A STUDY ON THE MIDGAP LEVEL (EL2) IN GaAs

(GaAs中のミッドギャップレベル(EL2)に関する研究)

A Thesis Presented to the Faculty of Electronic Engineering
of the University of Tokyo
in Partial Fulfillment of the Requirements
for the Degree of Doctor of Philosophy

by

Yasunori MOCHIZUKI

December 20, 1986

CONTENTS

CHAPTER 3 TRANSITIONS VIA EXCITED STATE OF EL2

CHAPTER 4 PROCESS DEPENDENCE AND ATOMIC STRUCTURE OF EL2

CHAPTER 1 INTRODUCTION

Abstract

Background of the present study is reviewed together with the basic knowledge on EL2 which have been widely accepted. Synopsis of the following chapters are also described.

1.1 Background

Recently, III-V semiconductor has drawn much attention and intensive studies have been carried out in this field. It is mainly because of the potential advantage of this material for the application for optical devices and very high speed integrated circuits. For the optical device applications, it is essential to use a direct-gap material as many of III-V semiconductors are. From the view point of the electronic device applications, large mobility and capability of achieving semi-insulating (SI) property are advantageous. Furthermore, alloy semiconductors and heterojunctions have brought about a new degree of freedom in designing devices, especially band structures and electronic states.

GaAs is one of the most important and intensively studied III-V semiconductor materials. This is the material which is already in practical use as, for instance, high frequency analogue amplifiers (FETs and MMICs) and laser diodes. For digital integrated circuits, fabrication of 16kbit SRAM has been reported and some digital LSIs have come to be commercially available. These digital ICs commonly consist of GaAs metal-semiconductor field effect transistors (MESFETs).

GaAs MESFETs in a VLSI are fabricated by direct ion implantation to the SI GaAs substrates. SI substrates not only makes the device isolation easy but also reduces unwanted parasitic

capacitance. The bandgap of GaAs at room temperature is 1.42eV which results in the intrinsic carrier concentration of 1.8×10^6 cm^{-3} (for instance, Sze 1981). This value is four orders of magnitude smaller than that of Si and semi-insulating GaAs substrates are available. Using the state-of-the-art bulk crystal growth technology, however, it is difficult to suppress the impurity contamination lower than 1×10^{15} cm^{-3} (Thomas et al. 1984). Therefore, it is necessary to compensate the residual carriers by midgap deep traps which pin the Fermi level at midgap in order to get a stable semi-insulating substrates.

Up to several years ago, bulk GaAs was mainly grown by horizontal Bridgman (HB) method. Since a silica boat is used in this method, residual Si impurity in HB GaAs is always more than 1×10^{16} cm^{-3} and it is necessary to intentionally dope deep acceptor impurity, such as Cr, to make a crystal semi-insulating. However, it was very difficult to fabricate LSIs on a Cr-doped HB crystal because of non-uniformity of Cr concentration within a wafer and pile-up of Cr (Vasudev et al. 1980) atoms toward surface after post-implantation annealing.

Now the trend is such that liquid encapsulated Czochralski (LEC) GaAs grown from a pyrolitic boron nitride (PBN) crucible is mostly used as a SI substrate for GaAs LSIs. It is mainly because that semi-insulating crystal is obtained without any intentional doping. Additionally, large diameter, round (100) crystals can be grown more easily. Carrier compensation

mechanism in undoped SI LEC GaAs is completely different from that in HB GaAs. Using a PBN crucible, Si contamination is very small and the major residual impurities in LEC GaAs are boron and carbon coming from B_2O_3 encapsulant and from graphite heater, respectively. Since carbon forms a shallow acceptor level in GaAs, residual carriers are compensated by a deep donor which exists even in an undoped material. Actually, such a trap is located at midgap and generally called EL2 (Martin et al. 1977).

The origin of this level has been argued since 1960's but not yet clearly determined. From the practical point of view, it is important to investigate its origin because it provides key knowledge to reproducibly assure the uniformity of electrical properties during GaAs LSI fabrication processes, which is not yet satisfactory. There also has been a lot of basic research works on EL2. In such cases, characterization and identification of this particular level called a physical interest.

1.2 Properties of EL2

In this thesis, characterization of EL2 is carried out and its atomic structure is discussed. Before proceeding to the following chapters, properties of EL2 so far reported are reviewed and summarized in this section. The purpose here is not to make a comprehensive review of the research works on EL2 but only to clarify the present status of understanding and what are still controversial on this level.

The name of EL2 was given to a midgap deep donor by Martin et al. (1977) who summarized data on thermal emission rates of various deep levels in GaAs. Thermal emission property of EL2 was first reported by Sakai and Ikoma (1974), and also by Lang and Logan (1975). Existence of this level was reported in early 1960's from Hall measurements, photoconductivity, optical absorption, photocapacitance (PHCAP) and thermally stimulated current (TSC) (Gooch et al 1961, Hambleton and Hall 1961, Ainslie et al. 1962, Haisty et al. 1964, Blanc et al. 1964).

Table 1-1 summarizes the trap parameters of EL2. Its energy level is located at midgap. Electron capture to this level occurs through multi-phonon emission (MPE) process, whose energy barrier has been determined to be 80 meV (Henry and Lang 1977). This means that the stable position of an occupied EL2 is slightly displaced from the normal lattice position (i.e. EL2 has a lattice relaxation). A description in detail on the treatment

Table 1-1 Trap parameters of EL2

Energy Level below the Conduction Band	E_T (eV)	0.75
Activation Energy for Thermal Emission of Electrons	E_a (eV)	0.815
Capture Cross Section for Electrons at T=∞	σ_n (cm^2)	1.2×10^{-13}
Activation Energy in Electron Capture Cross Section	ΔW (eV)	0.08
Franck-Condon Shift at the Normal State	d_{FC} (eV)	0.12~0.15
Absorption Cofficient at 1 μm per Unit Concentration	α (cm-4)	1.3×10^{16}

of lattice relaxation will appear in the following chapters and thus not discussed here. Anyway the Franck-Condon shift of EL2 has been also reported both from optical measurements and from electric field dependence measurements as shown in the table (Mircea-Roussel and Makram-Ebeid 1981, Chantre et al. 1981).

EL2 has a characteristic absorption band around 1.1eV (1.1um) as shown in Fig. 1-1 (Martin 1981). Using a calibration curve after Martin and Fermi level correction (Walukiewicz 1983), EL2 concentration can be estimated by measuring the absorption coefficient of this band. This method is convenient to estimate EL2 concentration in semi-insulating GaAs crystals where electrical measurements are difficult.

Besides usual trap parameters, some peculiar and interesting characteristics of EL2 are reported. One is the so called photoquenching effect first reported by Vincent and Bois (1978) from PHCAP measurements. This effect is due to the existence of metastable state. Another is the existence of the excited state of EL2, which is observed as an internal optical excitation from the ground state first reported by Kaminska et al (1983). Furthermore, it has been found that EL2 cannot be a well-defined unique level but is a family of midgap levels of similar properties (thus similar origins). This is the concept of EL2 family reported by Taniguchi and Ikoma (1983). These findings have brought a new class of experimental information which greatly contribute to elucidate the atomic structure of EL2.

(a)

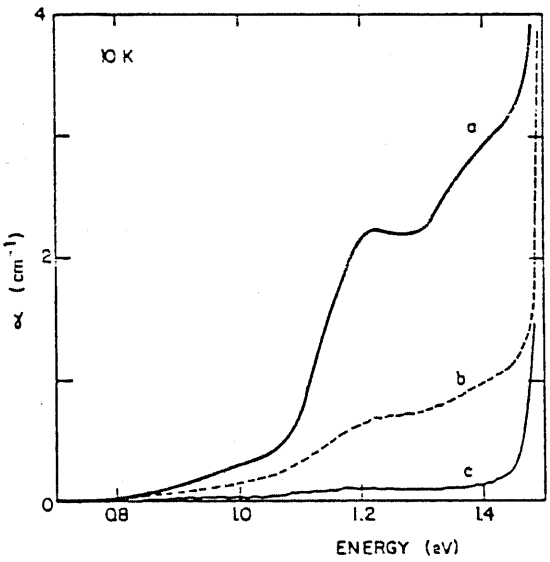

(b)

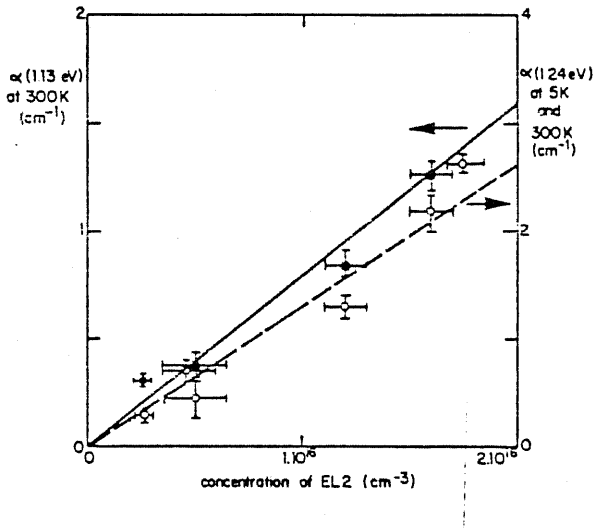

Fig. 1-1 (a) Characteristic absorption spectrum of EL2 measured at 10K. The band can be quenched by illumination as shown in curves b and c. (b) Correlation of absorption coefficient and EL2 concentration. (After Martin 1981).

Actually, these characteristics are what the following chapters of this thesis focuses on.

Back in 1961 it was reported that a midgap donor, which was speculated to be oxygen-related, plays a role in compensating shallow acceptors and making oxygen-doped HB GaAs crystals semi-insulating (Blanc and Weisberg 1961). The idea of oxygen-related defect was generally accepted until late 1970's, in which an oxygen atom substituting arsenic site (O_{As}) or a complex involving O_{As} should be EL2 (Ross and Jaros 1973, Fazzio et al. 1979). However, Huber et al. (1979) reported a negative experimental result against such a model. They compared concentration of EL2 measured from deep level transient spectroscopy (DLTS) to that of oxygen measured from secondary ion mass spectroscopy (SIMS) in GaAs crystals and found no quantitative correlation between each other. Later on, it was also found that EL2 had no correlation with Ga_2O_3 content in the melt used for bulk GaAs growth (Kaminska et al. 1981, Martin et al. 1982). These observations gave evidence that EL2 is no more likely to be related to oxygen.

It was also well-known that EL2 is not detected in liquid-phase epitaxial (LPE) GaAs which is always grown under a Ga-rich condition (Lang and Logan 1975). Increase of EL2 concentration with increase in the degree of arsenic rich conditions (As/Ga) during vapor-phase epitaxial (VPE) (Miller et al. 1977), organometallic vapor phase epitaxial (OMVPE) (Bhattacharya et al.

1980, Watanabe et al. 1981, Samuelson et al. 1981) and LEC growth (Holmes et al. 1982) has also been reported. As a natural consequence, it was suggested that EL2 may be related to a non-stoichiometric native defect such as gallium vacancy (V_{Ga}) or arsenic antisite (As_{Ga}). However, it is difficult to identify EL2 as an isolated V_{Ga} since this defect is not a donor but an acceptor in a GaAs crystal.

Lagowski et al. (1982a, 1982b) proposed an As_{Ga} model for EL2 in HB GaAs which should be formed through the mechanism of V_{Ga} diffusion. A possibility of antisite defect formation had been pointed out by Van Vechten (1975) from thermodynamical considerations. Actually, existence of this defect was confirmed through electron spin resonance (ESR) measurements on GaAs crystals which were either neutron irradiated, electron beam irradiated or plastically deformed (Wagner et al. 1980, Worner et al. 1982, Goswami et al. 1981, Weber et al. 1982). Recently, As_{Ga} defect is also detected even in as-grown bulk GaAs crystals (Elliott et al. 1984, Meyer et al. 1984).

Although there are many similarities between EL2 and As_{Ga}, some of the EL2 properties cannot be explained by assuming a single isolated As_{Ga} defect. A variety of native defect complex models have been also proposed. Discussion on the atomic structure of EL2 is made in Chapter 4.

1.3 Purpose of the study and synopsis

The purpose of this study is to clarify the origin of EL2 through carefully characterizing its properties. More in detail, the purposes are summarized as follows;

(1) to clarify the family nature of EL2 in photoquenching effect through a systematic characterization of the transition processes between the normal and the metastable state of EL2.

(2) to develop a new method to characterize the transition mechanisms via the excited state of EL2.

(3) to obtain a model which consistently describes the electrical and optical transitions at EL2.

(4) to examine the validity of the As cluster model for the atomic structure of EL2.

In Chapter 2, the photoquenching effect at the EL2 family is systematically studied using the photocapacitance method. It is shown that there exists a variation in the energy configurations of the normal and the metastable states based on the results of the recovery of photoquenching. A detailed study on the optical recovery process was carried out for the first time. These studies on the EL2 family provided a new insight into the transition mechanisms between the normal and the metastable states as also described.

In Chapter 3, a study is focused on the transition mechanisms via the excited state of EL2. A new method called Spectral

Photocapacitance Transient Analysis (SPTA) was developed and applied for the purpose. This method for the first time revealed that the excited state couples both with the metastable state and with the conduction band. A new configuration coordinate model for EL2 is proposed which can consistently explain the transition processes at EL2 so far reported. The atomic structure of El2 is also discussed.

Chapter 4 deals with the atomic structure for the origin of EL2. A change of EL2 is studied after process-induced damage and low temperature annealing. Thus, the defect component responsible for the EL2 formation is estimated. Arsenic cluster model for the origin of the EL2 family is proposed and discussed. After describing its advantages, comprehensive discussions are made together with other identifications so far reported by other researchers.

In Chapter 5, conclusions obtained in this study is summarized.

CHAPTER 2 PHOTOQUENCHING EFFECT AT EL2 FAMILY

Abstract

Photoquenching effect at the EL2 family is systematically studied by photocapacitance technique. A large variation in the photoquenching and the recovery characteristics indicates the existence of multiplicity in the energy configuration of the normal and the metastable states of EL2. It is found that the optical recovery process occurs only at a part of the EL2 family in LEC GaAs and that the transition energy for this recovery is 0.855eV. Inapplicability of a simple configuration coordinate model for the transitions between the normal and the metastable states is also clarified, which suggests that photoquenching can be identified as an optically-induced defect reactions accompanied by configuration changes.

2.1 Introduction

2.1.1 Photoquenching effect at EL2

EL2 is known to have a peculiar optical characteristic called photoquenching effect (sometimes called bleaching or optical fatigue). This effect has been first reported by Vincent and Bois (1978) from photocapacitance measurements. Under optical excitation in the energy range between 1.0eV and 1.3eV at temperatures below 130K, photocapacitance due to EL2 exhibits a non-monotonic transient as shown in Fig. 2-1. When photons are sent into the depletion region after filling the EL2 centers with electrons, capacitance first increases, passes a maximum and then gradually decreases to a stationary saturation value. The initial increase is attributed to photoionization processes of electrons and holes, which are common to deep levels. The successive decrease is due to the photoquenching. It is known that photoquenching most efficiently occurs around photon energy of 1.13 eV. When the light is off and again switched on, capacitance no more exceeds the saturation value. This state is persistent for a long time at low temperatures, at liquid nitrogen temperature for instance. Photoquenching effect is considered to be a transition from the normal state to the metastable state from which no excitation of electrons or holes take place to the conduction or valence band. Decrease of capacitance means that the metastable state only exists with an occupied condition and that the transition to the metastable

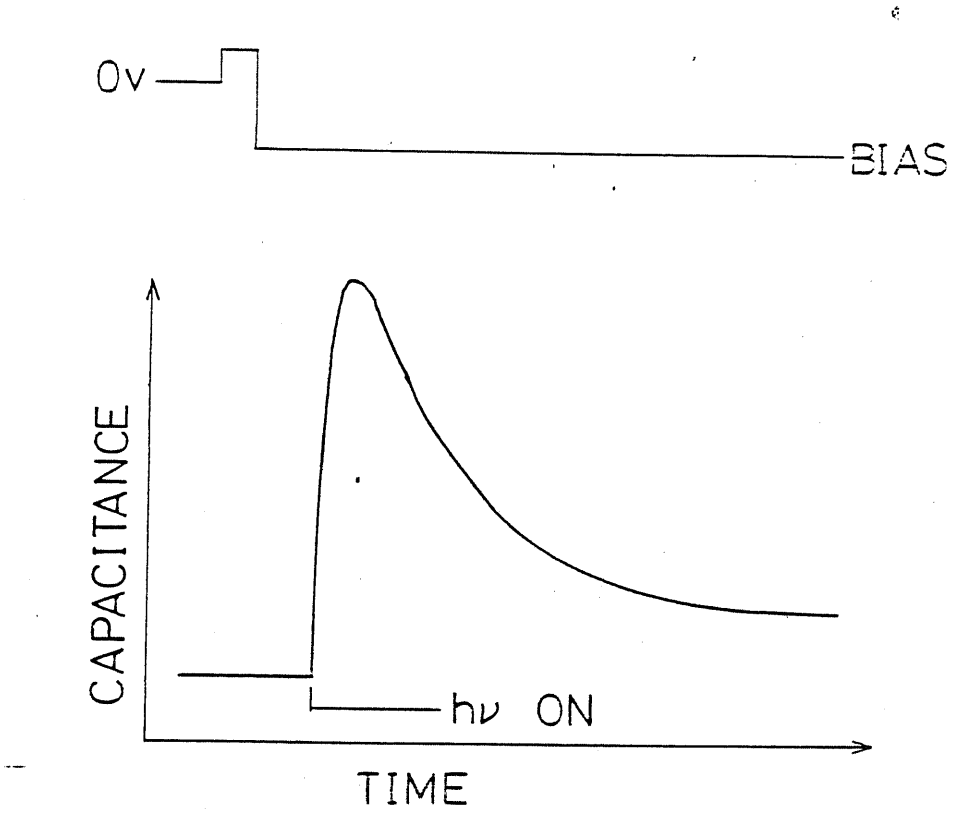

Fig. 2-1 A typical capacitance transient due to photoquenching of EL2. Temperature is 77K and the photon energy is 1.17eV. All the traps are filled with electrons before illumination.

state only occurs from a neutral normal state.

The photoquenching effect has been observed not only in photocapacitance but also in other optical properties. Martin (1981) showed a quenching in extrinsic optical absorption band around 1.1eV and concluded this band to be characteristic of EL2. Together with a Fermi level correction, his finding has provided a powerful tool for estimating EL2 concentrations in SI GaAs crystals where electric measurements can hardly be applied. A zero phonon line intensity of intracenter absorption, which will be discussed more in detail in the following chapter, is also quenched preserving a nice correlation with the main absorption band (Skowronski et al, 1986). However, it should also be noted that defects introduced by plastic deformation show no increase in the photoquenchable absorption, while the total absorption around 1.1eV is enhanced (Omling et al 1985).

Photoluminescence bands of a midgap energy also exhibits photoquenching. However, a situation is not so clear as for the absorption case. The controversial problem on the midgap photoluminescence is the presence of several emission bands: usually 0.64, 0.67 and 0.8eV bands are observed depending on the crystals under Ar or Kr laser excitation. It is, therefore, difficult to determine which band(s) is associated to EL2. The midgap luminescence in GaAs was first reported by Turner et al. (1963) in oxygen-doped HB crystals. The first observation of photoquenching of luminescence was reported by Leyral et al.

(1982) on the 0.65eV band. Later on, Shanabrook et al. (1983) observed a photoquenching at 0.63eV band but not for 0.68eV, while Yu (1984) observed the effect at 0.68eV band. Tajima (1985) found that the midgap luminescence band converge to 0.67eV band under an excitation of 1.32um. However, he also found that some of the midgap luminescence quench but others do not (Tajima 1984). Paget and Klein (1985) attributed the photoquenching of midgap luminescence bands not due to a direct involvement of EL2 but due to an indirect effect such as a change in Fermi level or absorption coefficient caused by photoquenching at EL2.

It has also been found that a quadruplet ESR signal, which has been attributed to As_{Ga}^{+}, shows photoquenching. However, it should be noted that the charge state is different from EL2 since photoquenching occurs at neutral EL2 centers. Furthermore, Meyer and Spaeth (1985) observed a difference in photoquenching characteristics. Relationship between this ESR signal and EL2 is discussed in chapter 4.

It is known that the initial state is restored by heating a sample above 130K (thermal recovery) (Vincent and Bois 1978). This process is explained as surmounting an energy barrier between the metastable state and the normal state. The barrier height can be determined by measuring thermal recovery rate as a function of temperature. So far, the values of 0.30eV and 0.34eV are reported by Vincent et al. (1982) and by Mittoneau and Mircea (1979), respectively.

Recovery to the normal state occurs also by free electron injection. Mittoneau and Mircea (1979) deduced an empirical expression for the recovery rate, r, to be

$$r = n*v_{th}*1.9x10^{-14}\exp(-0.107eV/kT) \qquad (2-1)$$

in the temperature range 50K<T<115K, where n and v_{th} are free electron concentration and thermal velocity of electrons. They proposed a model of an Auger-like process. There are some other interpretations for this recovery process. Levinson (1983) has proposed a complex defect model for EL2, where the metastability is considered as dissociation of the complex through a Coulombic interaction. According to his model, the recovery by free electron injection can be explained very naturally since they induce a motive force for Coulombic coupling. An $(As_{Ga})_2$ model for EL2 proposed by Figielski et al. (1985) can also successfully explain this recovery process. If an additional electron is captured at $(As_{Ga})_2^{++}$, the Jahn-Teller coupling strength is reduced and the metastability is no more expected.

A possibility of an optical recovery process has been also explored. Leyral et al. observed a recovery of 0.64eV luminescence intensity after a long time irradiation of intense above bandgap energy light (1982), while Tajima (1984) found that this emission band can be restored by 1.32um light irradiation. Nojima's observation (1985) of a spike conductivity also

indicates an existence of this type of process. Paget and Klein (1985) showed a similar effect in photoconductivity. However, a comprehensive study on this recovery process has not been made before the present study, which is described in the following (Mochizuki and Ikoma 1985).

Microscopic models of the photoquenching effect can be classified into two types. One is to assume a very large lattice relaxation at the metastable state, which was originally proposed by Vincent et al. (1982). As shown in Fig. 2-2, they correlated the peak energy of photoquenching to a vertical excitation energy from the normal to the metastable state and obtained a consistent diagram where the recovery barrier is 0.3eV. Their scheme, however, provides no explanation to the recovery by free electrons. The model by Figielski et al. (1985) belongs to this category since the the metastable state undergoes a large lattice relaxation due to a Jahn-Teller distortion which is caused by a redistribution of two trapped electrons at $(As_{Ga})_2^{2+}$. Levinson's model is the second type since the quenching is explained by assuming a difference in photoionization cross sections between the normal and the metastable state and no change in the lattice relaxation is necessary. Fillard et al. (1984) presented a supporting experimental evidence that new levels (E_t--100meV) appear in a thermally stimulated current (TSC) spectrum after photoquenching. Theoretically, metastability are predicted at $As_{Ga}+V_{As}$ and $As_{Ga}+As_I$ and will be discussed elsewhere.

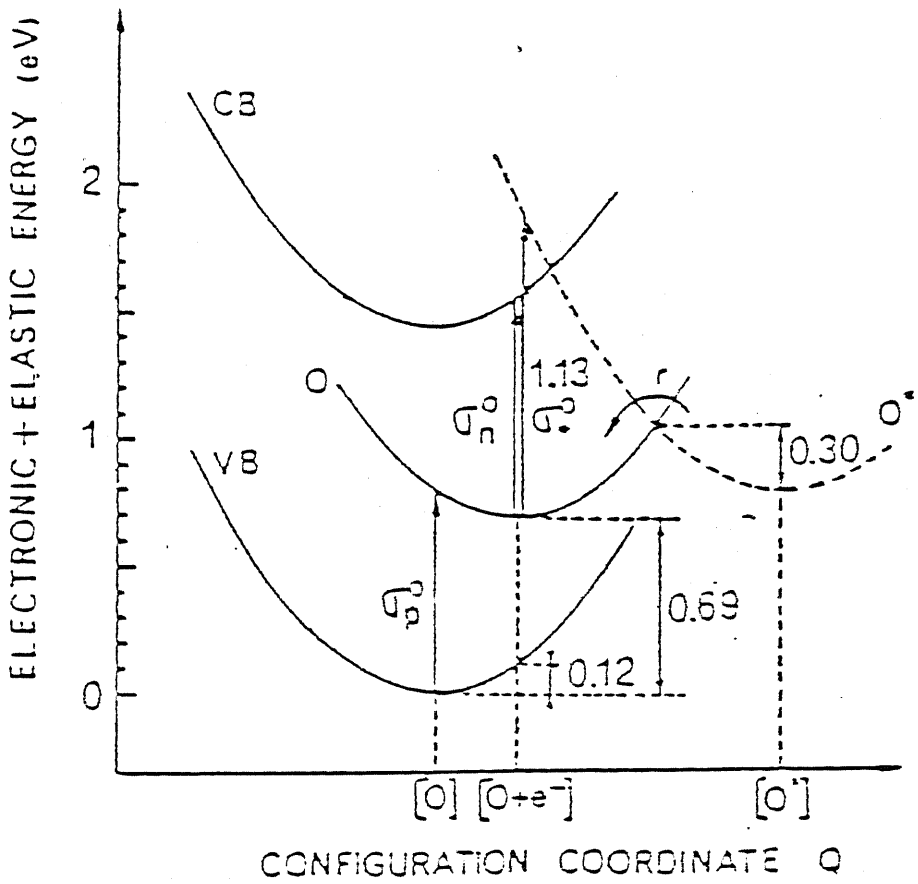

Fig. 2-2 The configuration coordinate model for the normal and the metastable states of EL2 (denoted as O-level) after Vincent et al. (1982).

Recently, several interesting experimental results are reported. Baranowski et al. (1986) reported a gradual increase in hole conductivity after the quenched condition is reached. This observation might correspond the observation by Tsukada et al. (1985). They found that a singlet component of ESR signal shows an increase under the photoquenching condition. The transient is much slower than that of quenching of the quadruplet signal and cannot be expressed by a simple exponential transient. However, there is no clear explanation to these results so far. Discher et al. (1986) monitored the photoquenching effect by an intravalence band absorption of holes in p-type LEC GaAs grown from Ga-rich melt. An interesting result is obtained that the recovery to the initial carrier concentration takes place at 65K which is much lower than 130K.

2.1.2 EL2 family

Taniguchi and Ikoma (1983b) first reported family like characteristics at EL2. They found that thermal emission rate of EL2 centers in LEC GaAs has a variation which cannot be simply explained by an experimental error. They also studied the photoquenching spectra of EL2 centers in various GaAs crystals (LEC, HB, VPE, oxygen-implanted and annealed LPE) and observed a variation among them (Taniguchi and Ikoma 1984). They found that some of the EL2 in LEC GaAs and the level artificially created by oxygen-implantation and successive annealing of LPE GaAs (Taniguchi and Ikoma 1983a) are unstable to annealing at 650C,

while EL2 in HB is always stable up to 850C. They concluded that EL2 is not a well-defined single level but a family of midgap levels of a similar origin since all of them exhibited a common characteristic of photoquenching effect. Thus, they proposed an idea of the EL2 family.

Supporting results were reported by other researchers. Watanabe et al. (1981) found that increasing rate of EL2 with [As/Ga] mole fraction in MOCVD GaAs are dependent on the growth temperatures. Lagowski et al. (1984) reported that a new midgap level appears by oxygen doping to HB GaAs. On the other hand, As_{Ga} defect detected by ESR, which is often discussed in conjunction with EL2, has been found to have a variation in its atomic structure from optically-detected electron-nuclear double resonance (ODENDOR) (Hofmann et al. 1984).

In this chapter, photoquenching properties at EL2 family is systematically studied using photocapacitance method.

2.2 Characterization of photoquenching effect by photocapacitance method

In the present study, photocapacitance method is adopted for the characterization of photoquenching effect of EL2. Although photoquenching effect can be observed by various techniques as already mentioned, photocapacitance measurement has advantageous in the following points:

(i) Re-capturing of electrons at the conduction band can be neglected because the measurement accesses to a depletion region.

(ii) Recovery from the metastable to the normal state is neglected because of a very low free electron concentration within the depletion region.

(iii) The concentration of traps responsible for a change of capacitance can be estimated much more easily than in photoluminescence and photocurrent measurements.

(iv) Photocapacitance can be applied to a thin layer of crystal such as epitaxial GaAs, while absorption measurement cannot be. The main disadvantage is that this method cannot be applied to a highly resistive materials.

Here, a transient due to the photoquenching effect is formulated based on a set of empirical rate equations. At low temperatures, no thermal emission takes place and the capture process can be neglected within a depletion region. Therefore, the rate equation can be formulated after Fig. 2-3 and is written for the

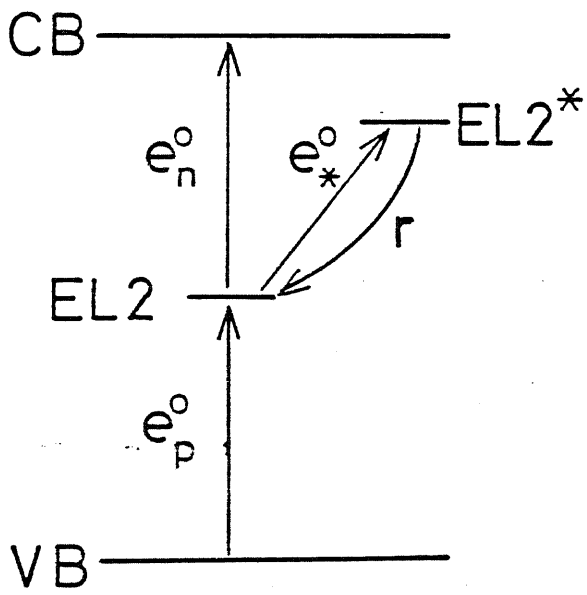

Fig. 2-3 Transition processes at EL2 under illumination. CB, VB, EL2 and EL2* correspond to the conduction band, the valence band, the normal and the metastable states of EL2, respectively.

concentration of electrons at the normal state of EL2, N, and for that at the metastable state, N^*, as

$$\frac{dN}{dt} = -e_n^{\circ}N + e_p^{\circ}(N_T-N-N^*) - e_*^{\circ}N + rN^* \qquad (2\text{-}2)$$

$$\frac{dN^*}{dt} = e_*^{\circ}N - rN^* \qquad (2\text{-}3)$$

where e_n°, e_p° are photoionization rates for electrons and for holes, respectively. e_*° is the optical transition rate for a transition from the normal to the metastable state. All of the three rates can be expressed as a product of incident photon flux, phai, and the corresponding transition cross sections, σ_n°, σ_p° and σ_*°, respectively. r is the recovery rate from the metastable state to the normal state. These rates are all constant at a fixed photon energy. r can be neglected at a considerably lower temperature than 130K. N_T is the total EL2 concentration. In an n-type semiconductor diode, an increase in capacitance is approximately proportional to an increase in positive space charge density, $P=N_T-N-N^*$. It should be reminded that there is no unoccupied (positively charged) centers at the metastable state. P can be calculated from the solution of (2-2)

and (2-3).

$$P(t) = N^{o}*[\ \exp(-b_2 t) - \exp(-b_1 t)\ ] \qquad (2\text{-}4)$$

where

$$b_1 = e_n^{\,o} + e_p^{\,o} \qquad (2\text{-}5)$$

$$b_2 = e_*^{\,o} e_p^{\,o}/(e_n^{\,o} + e_p^{\,o}) \qquad (2\text{-}6)$$

$$N^{o} = N_T e_n^{\,o}/(e_n^{\,o} + e_p^{\,o}) \qquad (2\text{-}7)$$

The first term in the right hand of (2-4) corresponds to photoquenching, while the second term does to photoionization. b_1, and b_2 correspond to photoionization rate and photoquenching rate, respectively. N^{o} is related to the unoccupied EL2 centers at the steady state. (2-6) gives an insight that the transition rate to the metastable state is proportional to the occupied portion of the normal state where electrons are supplied by hole photoionization process.

2.3 Transition between the normal and the metastable states of EL2

2.3.1 Transition from the normal state to the metastable (photoquenching)

A study on the transition from the normal state to the metastable state has been already described in Taniguchi and Ikoma (1984), Taniguchi et al. (1984) and in Mochizuki (1984). Therefore, it is not appropriate to go further than summarizing the results which would be necessary for discussions.

In Fig. 2-4, capacitance transients due to photoquenching, $C(t)-C_{\infty}$, at EL2 centers in various GaAs crystals are collectively shown. The measurements were carried out at 77K with an excitation photon energy of 1.17eV. It is apparent from the figure that photoquenching rates are different depending on the crystals. Furthermore, a strong non-exponentialities are observed for the levels in LEC and oxygen-implanted and annealed LPE GaAs (labeled as ETX-1 and EL2-O, respectively). Figure 2-5 shows spectral dependences of photoquenching rate for these GaAs crystals, which are normalized to the peak value. It can be seen that the spectra consist of Gaussians around 1.13eV and increase at the region above 1.3eV, the latter of which has an apparent variation among the EL2 levels in the various crystals (EL2 family).

Table 2-1 Sample description

sample	midgap level	n (cm^{-3})	growth conditions etc.
LEC1(T)	ETX-1	$0.8\sim1.7\times10^{16}$	undoped, SiO_2 cruicible
LEC2(F)	ETX-4	0.3×10^{16}	undoped, pBN cruicible, grown from poly crystalline GaAs
HB	EL2	1.6×10^{16}	undoped, SiO_2 boat
VPE	EL2	2.5×10^{15}	grown on n^+-substrate
LPE	EL2-0	1×10^{16}	undoped, O^+implantation at 100keV/$1\times10^{13}cm^{-2}$, annealed at 600C for 15min.
MOCVD	EL2	1.5×10^{15}	undoped, grown on n^+-substrate, T_{sub}=720℃, V/III=20

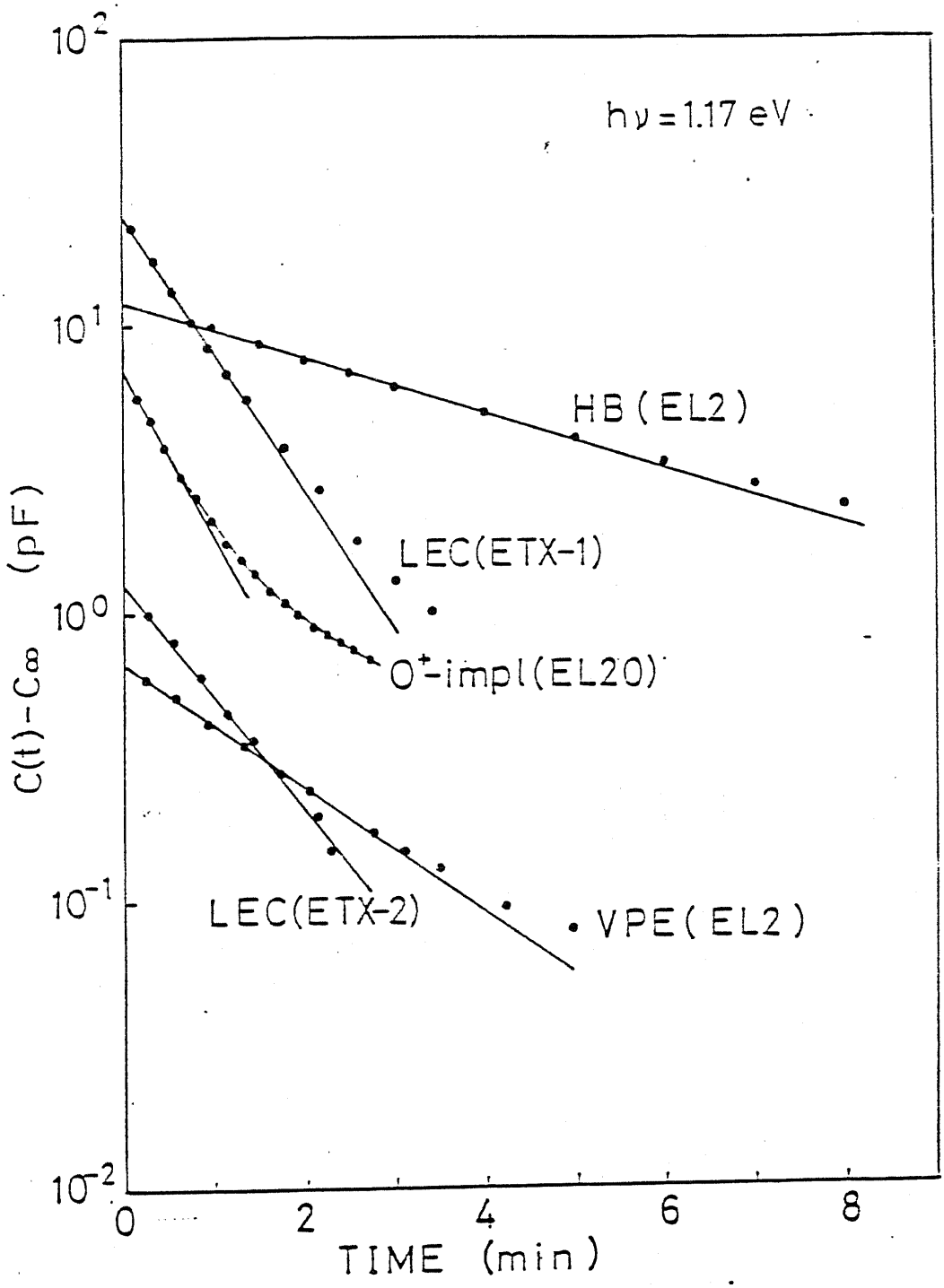

Fig. 2-4 Photoquenching transients of the EL2 family in various GaAs crystals.

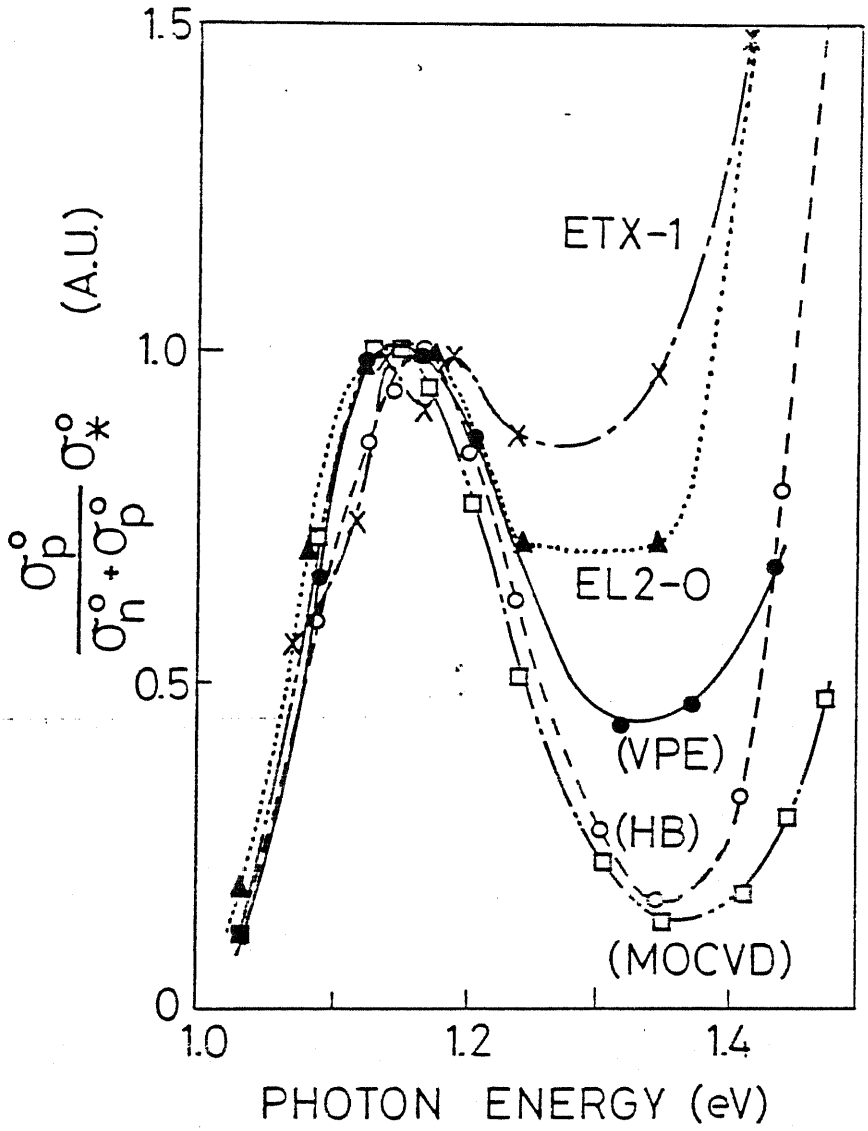

Fig. 2-5 Spectral distributions of photoquenching rate normalized by incident photon flux (photoquenching cross section) for the EL2 family.

A more extensive study was carried out on the non-exponentiality in the capacitance transient at ETX-1. A constant capacitance measurement was applied using a feedback circuit to eliminate the effect of non-linearity between capacitance and space charge density. Let $\Delta\rho$ be a change in the space charge density. Then, a change in bias voltage, ΔV, to keep a capacitance constant is,

$$\Delta V = \Delta\rho * (V_{bi} - V_{appl} - kT/q)/N_d \qquad (2\text{-}8)$$

where V_{bi}, V_{appl} and N_d are built-in potential, applied voltage and shallow donor density, respectively. It is clear that ΔV, instead of capacitance, is exactly proportional to $\Delta\rho$. Fig. 2-6(a) shows the result obtained by the constant capacitance method at three excitation photon energies. It is concluded that the non-exponentiality can be attributed not to experimental error but to the physical property of ETX-1: this level consists of traps with slightly different photoquenching rates. The rates are expected to have a broadening with a certain distribution. A Gaussian distribution was assumed for simplicity in the study. Figure 2-6(b) shows the distributions which gave the best fits (solid curves in Fig. 2-6(a)) to the experimentally obtained transients. Values of a measure of broadening (standard deviation/mean value) were 0.38, 0.52 and 0.69 at photon energy of 1.09, 1.17 and 1.48eV, respectively. However, distributions tend to extend to negative region which has no physical meanings. This may be due to an insufficient assumption of simple Gaussian distributions.

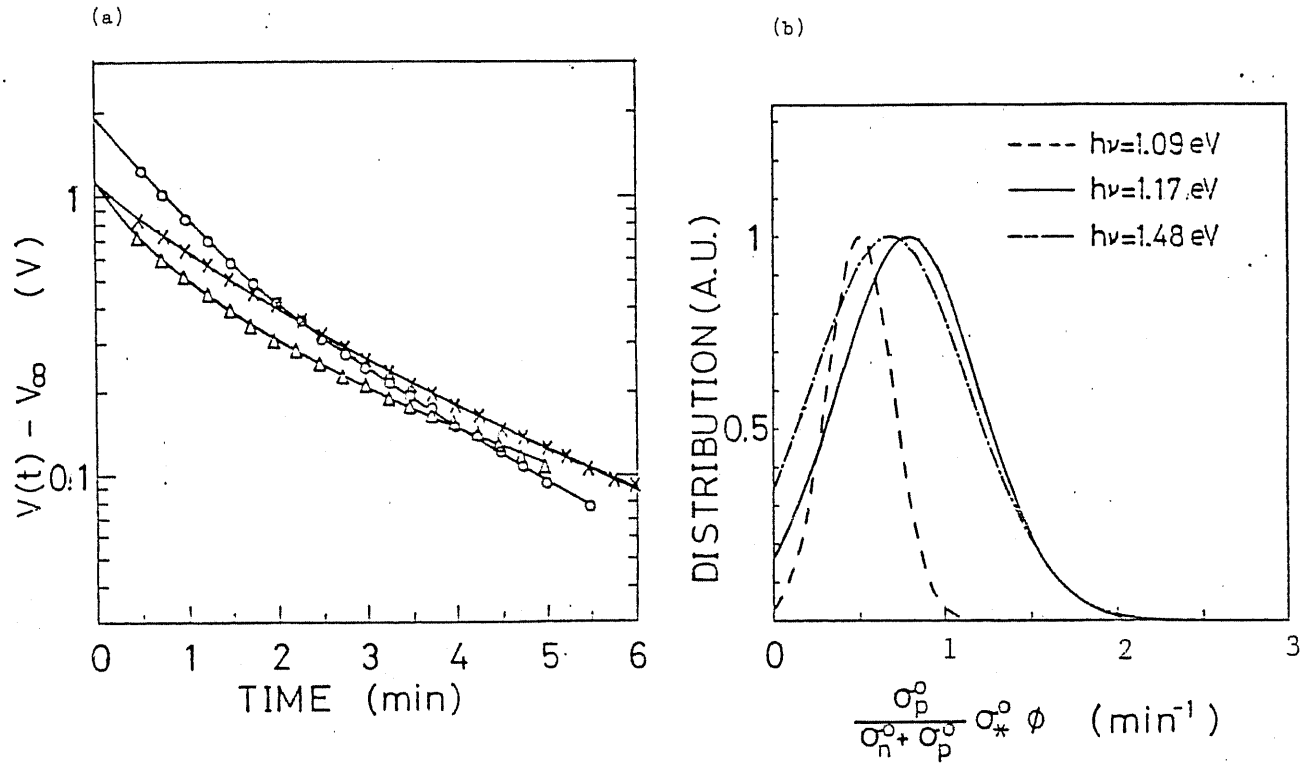

Fig. 2-6 (a) Photoquenching transients measured by constant capacitance technique for ETX-1 in LEC-1(T). Excitation photon energies are 1.48 (Δ), 1.17 (o) and 1.09eV (x). The solid lines are the calculated curves (see text). (b) Distributions of photoquenching rates used to reproduce the solid lines in (a) which give the best fit to the observed transients assuming single Gaussians.

2.3.2 Thermal recovery process

Thermal recovery rate, r, was characterized for ETX-1 in LEC GaAs by varying temperature as schematically shown in Fig. 2-7. Non-exponentiality was again observed as shown in Fig. 2-8(a). The result of Gaussian fitting (Fig. 2-8(b)) revealed that the average barrier height for the recovery is 0.305eV and the broadening in the barrier height is estimated to be less than 10meV, which is smaller than the thermal energy at the measurement temperatures.

Characterization of EL2-O was also carried out. This center is peculiar since no recovery occurs by a free electron injection as shown in Fig. 2-9. The barrier for the thermal recovery process at EL2-O was measured to be 0.41eV. The Arrhenius plot of the recovery rate is shown in Fig. 2-10 together with the data for ETX-1 as well as those already reported by other researchers. The barrier height of EL2-O is larger than that of other EL2 centers and indicated that the metastable state of EL2-O is distinctly different from that of other members of the EL2 family.

2.3.3 Optical recovery process

Optical recovery from the metastable state to the normal state is reported in "spike photoconductivity" (Nojima 1985) and in 0.64eV

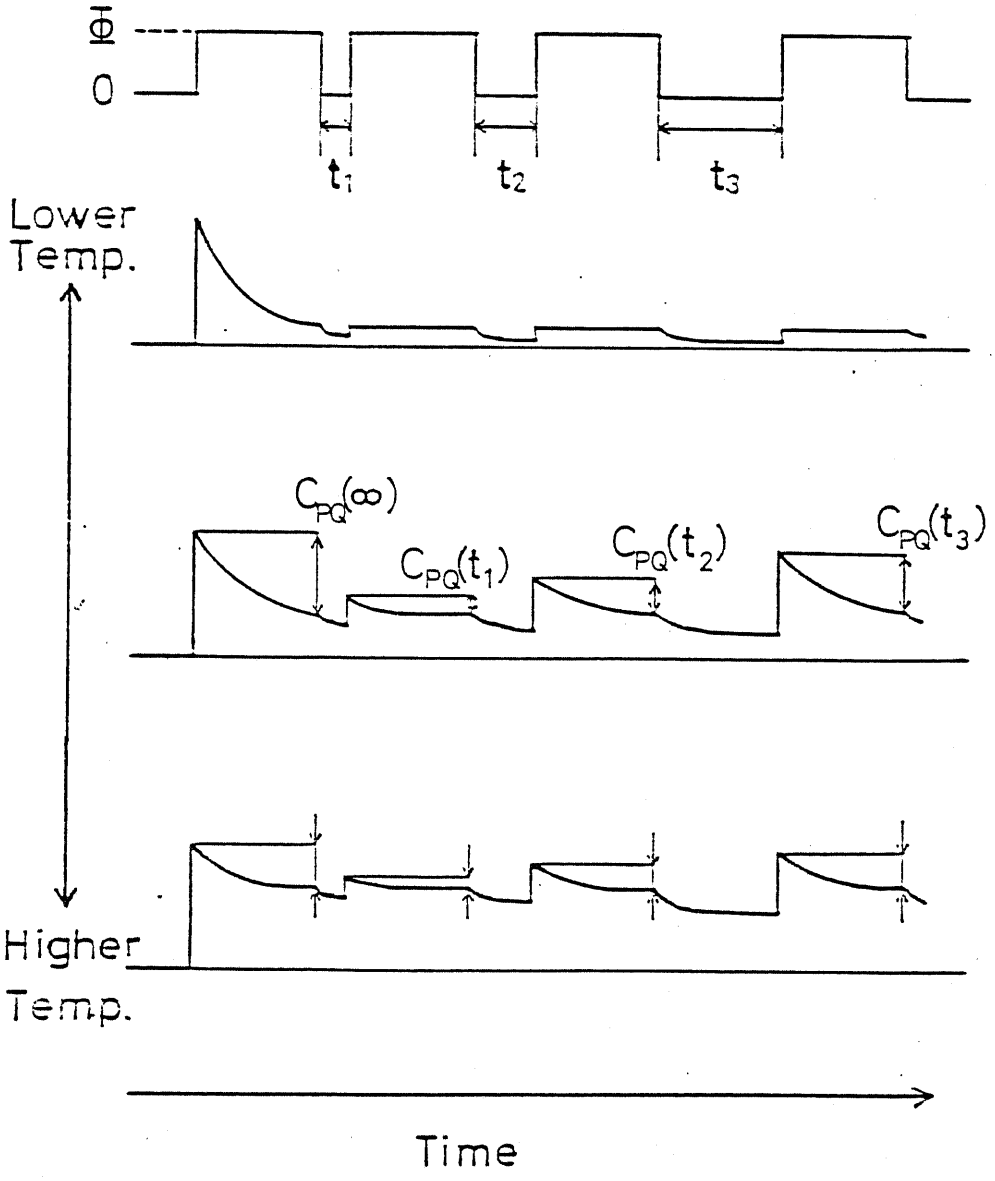

Fig. 2-7 An illustration of the measurement procedures for the thermal recovery rate from the metastable to the normal state of EL2.

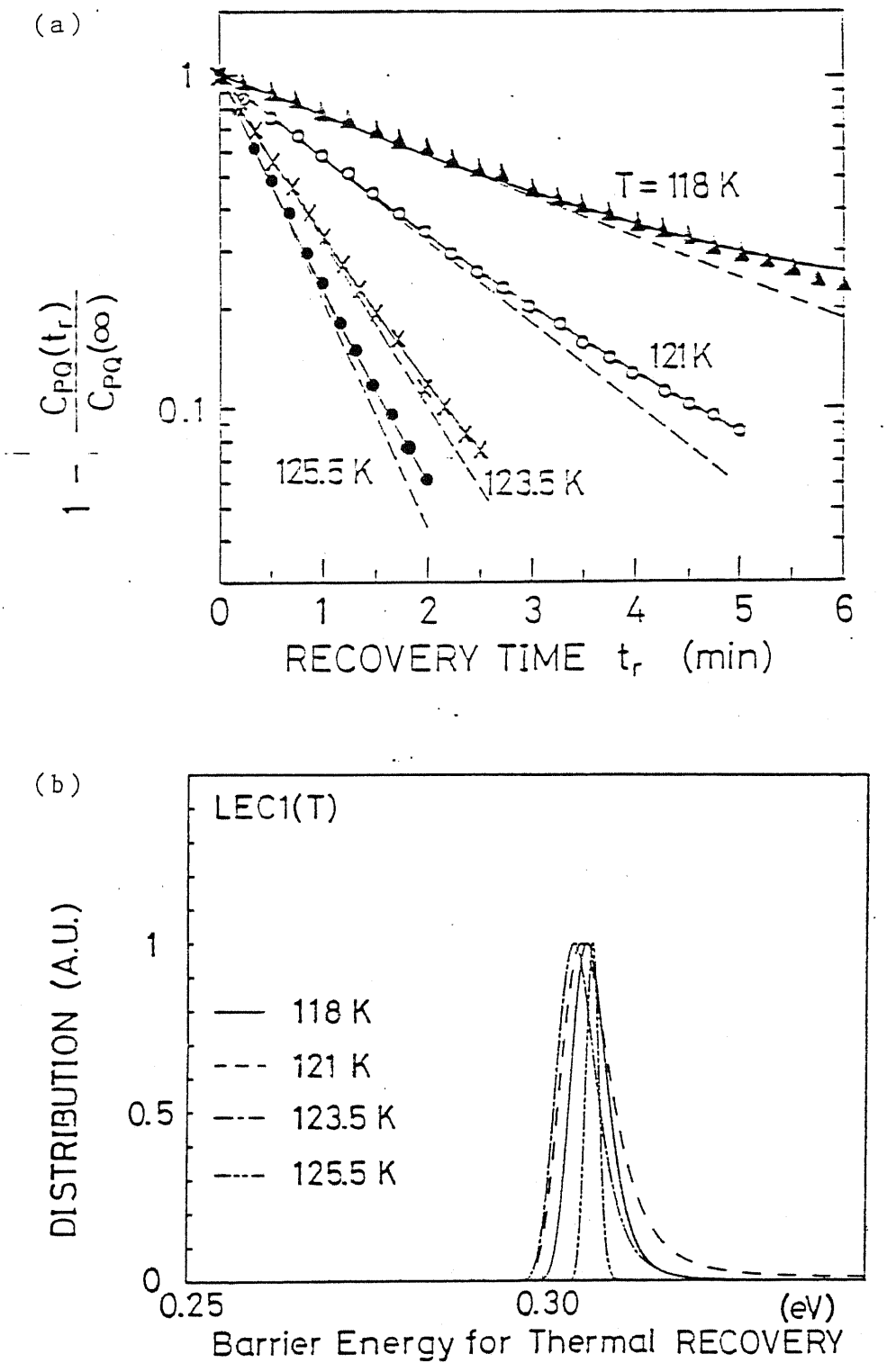

Fig. 2-8 (a) Transients of the thermal recovery process at ETX-1. (b) Broadening in the energy barrier for the recovery from the metastable state to the normal state of ETX-1, which gives the best fit to the observed transients.

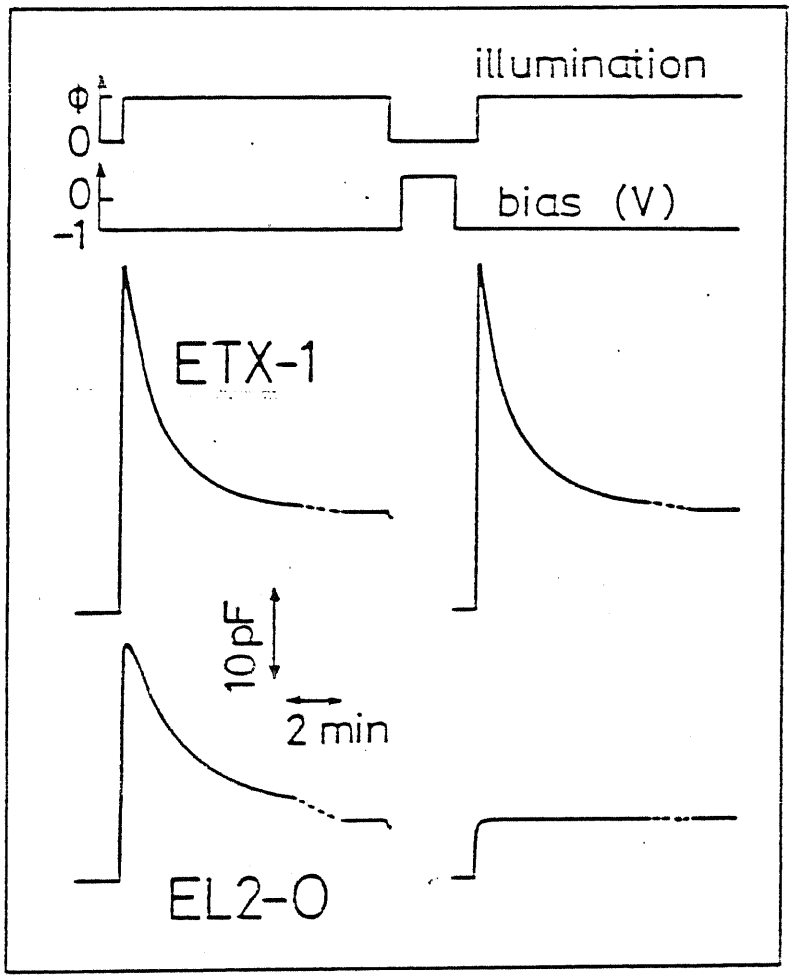

Fig. 2-9 Capacitance transients due to photoquenching at ETX-1 and EL2-O. No recovery by forward biasing was observed at EL2-O.

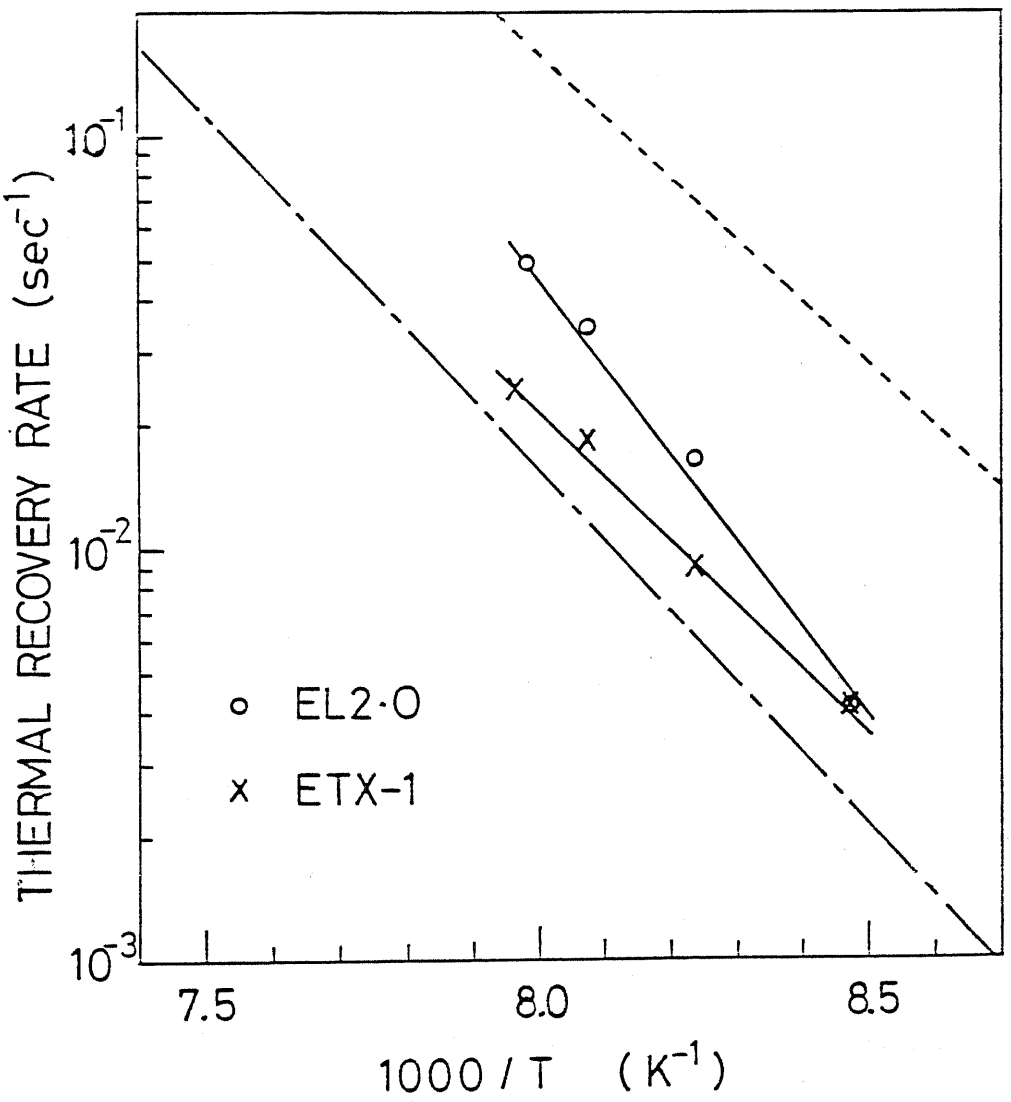

Fig. 2-10 Arrhenius plots of the thermal recovery processes at ETX-1 and EL2-O. Data of previous reports are also shown (Vincent et al. 1982, Mittoneau and Mircea 1979).

photoluminescence band (Tajima 1984). However, these measurements accessed to neutral regions and therefore the actual change of charge states due to transition between the two states of the EL2 center was not well measured. Furthermore, identification of photoluminescence emission band is still controversial. In the present study, optical recovery process is characterized carefully using a photocapacitance method on the EL2 family in various GaAs crystals.

The samples studied are LEC, HB, MOCVD and oxygen-implanted and annealed LPE GaAs crystals. Two wafers of LEC GaAs were examined, one of which was cut from the tail section of an ingot while the other is from the front section. Midgap levels in these wafers are labeled as ETX-1 and ETX-4, respectively. The level in the oxygen-implanted LPE GaAs is denoted as EL2-O as is in the previous section. All the samples were studied after forming Schottky diodes by Au deposition. Measurements were carried out with immersing the samples into liquid nitrogen (77K), at which temperature the effect of thermal recovery process can be neglected.

The measurement sequence is described in the following. First, all the traps were filled with electrons and the samples were illuminated with light, $h\nu_1$, of 1.17eV which efficiently induces photoquenching. The quenched magnitude of capacitance, C_{PQ}, represents a total amount of EL2 in a sample. After a sufficiently long time illumination, all the EL2 centers are

considered to have been transferred to the metastable state. To study the effect of optical recovery, the secondary light, $h\nu_2$, is sent. The recovered amount was monitored by the magnitude of photoquenching, C_r^o, under $h\nu_1$ illumination. This procedure eliminates the effect of photoionization, where the ratio of e_n^o to e_p^o is usually unknown. Here, we define the recovered amount of EL2 by illumination of $h\nu_2$ as,

$$F_r^o = C_r^o/C_{PQ} \qquad (2\text{-}9)$$

which is called a fractional recovery. F_r^o is functions of time and energy of the secondary illumination, $h\nu_2$.

Figure 2-11 shows transients of capacitance following the illumination sequence. Photon energy for the recovery is 0.855eV in this figure. Recovery by $h\nu_2$ was observed only for ETX-1 and ETX-4 in LEC GaAs while no recovery was observed for EL2 in HB, MOCVD GaAs and for EL2-O.

In Fig. 2-12, F_r^o for ETX-1 is plotted as a function of the time of $h\nu_2$ irradiation, t_r^o, where photon energy is taken as a parameter. F_r^o tends to saturate after a long time illumination of recovery light. The saturation value of F_r^o is independent of $h\nu_2$ but dependent on samples: it was 0.08 for ETX-1 and 0.12 for ETX-4. From the result, it is found that only part of EL2 centers, around 10% of EL2 in LEC GaAs, recover optically from the metastable state.

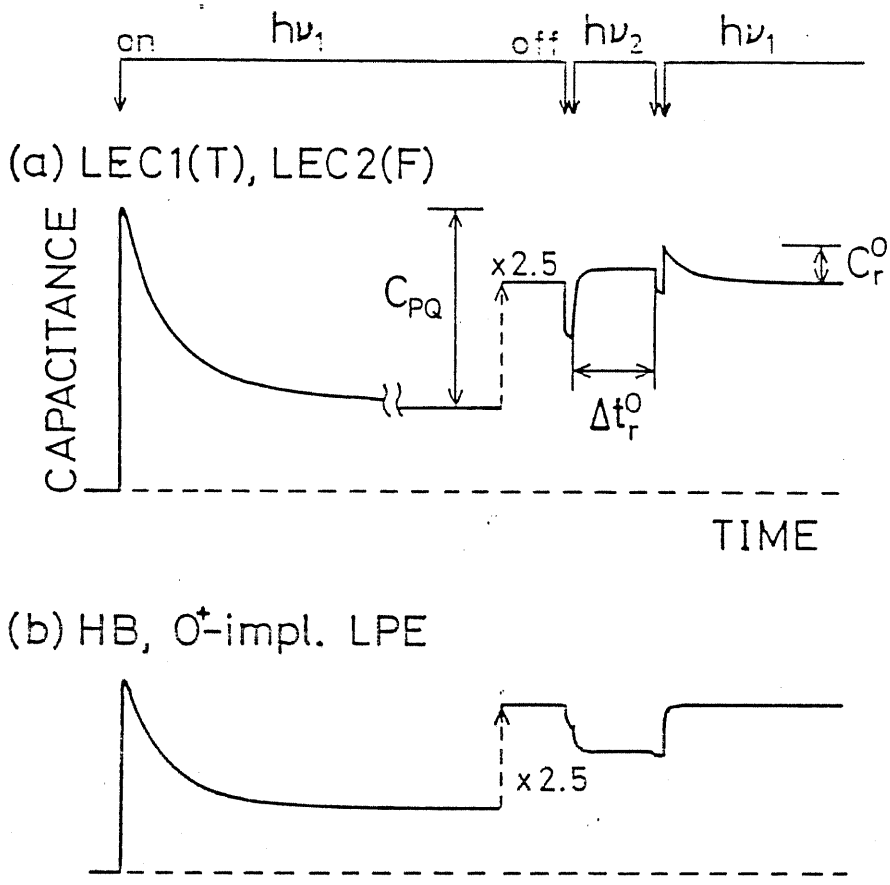

Fig. 2-11 Capacitance transients during the sequencial illuminations by hv_1 and hv_2. (a) Optical recovery of photoquenching was observed at LEC1-(T) and LEC2-(F) which contain ETX-1 and ETX-4, respectively. (b) No recovery was observed at HB and O^+-implanted LPE which contain EL2 and EL2-O, respectively.

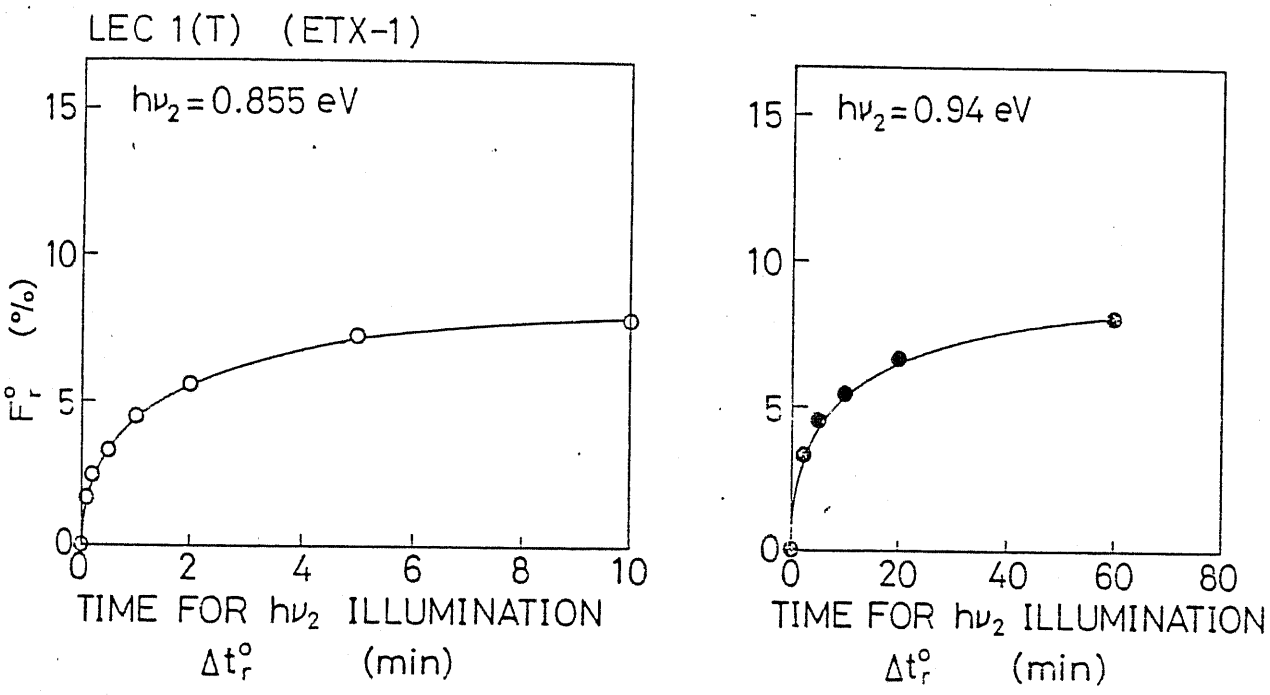

Fig. 2-12 Fractional recovery (F_r°) of photoquenched capacitance by 0.855eV- and 0.94eV-light as a function of time.

Spectral dependence of the optical recovery process was measured. F_r^o at Δt_r^o=10min was measured as a function of $h\nu_2$. This value approximately gives the spectral dependence of recovery rate. The results for ETX-1 and ETX-4 are exhibited in Fig. 2-13. Both of the spectra have peaks at 0.855eV with FWHM of 130meV. Thus, the vertical transition energy from the metastable state in the configuration coordinate diagram is determined to be 0.855eV for the EL2 centers which recover optically.

Capacitance transients of photoquenching (transition from the normal state to the metastable state) at the EL2 centers which recover optically are compared to that at all the EL2 as shown in Fig 2-14. In the figure, solid circles represent a transient recorded after all the EL2 is recovered to the normal state by forward biasing, while open circles represent transients to which only part of the EL2 centers that recover optically from the metastable state contribute. In the latter case, Δt_r^o was varied and the transients were recorded at various stages of the optical recovery. It is clear that the photoquenching rates are faster at the centers where the optical recovery is allowed. Furthermore, the photoquenching rate is faster when Δt_r^o is shorter. This result indicates that even the EL2 centers that recover optically cannot be regarded a single level and that EL2 which has a faster optical recovery rate has a larger cross section for transition from the normal state to the metastable state.

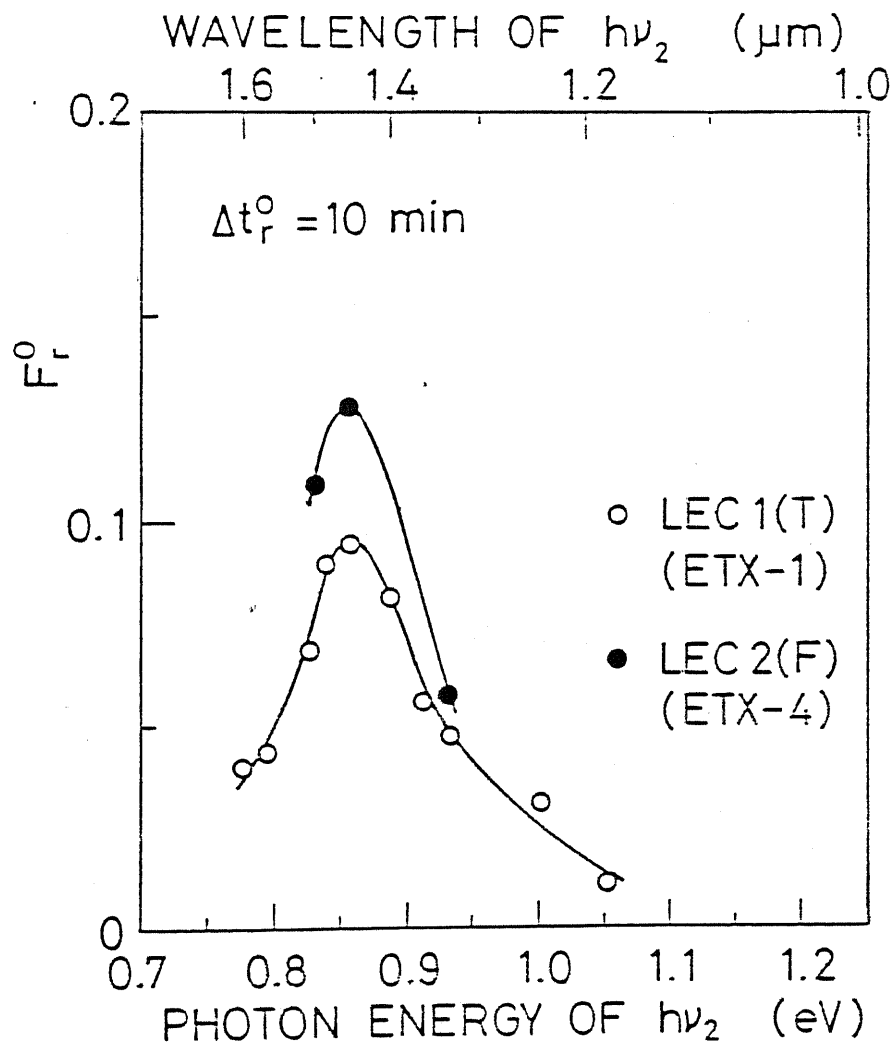

Fig. 2-13 Dependences of F_r° at ETX-1 (open circles) and ETX-4 (solid circles) on hv_2, where Δt_r° and hv_1 are 10 min and 1.17 eV, respectively.

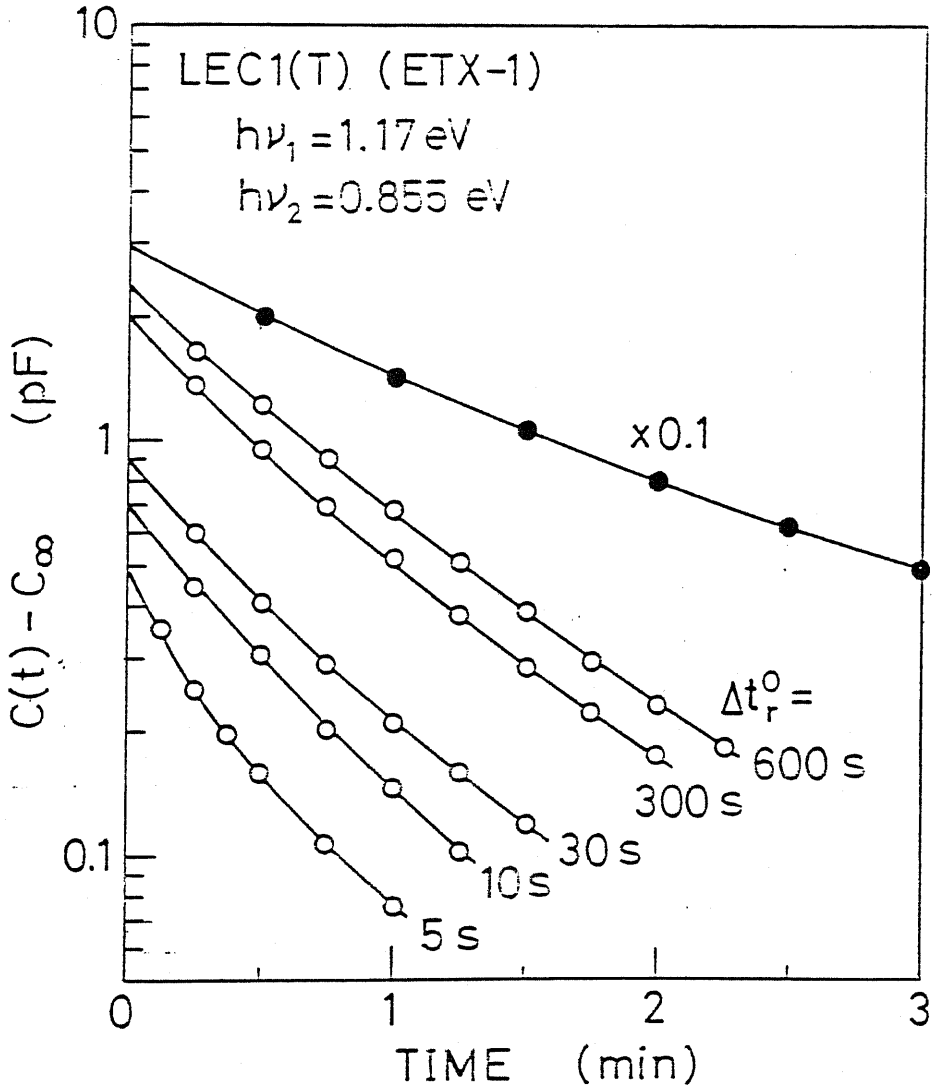

Fig. 2-14 Capacitance transients due to photoquenching at ETX-1 when hv_1=1.17eV. Solid circles represent a case where all the levels are in the normal state by forward biasing prior to the illumination by hv_1. Open circles represent cases where only the levels which can be recovered by hv_2 illumination contribute to the photoquenching transients.

The transient of optical recovery process is replotted from Fig. 2-12 in Fig. 2-15 in the form of $F_r^o{}_\infty - F_r^o(t_r^o)$. The transient of recovery process has a strong non-exponentiality. It is, therefore, indicated that there exist EL2 centers with a variation in the optical recovery cross section. This result coincides with the above observation that EL2 which recovers optically from the metastable to the normal state (around 10% of the total EL2 in an LEC GaAs crystal) has a variation and cannot be regarded as a unique level.

Optical recovery process gives another transition energy within a configuration coordinate (CC) diagram. In the following, a validity of the conventional CC diagram proposed by Vincent et al. (1982) is discussed. In their model, photoquenching corresponds to a direct excitation process from the normal to the metastable state. A diagram is shown in Fig. 2-16(a) where the transition energy of photoquenching, E_q^o, is taken to be 1.13eV from the photoquenching spectrum for LEC GaAs and the thermal recovery barrier, E_r^{th}, to be 0.3eV. Assuming the same phonon frequency for the normal and the metastable state, the resultant vertical transition energy from the bottom of the metastable state to the normal state is 1.18eV. This value is much larger than the experimental value of 0.855eV. There are two other ways for choosing two energies out of three, E_q^o, E_r^{th} and E_r^o. However, they both fail in giving a consistent diagram due to a smaller value in E_r^{th} or in E_q^o than the observed values.

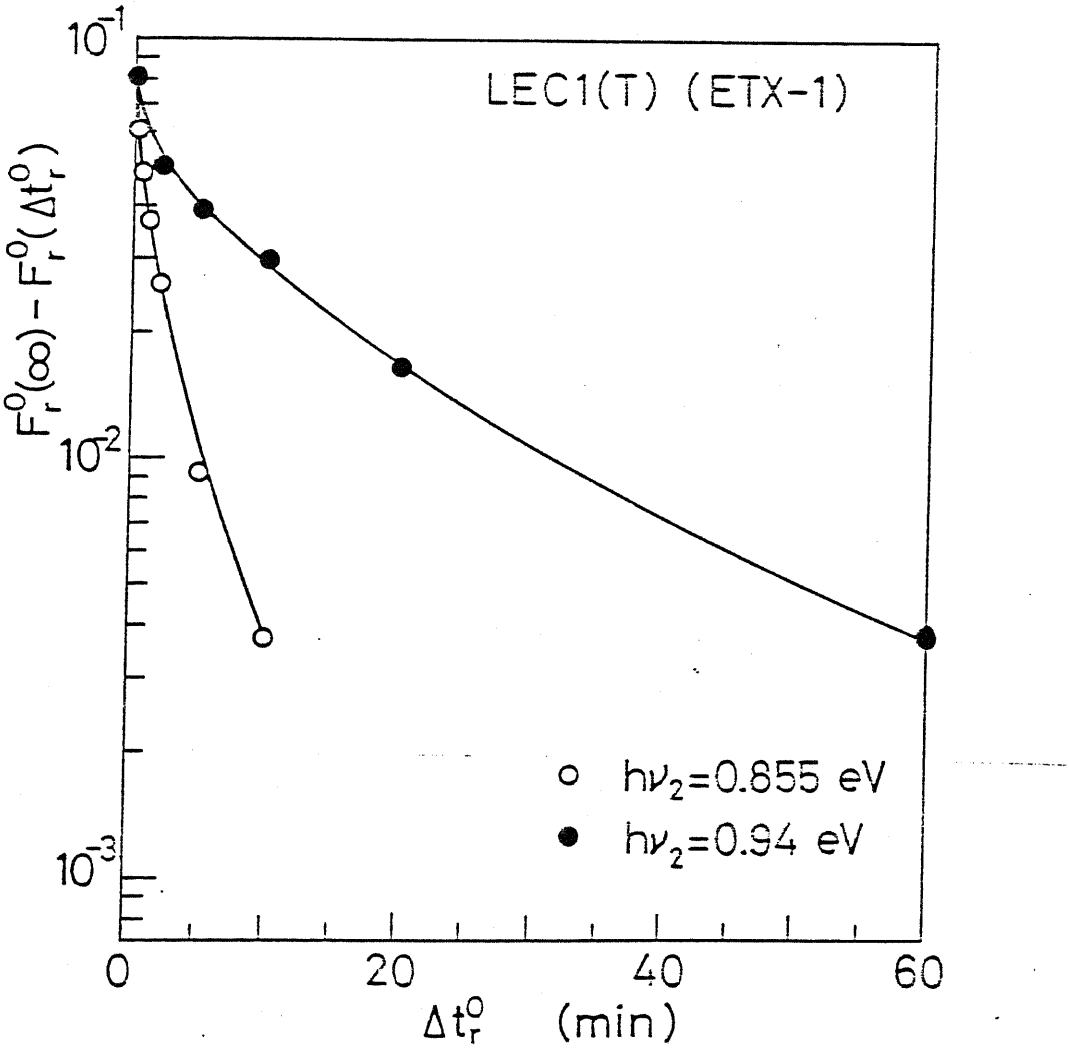

Fig. 2-15 Transients of optical recovery from the metastable state to the normal state of ETX-1.

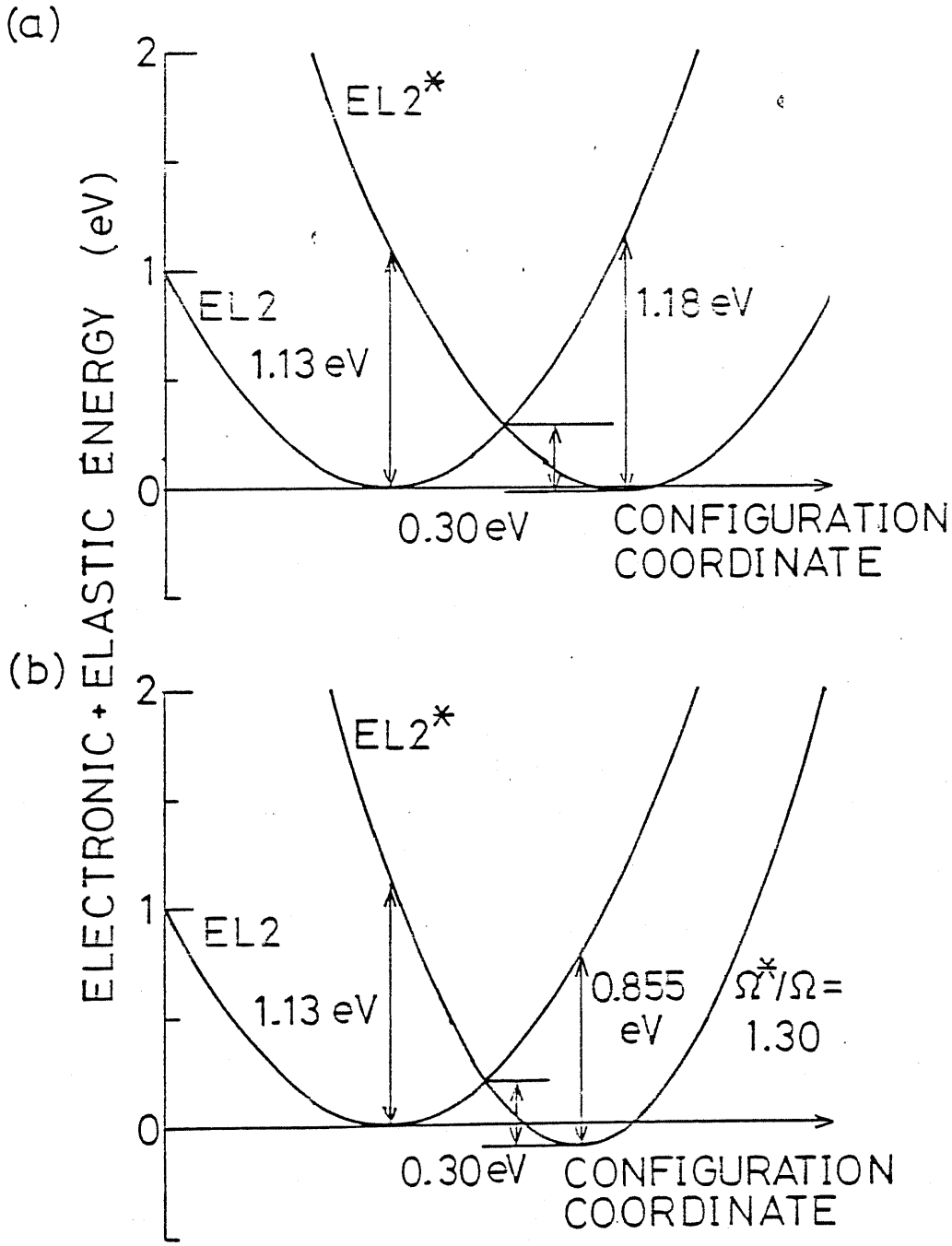

Fig. 2-16 Configuration coordinate model for the two states of EL2. (a) shows the scheme originally proposed by Vincent et al. (1982). (b) is the case where ratio of phonon frequencies is taken as a fitting parameter to make the three transition energies consistent.

A consistent diagram can be obtained by introducing a difference in phonon frequencies to which the normal and the metastable states couple. Fig. 2-16(b) shows a thus obtained CC diagram by assuming a ratio of $\Omega^*/\Omega=1.30$, where Ω^* and Ω denote the phonon frequencies to which the metastable state and the normal state couple, respectively. In this diagram, all of the three energies are consistent. However, the energy level of the metastable state becomes apparently lower than that of the normal state. This scheme is incorrect since the energy of the metastable state should be higher than that of the normal state.

Two possibilities are pointed out which may cause such inconsistency; (1) the values of E_q° and /or E_r^{th} are not appropriate for the states that recover optically, or (2) higher order terms in the expansion of the electron-lattice Hamiltonian cannot be neglected, that is, a harmonic approximation does not hold.

Case (1) is suggested because the fraction of EL2 states that recover optically is small, and therefore, true values of E_q° and E_r° for such centers could not be measured, being masked by other majority states. However, this possibility should be ruled out from the following argument. If we take $E_r^{\circ}=0.855$eV and $E_r^{th}=0.30$eV, then E_q° becomes 0.36eV, which is too small to explain the photoquenching spectrum. On the other hand, if we take $E_q^{\circ}=1.13$eV and $E_r^{\circ}=0.855$eV, then E_r^{th} becomes 0.18eV, which

is too small for a persistent photoquenching to occur at liquid nitrogen temperature.

Case (2) is likely at the EL2 centers. The harmonic approximation is too simple to quantitatively interpret characteristics of deep states. It is necessary to take into account terms higher than the second order in the expansion of the electron-phonon interaction Hamiltonian. Such a correction to the harmonic oscillation is too complex to treat quantitatively. However, this suggests that the EL2 centers have complex atomic structures and a simple CC model cannot apply to them. As already mentioned, the transition from the normal to the metastable state varies among the EL2 centers in different crystals. Here, it is also found that the optical recovery process is not always observed at the EL2 centers but only about 10% of the centers in LEC materials show such optical recovery.

These results suggest that the transitions between the normal and the metastable states should be regarded as optically excited defect reactions or configurational changes in complex defects. For instance, Baraff and Schluter (1985) calculated the total energy of a defect, $As_{Ga}+V_{As}$ <---> V_{Ga}, and found As atom is moved with 40% of the nearest neighbor distance due to a stable-metastable transition. Although this defect cannot be directly attributed to EL2, such an atomic shift can no more be in a regime where a harmonic approximation hold. In amorphous materials configurational changes such as changes in bond angle

and length take place by optical excitation or charge-state variation. Similarity in characteristics between amorphous semiconductors and EL2 is further discussed in chapter 4.

2.3.4 Summary of the results on photoquenching effect at the EL2 family

In this chapter the results of the study on transition processes between the normal and the metastable states of the EL2 family in various GaAs crystals has been described. Table 2-2 summarizes the recovery characteristics of the EL2 family from the metastable state to the normal state. It is clearly revealed that the thermal recovery takes place at all the EL2 centers, while EL2-O does not recover by free electron injection and only a limited number of the states show optical recovery. In other words, we observed a large variation in the recovery characteristics among the members of the EL2 family, which is suggestive of an existence of multiplicity in the energy configurations of the normal and the metastable states depending on the crystals.

On the other hand, a variation in the transition from the normal to the metastable states can be seen in the photoquenching spectra. The spectra shown in Fig. 2-5 can be interpreted as convolutions of a Gaussian distribution whose peak is at 1.13eV-1.18eV and an onset above 1.3eV. The latter has a more pronounced variation among the family, while the Gaussian

Table 2-2 Summary of the recovery characteristics from the metastable to the normal states of the EL2 family.

	Thermal	Pulse Injection	Optical
ETX-1,-4	Yes(non-exp. little)	Yes(non-exp.)	10%(non-exp)
EL2(HB, MOCVD)	Yes	Yes	No
EL2-O	Yes(non-exp. little)	No	No

component is rather common to all the EL2 states.

A comparison of the variation among the family in photoquenching with that in recovery characteristics gives an insight into an interpretation of the photoquenching spectra. It is more likely that the onset part above 1.3eV in the photoquenching spectra reflects the direct excitation process from the normal to the metastable state. In the Gaussian part of the spectra, it is suggested that the photoquenching effect takes place through other mechanism than the direct excitation. This point is further discussed in the next chapter.

2.4 Conclusions

In conclusion, a systematic study is carried out on the photoquenching effect at the members of the EL2 family in various GaAs crystals to characterize the transition processes between the normal and the metastable states. In particular the recovery process from the metastable state to the normal state is studied in detail. It is found that EL2-O, the midgap level created by oxygen-implantation and successive annealing to LPE GaAs, has a barrier of 0.41eV for thermal recovery process and that this level exhibits no recovery to the normal state by free electron injection.

The first comprehensive study on the recovery process by optical excitation is carried out on the EL2 family by photocapacitance method. It is found that this recovery occurs only at part (around 10%) of EL2 centers in LEC GaAs crystals. The vertical transition energy for the recovery from the metastable state was determined to be 0.855eV through the measurement of the spectral dependence of the recovery rate. It was further clarified that even the levels which recover optically from the metastable state to the normal state cannot be regarded as a unique level.

It is shown that there is no configuration for the normal and the metastable states, which consistently explain three energies, E_q^o, E_r^{th} and E_r^o, within a configuration coordinate under a harmonic approximation. A model is proposed that photoquenching

be due to a defect reaction in which configuration changes may accompanied.

A large variation in the recovery characteristics indicates existence of a multiplicity in the energy configuration of the normal and the metastable states of the EL2 family. The onset component rather than the Gaussian in the photoquenching spectra is tentatively attributed to the direct excitation process from the normal to the metastable state.

CHAPTER 3 TRANSITIONS VIA EXCITED STATE OF EL2

Abstract

Optical transition mechanisms via the excited state of EL2 is studied by using newly developed Spectral Photocapacitance Transient Analysis (SPTA) technique. It is found that the electrons at the excited state of EL2 have both probabilities of relaxing to the metastable state and to the conduction band. A new CC model for EL2 is proposed in which two excited states are considered with different degrees of lattice relaxation. This model is found to successfully explain the SPTA spectra (coupling to the final states and line shape) as well as the onset of photoquenching rate above 1.3eV. An asymmetric nature of the excited state branches favors the idea of As_{Ga}+As_{Ga} or As_{Ga}+As_I for a key defect structure of EL2. Additional defect should be involved in order to account for the variation in the SPTA spectra for different GaAs crystals.

3.1 Introduction

In 1983 Kaminska et al. (1983) reported the intracenter absorption at EL2. They compared the optical absorption spectrum of EL2 to that of photocurrent in the same photon energy range and found that EL2 has an absorption which does not contribute to photocurrent as shown in Fig. 3-1. Since photocurrent corresponds to photoionization of a deep level (i.e. excitation to the continuum bands), they interpreted the remained portion to be an intracenter absorption from the ground state to the internal excited state of EL2.

The spectrum of intracenter absorption, which has a Gaussian with a peak at 1.18eV, has a striking similarity to that of photoquenching rate. This is the reason why they tentatively attributed the excited state to an intermediate stage of the transition from the normal to the metastable state. They also observed a sharp zero-phonon line (ZPL) at 1.0395 eV accompanied with a series of phonon replica which has an interval of 11meV roughly corresponding to the TA-phonon energy in GaAs.

Uniaxial stress measurement (Kaminska et al. 1985) revealed that the splitting behavior of ZPL absorption follows the theoretical prediction assuming an A_1 to T_2 transition within the tetrahedral symmetry as shown in Fig. 3-2. This transition scheme agrees with an isolated As_{Ga} defect (i.e. an arsenic atom surrounded by four neighboring arsenic atoms) which has a tetrahedral symmetry

(a)

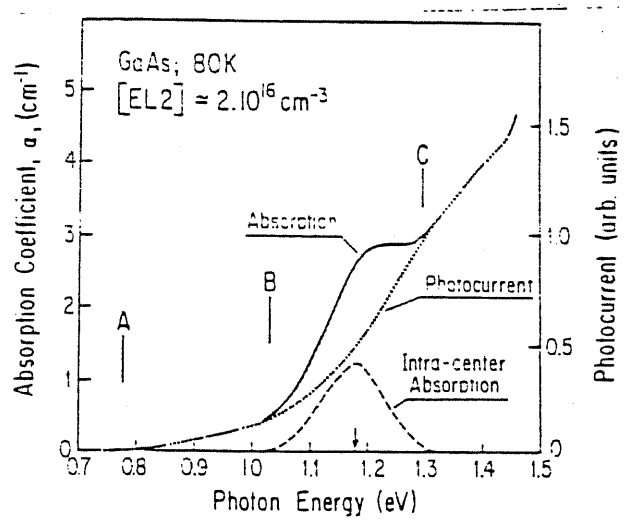

(b)

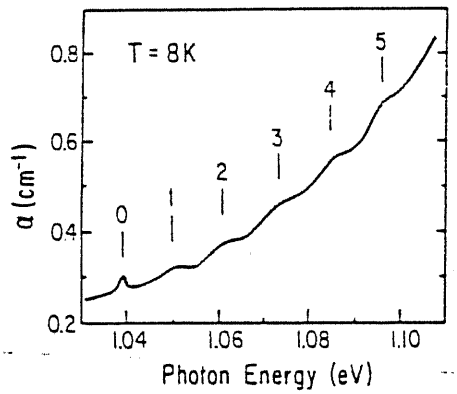

Fig. 3-1 (a) Intracenter absorption spectrum of EL2. (b) Fine structure in the intracenter absorption , which consist of a zero-phonon line at 1.039eV and phonon replica. (After Kaminska et al. 1983).

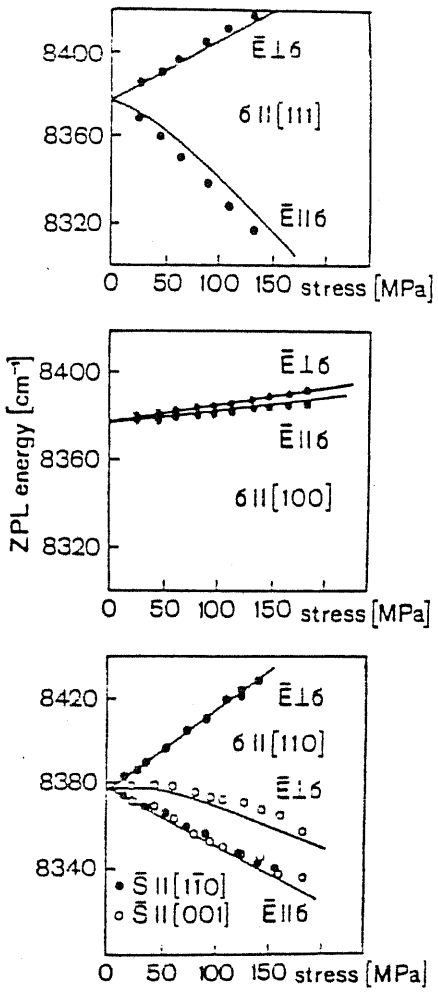

Fig. 3-2 Splitting of ZPL under uniaxial stress. the behavior is well-explained by assuming a transition from the A_1 ground state to a T_2 excited state within T_d symmetry. (After Kaminska et al. 1985).

and has an A_1 state within the bandgap. Based on these results, they concluded that EL2 be an isolated As_{Ga}.

Tsukada et al. (1985b) observed the intracenter transition also in a photocurrent spectrum of SI LEC GaAs. The ZPL and the oscillatory structure were observed similarly to those in an absorption spectrum. They attributed the reason why Kaminska et al missed the structure in photocurrent to be the use of n-type crystals which have large dark current. Tsukada et al. proposed an Auger-like process where the energy emitted by the relaxation from the excited state to the ground state excites electrons, from other deep levels than EL2 to the conduction band. According to their model, the excited state has no other final states than the ground state.

It is very important to know which is the final states that the excited state of EL2 couples to. Although Kaminska et al's result suggests the coupling with the metastable state, it is difficult to obtain the evidence only from the steady state measurements like absorption spectroscopy. (They actually pointed out a discrepancy in the transition cross sections of intracenter absorption and photoquenching.) It is, therefore, of interest to measure the spectral dependence of photoquenching rate in detail.

Such a measurement was actually carried out by Skowronski et al. (1985) who observed an increase in the photocapacitance

quenching rate near the ZPL energy of intracenter absorption. However, their result is preliminary and provides no information on the lower energy side and the phonon replica region. As far as a fine structure is concerned, a conventional photocapacitance measurement does not reveal enough information on the line shape.

In this chapter, a newly developed method (Spectral Photocapacitance Transient Analysis: SPTA) which can obtain a continuous spectrum of photoquenching or photoionization rate is described (Mochizuki and Ikoma 1986a). The result was found to give insight into the optical transition mechanisms at EL2. Based on the experimental results, a new configuration coordinate (CC) model of EL2 is proposed to overcome the inconsistencies arising in the conventional one which has been widely accepted so far. An atomic structure of EL2 is also discussed in terms of the new CC model (Mochizuki and Ikoma 1986b).

3.2 Spectral Photocapacitance Transient Analysis (SPTA)

3.2.1 Principle

In the SPTA measurement, a photocapacitance transient is recorded with very slowly scanning the excitation photon energy. Local derivative of this transient gives a continuous spectrum of photoquenching or photoionization rate (thus, an SPTA spectrum). Either photoquenching or photoionization can be measured by simply changing the photon flux or measured time range.

When an n-type sample (diode) is at low temperature (<<130K) and the photon energy is in the region of photoquenching, the transient of positively photoionized charge, P(t), is approximately written as

$$P(t) = N^{o}[\ \exp(-b_2 t) - \exp(-b_1)\ ] \tag{3-1}$$

here,

$$b_1 = e_n^{o} + e_p^{o} \tag{3-2}$$

$$b_2 = e_*^{o} e_p^{o}/(e_n^{o} + e_p^{o}) \tag{3-3}$$

$$N^{o} = N_T e_n^{o}/(e_n^{o} + e_p^{o}) \tag{3-4}$$

and all the EL2 centers are assumed to be filled before

irradiation as already mentioned in the preceding chapter.

Let us take two types of transients, log[P(t)] and log[N_0-P(t)]. If we neglect the possible non-exponentialities in the transients, derivatives of these transients are

$$\frac{d}{dt}\left(\log[P(t)]\right) = \frac{d}{dt}(\log N^\circ) + \frac{-(b_2 \pm at\frac{db_2}{d\lambda})e^{-b_2 t} + (b_1 \pm at\frac{db_1}{d\lambda})e^{-b_1 t}}{e^{-b_2 t} - e^{-b_1 t}} \qquad (3\text{-}5)$$

and

$$\frac{d}{dt}\left(\log[N^\circ - P(t)]\right) = \frac{d}{dt}(\log N^\circ) + \frac{(b_2 \pm at\frac{db_2}{d\lambda})e^{-b_2 t} - (b_1 \pm at\frac{db_1}{d\lambda})e^{-b_1 t}}{1 - e^{-b_2 t} + e^{-b_1 t}} \qquad (3\text{-}6)$$

Here, the excitation wavelength is assumed to be expressed as $\lambda=\lambda_0$+-a*t, where a is the scanning speed. The first terms are actually expressed as

$$\frac{d}{dt}(\log N^\circ) = \pm a\left(1 - \frac{N^\circ}{N_T}\right)\left(\frac{1}{e_n^\circ}\frac{de_n^\circ}{d\lambda} - \frac{1}{e_p^\circ}\frac{de_p^\circ}{d\lambda}\right) \qquad (3\text{-}7)$$

by using (3-3). (3-5) corresponds to photoquenching, while (3-6) does to photoionization. This is understood more clearly if the photon energy is fixed. In this case (3-5) and (3-6) reduce to

$$\frac{d}{dt}\left(\log[P(t)]\right) = \frac{-b_2 e^{-b_2 t} + b_1 e^{-b_1 t}}{e^{-b_2 t} - e^{-b_1 t}} \qquad (3\text{-}8)$$

and

$$\frac{d}{dt}\left(\log[N^0 - P(t)]\right) = \frac{b_2 e^{-b_2 t} - b_1 e^{-b_1 t}}{1 - e^{-b_2 t} + e^{-b_1 t}} \qquad (3\text{-}9)$$

respectively. They become $-b_1$ at $t \gg \log(b_1/b_2)/(b_1-b_2)$ and $-b_1$ at $1-\exp(-b_2 t) \ll \exp(-b_1 t)$. Although the latter inequality is implicit, it is easily seen that $\exp(-b_2 t)$ is very close to unity at small values of t.

In obtaining SPTA spectra, it is assumed that the slow scanning makes (3-8) and (3-9) hold. This point will be discussed later in this chapter.

3.2.2 Experimental

Experimental setup for measuring photocapacitance transients are almost identical to that already described in Chapter 2. However, capacitance values are digitized and directly stored in a micro-computer, HP-9816, to make the numerical calculation of time derivatives easier. A closed cycle refrigerator using He gas, (an Air Product Displex system), was also employed to

observe fine structures. This system is capable of cooling samples at various temperatures and down to 22K.

Before measuring, samples were heated up to 130K and forward biased at +0.7V. This procedure ensures that all the EL2 centers are in the normal state and filled with electrons. Then they were cooled and reverse biased.

For the measurement of photoionization spectra, a neutral density (ND) filter was used to reduce excitation photon flux to 0.6%. This procedure is in an attempt to make the required condition of $1-\exp(-b_2 t) \ll \exp(-b_1 t)$ hold under the limitation in the sampling rate of the digital multimeter.

A problem arises when a structure is observed in a photoquenching spectrum. Since b_2 consists of photoionization term (the transition from the normal state to the band) and the term for the transition form the normal to the metastable state, it should be examined to which transition the structure be attributed. This difficulty was actually overcome by comparing SPTA spectra for photoionization and for photoquenching in the same energy range because the former consists of only photoionization rates.

The samples studied are an undoped n-type MOCVD GaAs grown on an n^+-substrate and an undoped n-type LEC GaAs. Growth conditions for the MOCVD sample and the carrier concentrations as well as

EL2 concentration for both of them are listed in Table 2-1. It should be noted that, in the MOCVD sample, photoquenching transients at fixed photon energies are purely exponential. This result suggests that EL2 in MOCVD GaAs is a well-defined level, which is in agreement with a previously reported result (Zhu et al. 1981). Furthermore, photoionization at traps other than EL2 was insignificant in the photon energy range where photoquenching occurs.

3.3 Results and Discussions

3.3.1 Features of photoquenching SPTA spectra

(a) Overall spectra

Figure 3-3 shows an SPTA spectrum for photoquenching rate of MOCVD GaAs measured at 22K (the lowest temperature achieved with the present system). This spectrum was obtained by scanning the photon energy from low to high. The whole spectrum is a Gaussian shape whose peak is at 1.18eV with a full width at half maximum (FWHM) of 150meV.

The result is in agreement with the photoquenching rate spectrum obtained by the conventional point-by-point measurement. A slight peak shift to higher energy is due to the temperature dependence as pointed out by Omling et al. (1982). FWHM is smaller than that in a spectrum measured at 77K. This is quite natural again taking into account the temperature difference. The result is also in agreement with the spectral dependence of intracenter absorption measured at 8K (Kaminska et al. 1983).

Additionally, an oscillatory structure is observed in the lower energy region of the peak, which was observed in a spectrum of photoquenching rate for the first time. This result indicates the potential advantage of the continuous measurement, i.e. the SPTA method.

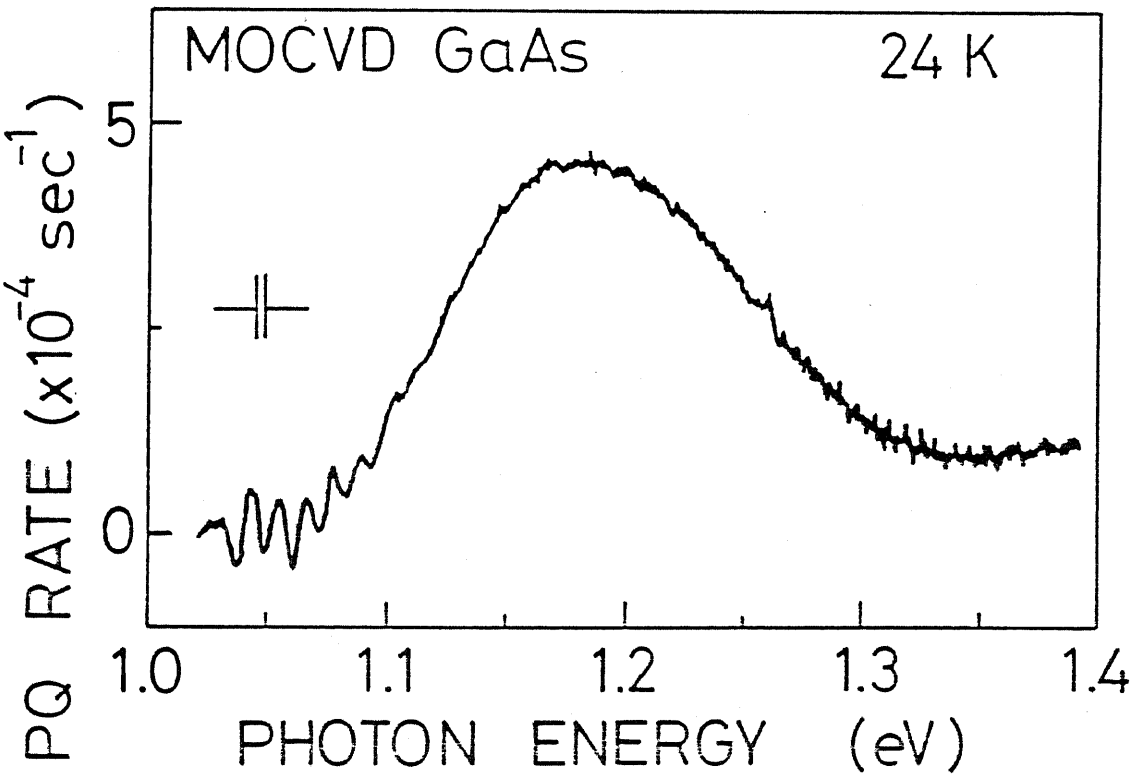

Fig. 3-3 The spectral dependence of photoquenching rate at EL2 in MOCVD GaAs measured by SPTA technique.

(b)Fine Structure

Temperature dependence of the oscillatory part is shown in Fig. 3-4. The structure becomes vague as the temperature is raised and almost difficult to be observed above 62.5K. Energy shift is observed but not significant in this energy range. It is confirmed from this series of measurement that the oscillatory structure is not due to a spurious effect of spectral response of the system. It is reported that the fine structure observed in intracenter absorption is not observed at high temperatures in agreement with the present result.

SPTA spectra for both photoionization (b_1) and photoquenching (b_2) measured in the same photon energy range are shown in Fig. 3-5. It is clear from the figure that the oscillatory structure is not observed in the b_1 spectrum. It is, therefore, concluded that this structure is attributed to the spectral dependence of the optical transition cross section from the normal state to the metastable state of EL2 and not to that in the direct photoionization processes. This result also provides evidence that the structure is not due to the spectral dependence of photon flux reduction which might arise from the fine structure of intracenter absorption at EL2.

The result of a higher resolution measurement is shown in Fig. 3-6. A sharp peak is observed at 1.039eV followed by an

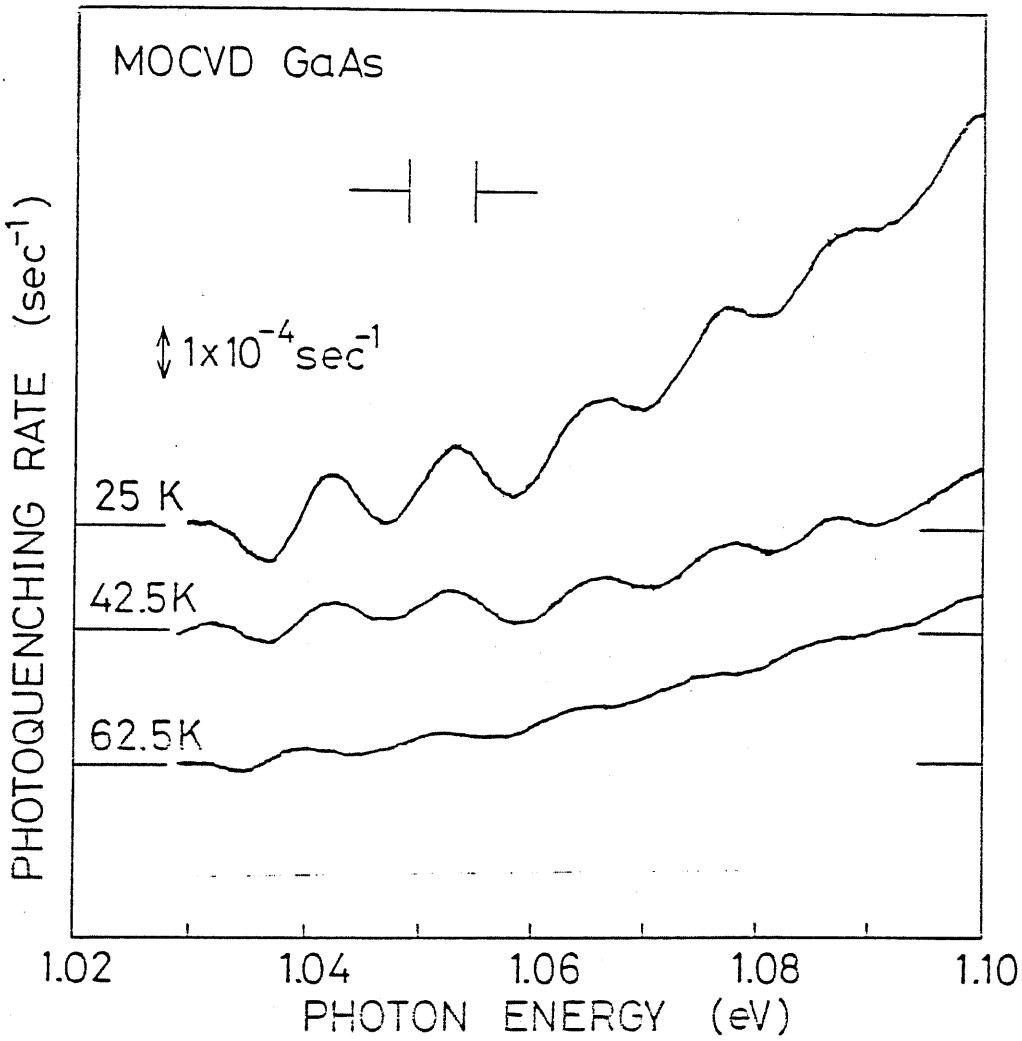

Fig. 3-4 Temperature dependence of the oscillatory spectrum of photoquenching rate of EL2 in MOCVD GaAs.

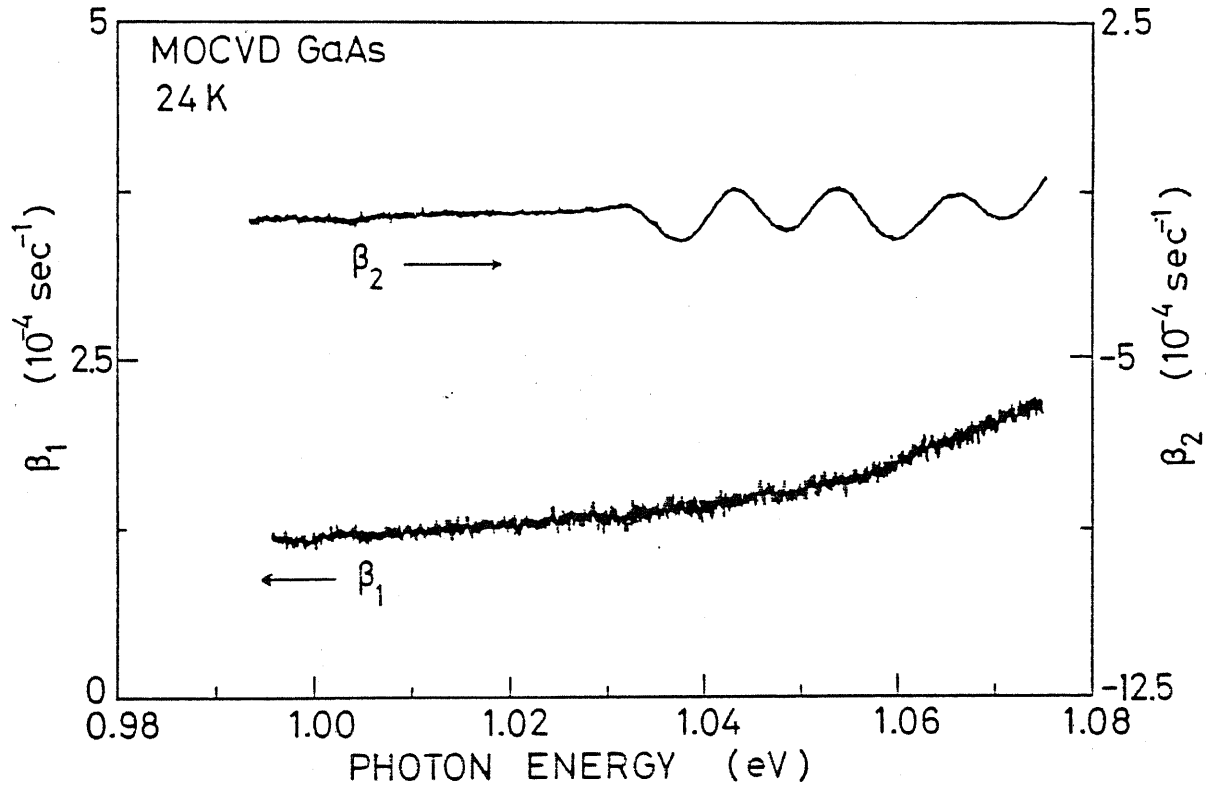

Fig. 3-5 A comparison of SPTA spectra for photoionization rate (b_1) and photoquenching rate (b_2) for EL2 in MOCVD GaAs measured in the same energy range.

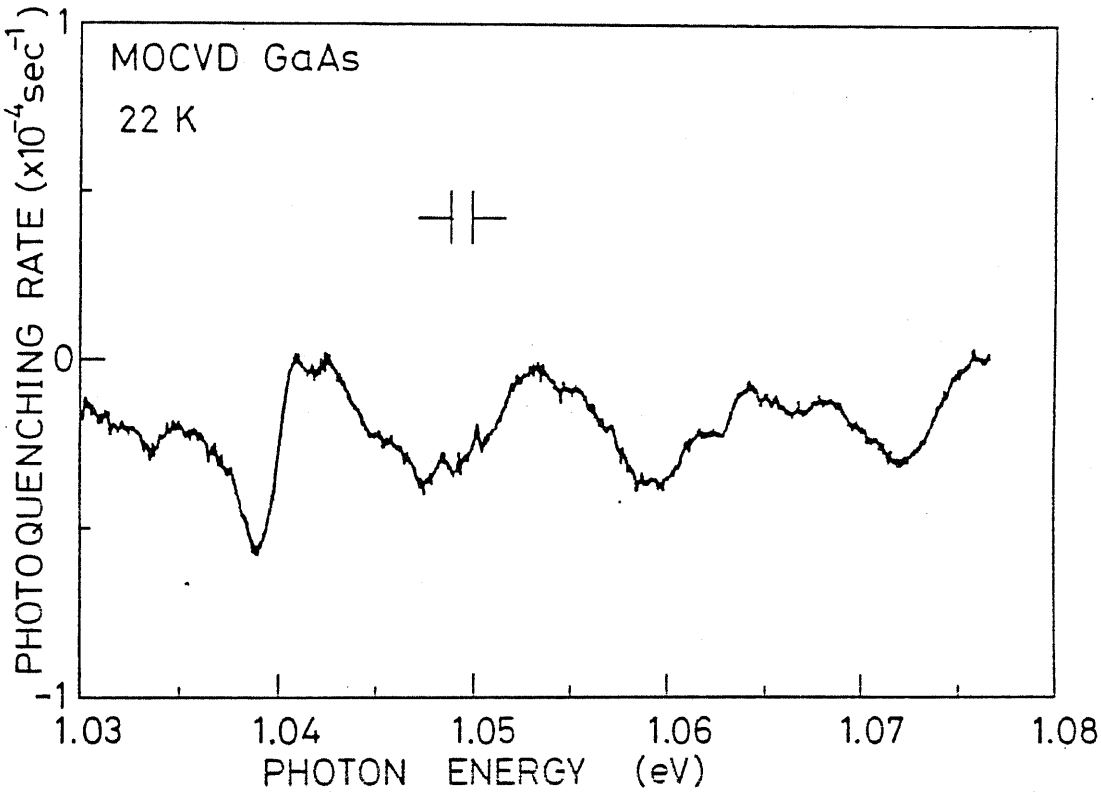

Fig. 3-6 An SPTA spectrum of photoquenching rate measured with a high resolution.

oscillation with an interval of approximately 11meV at the higher energy side. The feature is similar to the fine structures observed in intracenter absorption, where ZPL is at 1.039eV and the interval of phonon replica is 11meV. Therefore, it can be concluded that the zero-phonon transition and its interaction with phonon(s) are also observed from SPTA measurements.

However, additional information of significant importance is obtained from SPTA measurements. The ZPL at 1.039eV is a "valley" in the SPTA spectrum. Since an increase in Fig. 3-6 corresponds to an increasing rate of negative charge or decreasing rate of positive charge within the space charge region, it is concluded that the ZPL transition does not enhance photoquenching (increase of negative charge). This result can be interpreted by assuming that the ZPL transition acts as a path for electrons to relax to the conduction band.

Another feature in Fig. 3-6 that should be noted is that a breakdown in the energy separation of the oscillatory structure. The separation between the ZPL and the first negative peak is 9meV while the others are almost 11meV. Furthermore, each subsidiary peak of ZPL has small dips all of which are not due to noise. These features indicate a difficulty in simply attributing the oscillation to a phonon replica of a single mode of phonon.

3.3.2 Effect of wavelength scanning

In making SPTA measurements, effects of scanning wavelength should be checked. First, a mechanical effect which occurs due to a backlash in a grating was checked using a Kr^+ laser line. The result was that this effect can be neglected even at the highest resolution adopted in the present study.

Another effect that should be checked is the one arising from the term $(db_2/d\lambda)$ in (3-6). In the energy region where the fine structure of b_2 was observed, the absolute value of $(db_2/d\lambda)$ is large. Effect of scanning wavelength was examined in this region by taking SPTA spectra with reversing the scanning direction. This procedure corresponds to changing the sign of the scanning speed, a. The result is shown in Fig. 3-7.

In the figure, each arrow indicates the scanned direction of excitation photon energy:(a) corresponds to "-" and (b) corresponds to "+" in (3-5), respectively. If the effect of $db_2/d\lambda$ is large, then the absolute value of $[t*(db_2/d\lambda)*(d\lambda/dt)]$ should prevail b_2. In such a case, the direction of ZPL is expected to be reversed and its magnitude should change according to the scanning direction. From the figure, however, it is clear that the direction, magnitude and energy position of the ZPL are all unchanged independent of change in the scanning direction. This is the indication that b_2 term is predominant. Energy positions of the oscillatory part, however, change due to scanning direction. The reason why is not clear at present. It

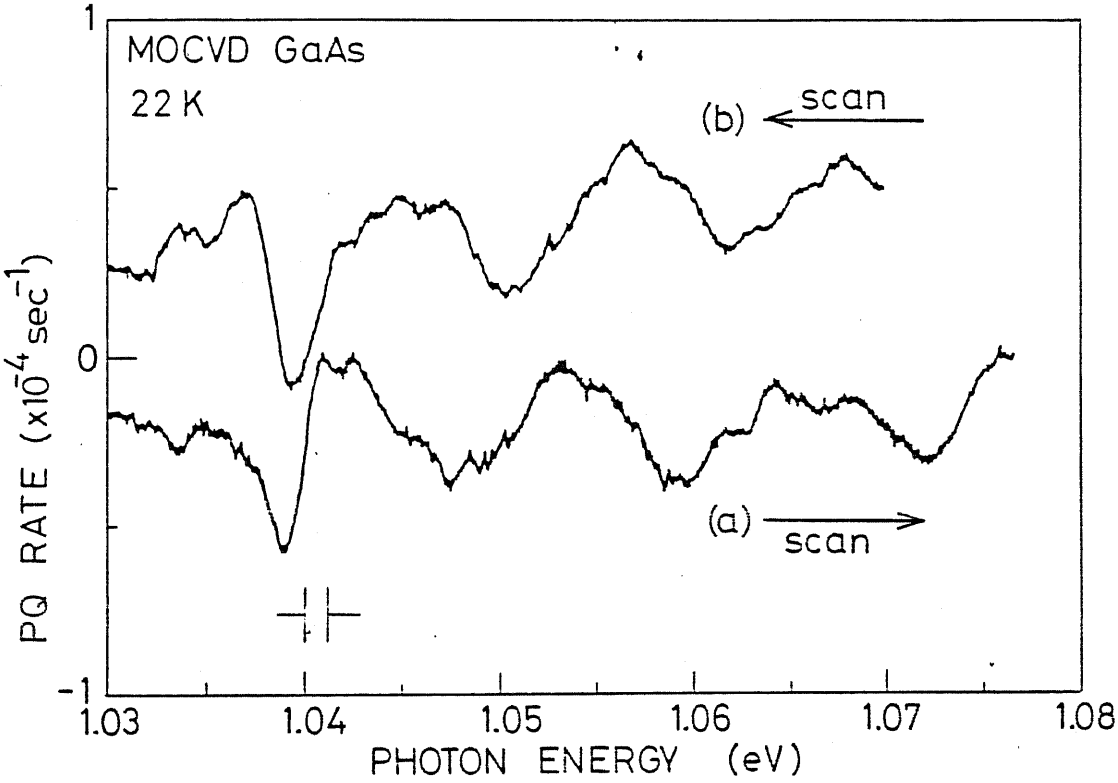

Fig. 3-7 SPTA spectra of photoquenching rate with changing the scanning directions, which are indicated by arrows.

can be speculated that the energy level of the excited state might be shifted due to the difference in occupation.

The first term in the right hand of (3-5), thus (3-7), consists only of photoionization cross sections which have no fine structures. This term, therefore, acts as a dc contribution to Fig. 3-7. Actually, spectra (a) and (b) in Fig. 3-7 have almost the same value with opposite directions in the lower energy side of ZPL as naturally expected. This result gives evidence that we can subtract this dc contribution in obtaining a true b_2 spectrum.

3.3.3 Interpretation of the SPTA spectra

Charge transfer mechanisms at EL2 are discussed in this section. It should be noted that the SPTA spectrum, the photoquenching spectrum and the intracenter absorption spectrum are in principle the same. Therefore, the Gaussian spectrum around 1.1eV is responsible both for the electron transfer to the metastable state and for the steady state excitation to the excited state. Since no transfer to the metastable state takes place during the intracenter absorption measurement, it is not appropriate to attribute the Gaussian spectrum to a direct excitation to the metastable state. Instead, it is naturally concluded that photoquenching should be a two step process; an optical excitation to the excited state followed by a non-radiative relaxation from the excited state to the metastable

state.

This assignment is supported by another fact. The FWHM of the Gaussian spectrum is too narrow to be accounted for with the direct transition from the ground state to the metastable state. In the conventional CC model for EL2, as reproduced in Fig. 3-8, a Franck-Condon shift of the metastable state from the normal state is of the order of 1eV. Using the classical theory for the relationship between a Franck-Condon shift, d_{FC}, and a half-width at low temperature limit, W_0,

$$W_0^2 = 8*\ln 2*d_{FC}*\hbar w \qquad (3\text{-}10)$$

an energy of the relevant phonon, hw, is estimated to be 4.05meV. This value is unusually small and suggests that observed W_0 does not directly correspond to the transition with this value of d_{FC}. Therefore, it is unlikely that this spectral shape reflect an direct optical excitation from the normal state to the metastable state of EL2.

Such an idea of the two step process is in agreement with the previous assignment by Kaminska et al. (1983) that the intracenter absorption does not correspond to the transition to the metastable state but to the excited state which might be the intermediate stage of photoquenching. They pointed out a difference in the optical cross section for photoquenching and for the intracenter absorption. Based on the present scheme,

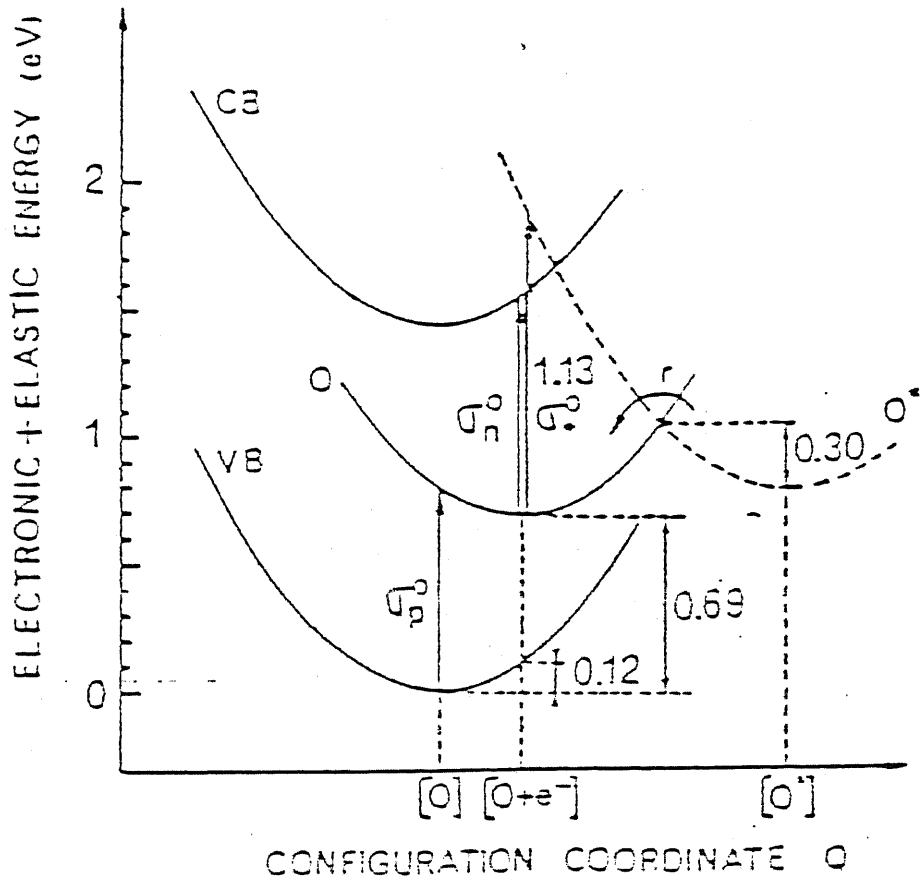

Fig. 3-8 A conventional CC model for EL2 after Vincent et al. (1982).

this difference is explained by assuming that the relaxation from the excited state to the metastable state is much slower than the relaxation to the ground state. In this case, the photoquenching rate (the cross section for photoquenching) is not determined by the transition rate to the excited state but by a product of the relaxation rate from the excited state to the metastable state and a steady state occupation of the excited state. This assumption is not surprising since a lattice relaxation occurs much more slowly than an optical transition.

An advantage is brought about if we regard the onset of the photoquenching rate above 1.3eV (reproduced in Fig. 3-9) as the direct transition to the metastable state. As can be seen, differences among the EL2 family are more remarkable in the energy region above 1.3eV than in the Gaussian peak. Since the recovery characteristics from the metastable to the normal state are different as summarized in Table 2-2, it seems the metastable state can have a variation, which also supports a hypothesis that the scattering in the photoquenching spectra at $h\nu > 1.3$eV is caused by the existence of different metastable states.

Based on this argument, it can be concluded that the Gaussian spectra corresponds to the optical excitation from the ground state to the internal excited state. The lattice relaxation of the excited state can be much smaller than that of the metastable state, which can properly explain the observed line width of the Gaussian. This point will be discussed more in detail later. On

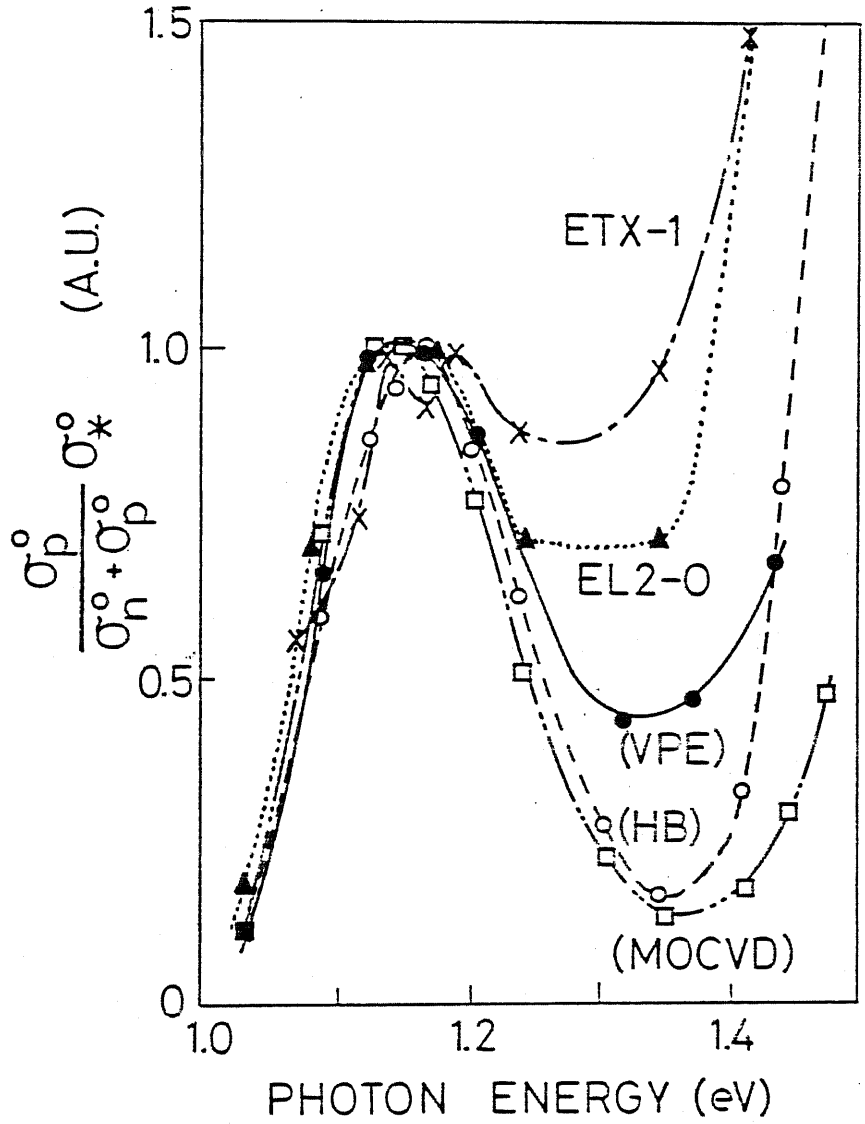

Fig. 3-9 Spectral dependences of photoquenching rate at EL2 family (measured by photocapacitance technique).

the other hand, newly obtained information using SPTA is that the ZPL transition acts as a path for electrons to relax to the conduction band. Since the excited state is apparently involved in this transition, it is also required that the excited state is resonant with the conduction band.

Here, a transition process of the oscillatory part following the ZPL will be discussed. In Fig. 3-10, fine structures observed by three different measuring techniques, SPTA, optical absorption and photocurrent are compared. A nice alignment of ZPL energy is obtained. Furthermore, minima in the SPTA spectrum almost correspond in energy positions to maxima of phonon replica measured by absorption and photocurrent. This result suggests that the ZPL and the following oscillation belong to the same transition process. However, the difference in direction indicates that the transition for this fine structure belongs to a different process which is responsible for the Gaussian spectrum.

Another feature that should be noted is the difference in the magnitudes of the fine structure peaks relative to the main Gaussian peak. According to Skowronski et al., the intensity ratio of ZPL to the Gaussian in the intracenter absorption is 0.03. On the other hand, the relative ZPL intensity in the SPTA spectrum is 0.08 which is more than twice larger. To account for this difference, a difference in the nature of measurements should be considered. An optical absorption is carried out under

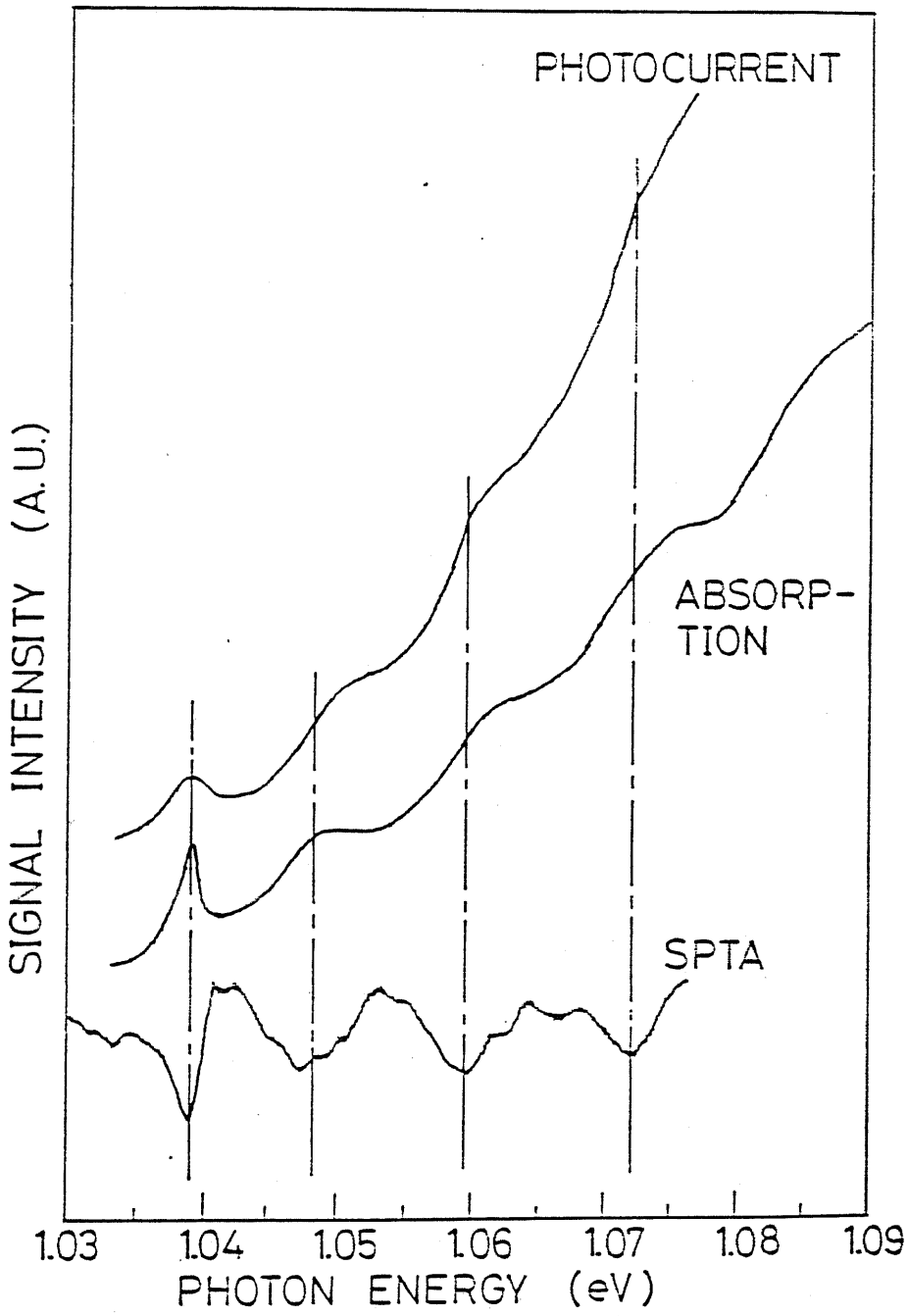

Fig. 3-10 A comparison of the fine structures measured by absorption (Skowronski et al. 1986), photocurrent (Tsukada et al. 1985b) and SPTA.

a steady state condition that no change in the occupation at the normal states (i.e. ground and excited states) occur. However, SPTA directly monitors the rate of occupation change, and therefore, monitors the rate including the relaxation to the final states other than the ground state. The difference in the relative height can be explained by assuming that the fine structure and the Gaussian are associated to different relaxation processes. This conclusion supports the former assignment that electrons excited through the ZPL transition have a probability of relaxing to the conduction band. Furthermore, it is found that the electron transfer to the conduction band is more efficient than that to the metastable state.

Summarizing this section, it is concluded that the Gaussian and the oscillatory structure observed in the absorption and in the SPTA are due to an electron transfer to the excited state of EL2. Electrons at the excited state have two final states other than the ground state; the metastable state and the conduction band. Such an interpretation also supports the idea that the direct excitation to the metastable state takes place, which contributes to the increase of photoquenching rate above 1.3eV. A comparison between the absorption and SPTA spectra indicates that the ZPL and the oscillatory part belong to the same mechanism where electrons are transferred to the conduction band, while the main Gaussian peak does to the process where electrons are transferred to the metastable state via the excited state. The conclusion is illustrated in Fig. 3-11.

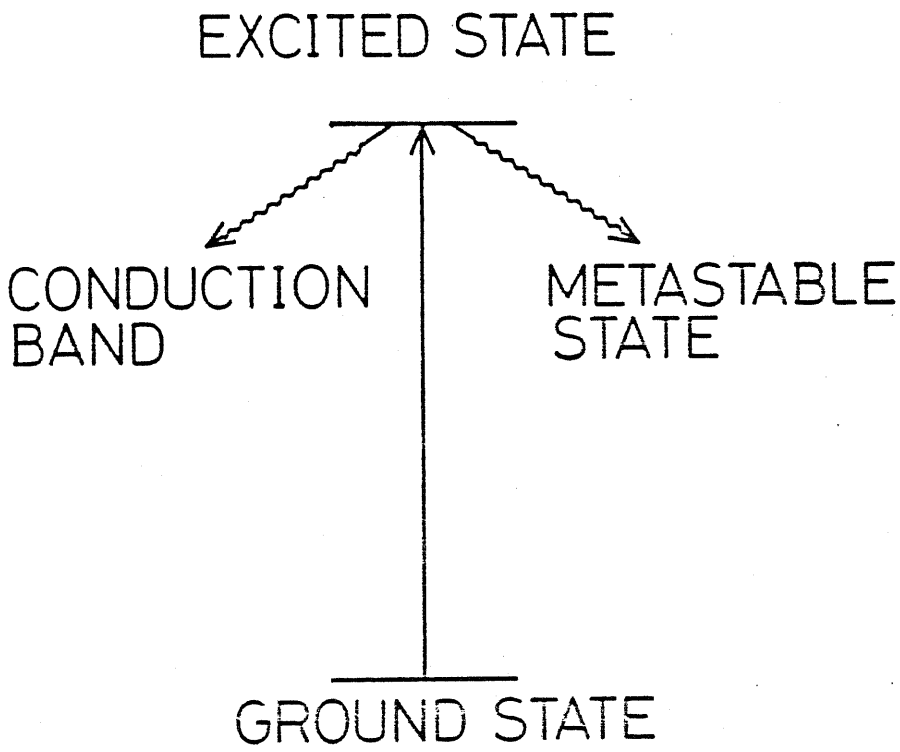

Fig. 3-11 The illustration of the results obtained by the SPTA measurements.

3.3.4 Sample dependence

Study on the family nature of EL2 revealed in SPTA spectra was carried out by comparing results of different GaAs crystals. Figs. 3-12 and 3-13 shows a comparison of SPTA spectra of between MOCVD and LEC GaAs. It has been found that EL2 in LEC GaAs exhibits broader spectra than that of EL2 in MOCVD GaAs. FWHM of overall spectrum for LEC GaAs is 162meV, while it was 150meV for MOCVD GaAs. FWHM of ZPL for LEC GaAs was 3.6meV which is also larger than that for MOCVD GaAs, 1.9meV.

The broadening of the overall photoquenching spectrum in LEC GaAs is consistent with the result obtained from point-by-point photocapacitance measurements, in which a large non-exponentiality was observed indicating a larger variation among the EL2 family in LEC crystals than in MOCVD crystals. Its overall shape is deviated from a Gaussian and again consistent with the previous result that sometimes a double-peak spectrum was observed in LEC GaAs (Taniguchi and Ikoma 1984).

It seems reasonable that the ZPL for LEC GaAs is broader than that for MOCVD GaAs. Such a comparison is very difficult to be made by absorption measurements since a thick epi-sample is hardly obtained. Therefore, this is the first observation of the family nature of EL2 in ZPL spectra. However, it should be pointed out that the ZPL of intracenter absorption reported by Skowronski et al. (1986) (reproduced in Fig. 3-14) is not so

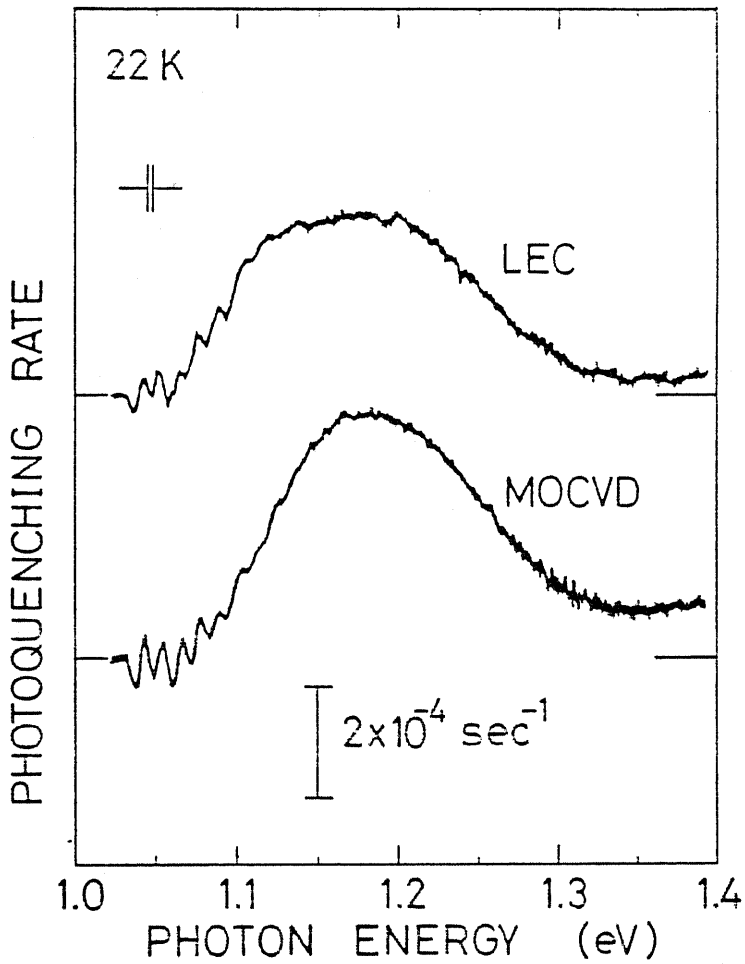

Fig. 3-12 A comparison of SPTA spectra of EL2 in MOCVD and LEC GaAs (Overall spectra).

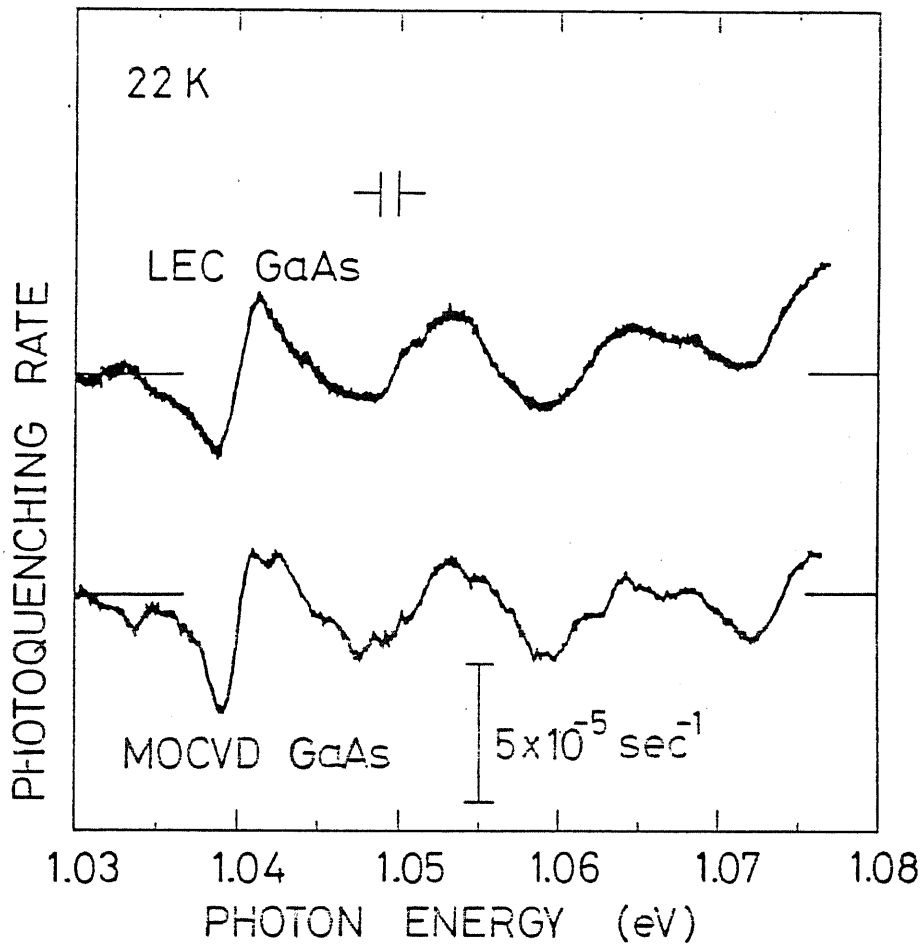

Fig. 3-13 A comparison of SPTA spectra of EL2 in MOCVD and LEC GaAs (Fine structure spectra).

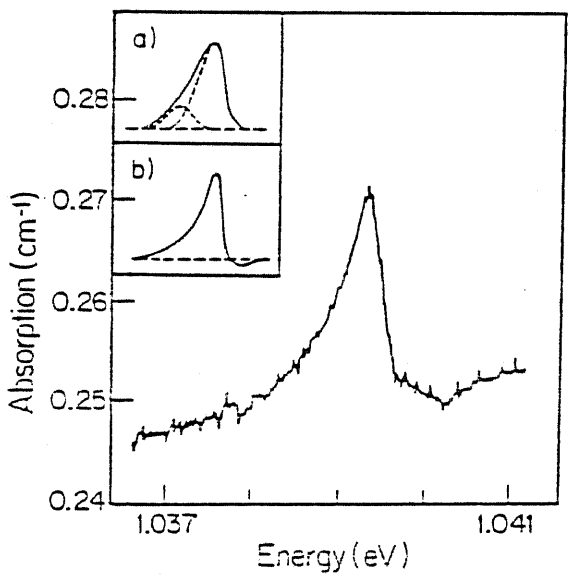

Fig. 3-14 ZPL spectra in intracenter absorption reproduced from Skowronski et al. (1986).

broad as that of SPTA. Although the ZPL spectra of absorption cannot be attributed to a single optical transition line but a convolution of two (or more) lines, the FWHM is much less than the value for the SPTA result.

The reason for this discrepancy is explained as follows. In LEC GaAs, EL2 seems to be a group of defects which have a slight modification in atomic structure among each other. Although the main characteristics such as a ZPL transition to the excited state is unchanged due to a common involvement of a certain defect, a variation in the additional defect may cause a slight change in the energy splitting between the ground and the excited state. Such a scheme is consistent with the larger variation observed in LEC GaAs rather than in MOCVD GaAs. At a more distorted center, transition probability to the excited state should be smaller. A rapid decrease in the probability may give rise to a rather sharp ZPL which has been observed in intracenter absorption. However, the lattice relaxation may also change, which would enhance a probability of electron transfer from the excited state to the conduction band. This enhancement may cause a more pronounced broadening in SPTA spectra, since this method monitors the overall transfer rate to the final state, i.e. to the conduction band.

3.4 A new configuration coordinate (CC) model of EL2

3.4.1 Configuration coordinate model and line shape of an optical transition

Based on the results on optical transition mechanisms of EL2 obtained by SPTA, a new CC model is proposed. First, in this subsection, a treatment of dynamic processes using a configuration coordinate is reviewed to make it easier to understand the following discussions.

Trap energies of a localized state are sometimes different depending on the measurement method. Such an inconsistency is often overcome by assuming a lattice relaxation within a configuration coordinate.

Configuration coordinate can be introduced by adopting an adiabatic approximation (Born-Oppenheimer approximation) in a system where electrons and phonons interact strongly each other. In this approximation, a fast varying system (electrons) and a slowly varying system (lattice) are treated separately. Thus, the lattice displacement is fixed in obtaining the eigen state of electron. The solution for electrons is taken as a potential energy for the Schroedinger equation for the lattice. Usually, the lattice vibration is approximated by a harmonic oscillator and the first term of the electron-phonon interaction, expanded near an equilibrium position of the lattice, is taken into

account. Hereafter, a brief review on the formalism of electron-phonon interaction is made. Next, an optical line shape due to a transition at localized states with lattice relaxation is deduced. For a more complete treatment, see Jaros (1982), for instance.

Let us consider an electron system of conduction electrons and a lattice system near a localized trap level. Let H be the total Hamiltonian. Under one-electron approximation, and assuming a linear coupling at a single configuration coordinate, H can be written as,

$$H = H_e(r) + H_L(Q) + H_{eL}(r,Q) \qquad (3\text{-}11)$$

Here, H_e, H_L and H_{eL} correspond to Hamiltonians for the electron, for the lattice and for the electron-phonon interaction, respectively. Here, it is assumed that the vibronic system can be treated with a dominant single mode expressed by using a configuration coordinate Q. The eigen state L(r,Q) of the Schroedinger equation using H is a product $\varphi(r,Q)*\eta(Q)$ where

$$H_e\varphi(r,0) = E(0)*\varphi(r,0) \qquad (3\text{-}12)$$

is satisfied. Here, E(0) is the electronic contribution to the total energy with the potential at Q=0. It is assumed that the nuclei moves so slowly that electrons have sufficient time to follow the lattice. This adiabatic approximation is probably

quite adequate even in the strong coupling limit provided that the vibrational amplitudes are small enough to prevent level crossing. In the absence of H_{eL}, the electronic and nuclear motions are completely decoupled and the total solution of the Schroedinger equation is $\varphi(r)*\eta(Q)$. H_{eL} describes the change in V(r,Q) as a function of Q. Expanding V(r,Q) around Q=0 gives

$$V(r,0) + Q \left.\frac{\partial V(r,Q)}{\partial Q}\right|_{Q=0} + \cdots\cdots \qquad (3\text{-}13)$$

If only the linear term is retained then

$$H_{eL} = Q \frac{\partial V}{\partial Q} \qquad (3\text{-}14)$$

The total energy of the j-th electronic state in the presence of H_{eL} is, by perturbation theory,

$$e_j(Q) = E_j(0) + Q\left\langle \varphi_j(r) \left| \frac{\partial V}{\partial Q} \right| \varphi_j(r) \right\rangle + \frac{1}{2} k_j Q^2 \qquad (3\text{-}15)$$

where k_j is the force constant. At the equilibrium coordinate the first order term must vanish (harmonic approximation)

$$\left.\frac{\partial e_j}{\partial Q}\right|_{Q_j} = \left\langle \varphi_j \left| \frac{\partial V}{\partial Q} \right| \varphi_j \right\rangle + k_j Q_j = 0 \qquad (3\text{-}16)$$

which defines Q_j in terms of the coupling term. The total energies e_j can be plotted in the usual CC diagram (Fig. 3-15). The The vibrational levels correspond to the oscillator eigen values $(m+1/2)\hbar w_j$ with the oscillator eigenfunctions $\eta_j = \eta_{j,m}$ (m=0, 1, 2, ---). Consider, for the sake of simplicity, two electronic states, j and j', only and set $Q_j=0$ and $Q_j=Q_0$. The transition takes place between the two states $|j,m\rangle$ and $|j',m'\rangle$ is proportional to the square of the dipole matrix element

$$\mathcal{P}^2 \left| \langle \varphi_i \eta_{j,m} | ir | \varphi_{j'} \eta_{j',m'} \rangle \right|^2 = \mathcal{P}^2 \left| \langle \varphi_j | ir | \varphi_{j'} \rangle \right|^2 \left| \langle \eta_{j,m} | \eta_{j',m'} \rangle \right|^2 \qquad (3\text{-}17)$$

Since $Q_0 \neq 0$ there is a finite overlap between the vibrational functions $\eta_{j,m}$ and $\eta_{j',m'}$. The transition probability corresponding to the j--->j' transition consists of a band of lines at transition energies hv connecting any two vibrational states, m and m', in Fig. 3-14, i.e.

$$\sigma^c \sim \mathcal{P}^2 \left| \langle \varphi_j | ir | \varphi_{j'} \rangle \right|^2 \sum_m f_m \sum_{m'} \left| \langle \eta_{j,m} | \eta_{j',m'} \rangle \right|^2$$

$$\times \delta \left[E_0 + (m+\tfrac{1}{2})\hbar w_j - (m'+\tfrac{1}{2})\hbar w_{j'} - h\nu \right] \qquad (3\text{-}18)$$

where f_m is the occupation number of the m-th level. The overlap integral can be evaluated analytically. In the simplest model $k_{j'}=k_j=k$ and the frequencies of both oscillators are the same. Then the coupling between the electronic and nuclear motions depends only on the difference between the equilibrium

coordinate (Q_0). Introducing the Huang-Rhys dimensionless coupling parameter $S=(1/2)kQ_0^2/\hbar w$, one obtains

$$\langle \eta_{j,m} | \eta_{j',m'} \rangle = e^{-S/2} \left(\frac{m!}{m'!}\right)^{1/2} S^{(m'-m)/2} L_m^{m'-m}(S) \qquad (3\text{-}19)$$

where $L_m^{m'-m}(s)$ is the associated Laguerre polynomial. If only the lowest state m=0 is populated significantly (low temperature limit), the result in (3-19) reduces to

$$\left|\langle \eta_{j,m} | \eta_{j',m'} \rangle\right|^2 = e^{-S} S^{m'}/m'! \qquad (3\text{-}20)$$

The vibrational contribution to the optical band (3-19) is shown in Fig. 3-16 for three different values of S. If the phonon energy $\hbar w$ is larger or comparable to the displacement energy $(1/2)kQ_0^2$, that is for S<1 (weak coupling limit), the zero phonon line dominates the vibrational contribution. The spectral lines are well separated by hw and their height decreases rapidly with increasing m. As the strength of coupling increases, the peak due to the ZPL is reduced and the maximum intensity shifts to an energy corresponding to m=S. For S>>1 (strong coupling limit), the vibrational spectrum approaches the bell-like shape resembling the Gaussian distribution. One expects many short-wavelength phonons to contribute and the result is a smooth broad band. Experimentally, the strength of coupling can be evaluated from the Stokes shift, $2d_{FC}$, between absorption and emission.

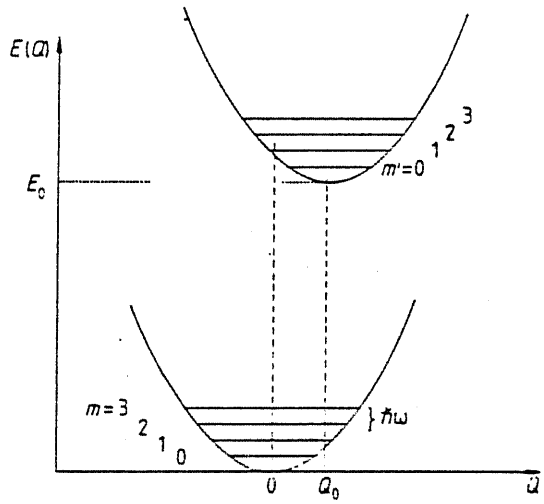

Fig. 3-15 Configuration coordinate diagram for two electronic levels j and j' as a function of the lattice coordinate Q. E_0 is the zero-phonon transition energy.

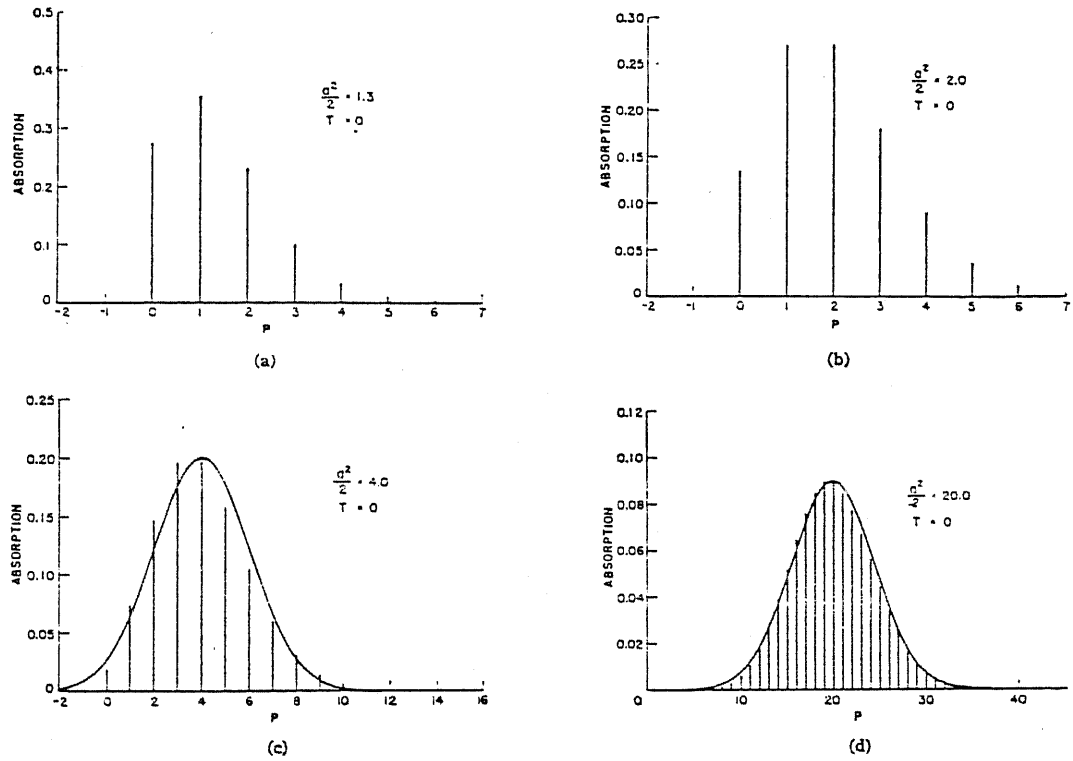

Fig. 3-16 The line shape due to a linear mode at T=0 for four values of S. The energy coordinate is P=(E-E_{ab}-Shw)/hw, where E_{ab} and hw are energy difference of two levels at no displacement and the phonon energy, respectively. (After Keil 1965).

Franck-Condon shift d_{FC} is a product of S and hw as can be easily understood from Fig. 3-15. In order to uniquely determine S and hw, additional information is necessary usually obtained through temperature dependence measurements of a line width.

3.4.2 Problems in the Conventional CC model for EL2

The CC model for EL2 has to account for the experimental results so far obtained. For the purpose of making discussions, they are summarized first as follows:

(i) The spectral dependence of photoquenching rate is a Gaussian whose peak is at 1.18 eV and FWHM is 150meV at low temperatures.

(ii) Photoquenching rate increases at higher energy region than 1.3eV.

(iii) The ground state of EL2 is located at 0.74eV below the conduction band and has an energy barrier of 80meV in the electron capture process.

(iv) An activation energy of 0.3eV exists in the thermal recovery process from the metastable to the normal state.

(v) The excited state of EL2 couples both with the metastable state and with the conduction band. (The result of SPTA)

So far, a CC model proposed by Vincent et al. (1982) has been widely accepted, which was in an attempt to account for their results on the photoquenching effect of EL2. In this model

photoquenching is considered to be a direct excitation from the normal state to the metastable state. However, several inconsistencies arise in this CC model.

First, it should be pointed out that energy levels of the normal and the metastable states are very close to each other. Therefore, it becomes rather sensitive to the transition energy determined by experiments, which of these states is lower in energy. Sometimes the metastable state is lower than the normal state, especially when a photoquenching spectrum is measured at rather high temperatures (liquid nitrogen temperature, for instance) at which the peak photon energy of the Gaussian is lower than that at the low temperature limit region. This result claims a strange conclusion that the metastable state should be more stable than the normal state and preferentially occupied at thermal equilibrium. This is contradictory to the fact that the metastable state is no more stably occupied (or exist) at higher temperatures than 130K.

Furthermore, this simple CC diagram provides no explanation on the observation (i) and (v). The conventional scheme brings a further inconsistency on the line width of photoquenching spectra and the expected d_{FC} as already mentioned in Section 3.3.3. These inconsistencies are mainly due to the oversimlpification of the transition scheme where the contribution of the excited state is not considered.

3.4.3 A new CC model for EL2

A new CC model for EL2 proposed in the present study is shown in Fig. 3-17. In this model photoquenching is considered as a two step process. First an electron is excited from the ground state to the normal state, and then relaxes to the metastable state by emitting phonons. The main feature of this model is the association of two excited states, Ex1 and Ex2, for EL2 with an asymmetric configuration. An involvement of two excited states is a consequence of the following argument.

First, the position of the excited state which couples with the metastable state is determined from the experimentally obtained Franck-Condon shift of approximately 0.14eV. However, only with this excited state branch, there still remain two inconsistencies. One is that the branch Ex2 has no configuration which satisfies (v). It may appear that the level crossing of the metastable state and Ex2 branches in the resonance region with the conduction band be a solution. However, in such a case, one finds that the re-excitation from the metastable state to the conduction band occurs by photons with smaller energies than bandgap and that the metastable state is no more "metastable".

The other one is concerned with the line shape. A simultaneous appearance of a well resolved ZPL and a broad Gaussian is hardly explained by assuming only a single transition since they are in a complementary relationship according to S as described in

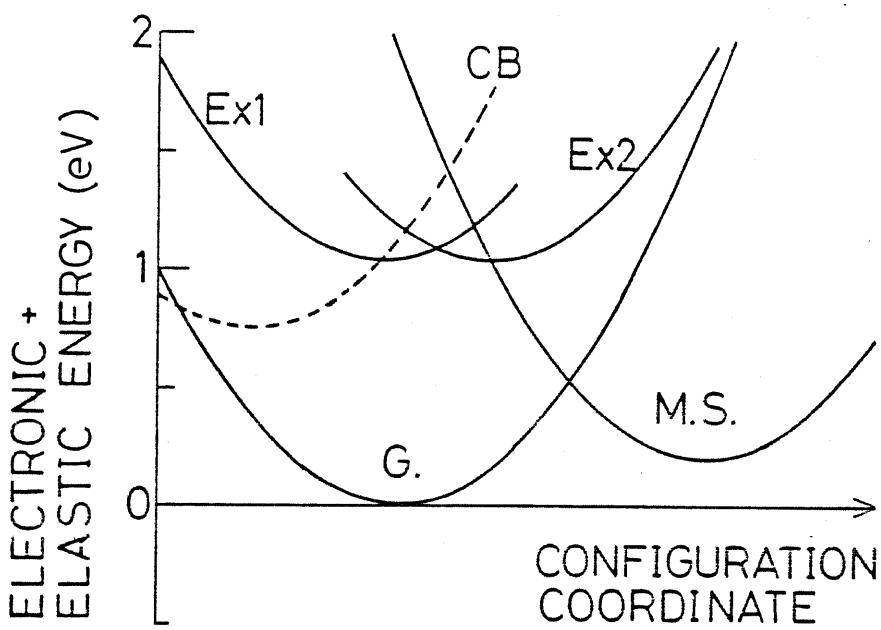

Fig. 3-17 A new CC model for EL2, which has two excited states (Ex1 and Ex2). G., M.S. and CB represent the ground state, the metastable state and the conduction band, respectively.

3.4.1. Since the Gaussian part is well described by assuming a reasonable value of S=33 for Ex2, we have to assume another transition process with a smaller S. In this case, the phonon energy for Ex2 is no more required to be 11meV which has been determined by the fine structure spectrum although the figure is simply written with a single configuration coordinate.

In order to overcome these inconsistencies, the second excited state branch, Ex1, was introduced which is resonant with the conduction band. Energy level of Ex1 is determined to be 1.039eV above the ground state using the ZPL energy in the SPTA spectrum. It is not possible to uniquely determine S of Ex1 even we know that $\hbar w$ is likely to be 11meV. It is, however, possible to know the smallest limit of S using the limiting condition that Ex1 is resonant with the conduction band. Such an S can be actually obtained by calculating the Ex1 branch whose stable point just crosses the conduction band edge. The value of thus evaluated smallest S is 0.53 if the phonon energy is assumed to be 11meV. The $1/2\hbar W$ term in the vibronic energy was neglected because an accuracy to such an extent is no more expected due to a level crossing. However, at least, this result means that S can be considerably smaller than 1 and is consistent with the experimental result that the well resolved ZPL and phonon replica are observed.

These two branches of Ex1 and Ex2 can, in principle, account for the line shape of SPTA spectrum as well as intracenter

absorption. However, there still remain a problem on the line shape of the fine structure. The position of Ex1 relative to the ground state gives a certain S, which simultaneously determines the relative intensities among m-th peaks. A comparison is made in Fig. 3-18 where the fine structure part of the SPTA spectrum and normalized envelope functions calculated from (3-20) with assuming several S are shown. It is readily seen that no choice of S gives even a qualitative agreement. It is because of the dominant intensity of ZPL and a long lasting phonon replica, while the theory predicts a rapid decrease when S is small and a ZPL dominates. A breakdown in the energy separation, 9meV between the ZPL and the neighboring negative peak instead of other separations of 11meV, also questions the attribution of the whole fine structure to a single series of transitions. The reason for the problem might be a contribution of other phonons than a symmetrical breathing mode. As far as we insist on the simple configuration coordinate theory, the fine structure should be considered to originate from two excited states, tentatively labeled as Ex1-a and Ex1-b (not shown in Fig. 3-17). Ex1-a is 1.039eV above the ground state and is resonant with the conduction band with a very small S, while Ex1-b has a larger S than that for Ex1-a and couple with phonons whose energy is 11meV. Such a scheme might also account for the asymmetrical shape of ZPL of intracenter absorption (Skowronski et al. 1986).

In the new CC model, the increase in photoquenching rate above 1.3eV is tentatively attributed to the tail of the direct

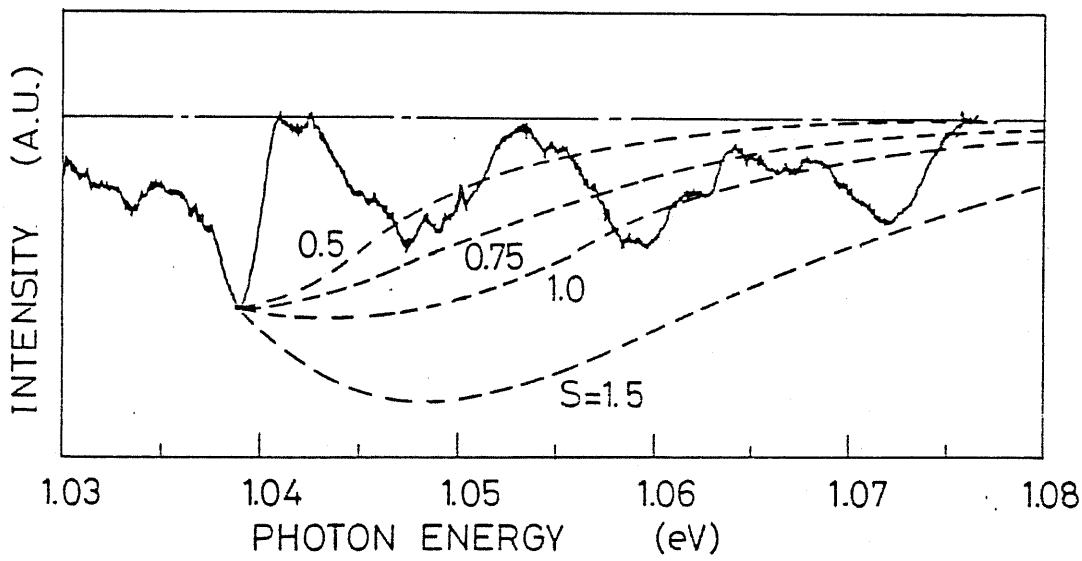

Fig. 3-18 Comaprison of the SPTA spectum and the envelopes of transition intensities assuming S=1.5, 1.0, 0.75 and 0.5.

transition to the metastable state, which is expected to be centered around 1.9eV. As discussed in the previous chapter, it is likely that an expansion of the electron-phonon interaction term only to the first order is no more a good approximation in such a largely displaced regime and that the direct transition process shows a variation among the EL2 family.

3.4.5 On the atomic structure of EL2

The zero phonon transition to the excited state has been found to belong to A_1 ---> T_2 transition at a center with T_d symmetry (Kaminska et al. 1985). This fact indicates an involvement of As_{Ga} in the EL2 center. A CC model has been proposed by Baranowski et al. (1985) in which a metastability is predicted at an isolated As_{Ga}. However, a theory predicted only a small lattice relaxation at an isolated As_{Ga} (Bachelet and Scheffler 1985). Further, a recent total energy calculation by Bar-Yam and Joannopoulos (1986) finds no metastable point assuming an isolated As_{Ga} and this conclusion has come to be more widely accepted. Actually, the CC diagram proposed in this study is not in accordance with the scheme by Baranowski et al. especially on the shape of the excited state.

It is interesting to note that the Ex1 branch has almost no relaxation relative to the ground state, while the metastable state and the Ex2 branch are rather largely displaced. The former suggests an involvement of a defect with a rigid structure

such as As_{Ga}. while the latter a defect with a soft bonding which can be displaced easily. This scheme, therefore, gives an insight that the key characteristics EL2 is determined by a complex of two point defects in which As_{Ga} may be involved.

Figielski et al. (1985) proposed an $(As_{Ga})_2$ molecule for the origin of EL2. They successfully predicted a metastability and the existence of an internal excited state with nearly T_d symmetry as well as an ESR-active center and recovery from the metastable state by electron injection, According to their model, the transition from the normal to the metastable state takes place via the excited state through a Jahn-Teller instability. However, their shape for the excited state is symmetrical relative to the ground state and not in agreement with that for the excited state obtained in the present study.

The present CC model is rather in agreement with that by Baraff and Schluter (1985), who predicted the dual minima in the excited state of the "actuator defect", V_{Ga} <----> $As_{Ga}+V_{As}$. Therefore, EL2 is more likely to be a defect involving As_{Ga}. As a counterpart of the As_{Ga}-complex, As_I is another candidate. Although atomic structure of EL2 will be discussed in another chapter, it should be pointed out here that a metastability at $As_{Ga}+As_I$ has been also predicted mainly due to the configuration change by a Coulombic interaction (Schluter and Baraff 1986, Bardeleben et al. 1986a).

The present results of SPTA claim that a complex defect like $As_{Ga}+V_{As}$ or $As_{Ga}+As_{I}$ should be the key structure of EL2. However, a variation in the SPTA spectra observed in LEC GaAs should be noted. Such a variation indicates an involvement of the third (or more) defect in EL2, which slightly changes the characteristics to form a family of traps, the EL2 family.

3.5 Conclusions

A new method called Spectral Photocapacitance Transient Analysis (SPTA) is developed and is found to be useful for the characterization of electron transitions at EL2. SPTA revealed a new result that the excited state of EL2 couples both with the metastable state and with the conduction band. Optical transition mechanisms via the excited state of EL2 is studied based on the results obtained by SPTA. A new CC model for EL2 is proposed in which two excited states are considered with different degrees of lattice relaxation to account for the SPTA spectrum. This CC model can successfully explain the SPTA spectra (coupling to the final states and line shape) as well as the onset of photoquenching rate above 1.3eV. An asymmetric nature of the excited state branches favors the idea of $As_{Ga}+V_{As}$ or $As_{Ga}+As_{I}$ for a key defect structure of EL2. Additional defect should be involved in order to account for the variation in the SPTA spectra for different GaAs crystals.

CHAPTER 4 PROCESS DEPENDENCE AND ATOMIC STRUCTURE OF EL2

Abstract

Atomic structure of EL2 is discussed based on the study of its change under damage which is introduced by device processes such as sputtering and reactive ion etching, together with the results described in the previous chapters. It is shown that EL2 has a mobile defect specie in its atomic structure like As_I. The family nature of EL2 suggests that EL2 family originates from amorphous arsenic clusters formed by reaction of excess arsenic atoms in the form of As_I.

4.1 Introduction

There has been growing evidence that EL2 is related to excess arsenic atoms in GaAs crystals. Especially, magnetic resonance measurements keep presenting a detailed information on the defect structure of As_{Ga}. First, these studies are surveyed in the following section to provide a perspective on the present status of defect identification in GaAs.

It is known that annealing study also provides information on the defect structure. Change of EL2 under sputtering and low temperature annealing is studied. The effect of another process induced damage by reactive ion etching (RIE) is also studied. Based on the experiments, atomic species which contribute in the formation of EL2 are discussed.

Finally, validity of the As-cluster model of the atomic structure for the EL2 family is discussed together with models proposed by other researchers so far.

4.2 Correlation of EL2 and excess arsenic defects

Simple point defects related to excess arsenic atoms in GaAs are As_{Ga} (antisite arsenic), V_{Ga} (gallium vacancy) and As_I (interstitial arsenic). As_{Ga} was first identified by Wagner et al. (1980) by submillimeter ESR measurements. They observed an isotropic quadruplet as reproduced in Fig. 4-1. This quadruplet is due to a hyperfine interaction of the unpaired electron with a host nuclei with a nuclear spin 3/2. After excluding the possibilities of Cu and Ga, they attributed the signal to be due to As surrounded by four neighboring As atoms. Their identification was based on the coincidence of the hyperfine constant with that of PP_4 (P_{Ga}) in GaP. Although no ligand-hyperfine splitting was observed, Worner et al. (1982) reconstructed the broad signal of the quadruplet assuming theoretically expected 13 ligand lines. It should be pointed out, however, that such an identification still leaves two possibilities; As_{Ga} and a tetrahedral As_I surrounded by four As atoms. These two defects has a difference in the electronic states which appears in the bandgap: A_1 ground state for As_{Ga} and T_2 state for As_I are expected from theory (Vigneron et al. 1983). The first exclusive identification was made by Meyer et al. (1984) from the MCD (magnetic circular dichromism) measurement, in which they found a large spin-orbit splitting in the excited state and found that the resultant ground state should belong to A_1.

After the oxygen-related model for EL2 was denied (Huber et al. 1979), a correlation of As_{Ga} with EL2 has come to be studied

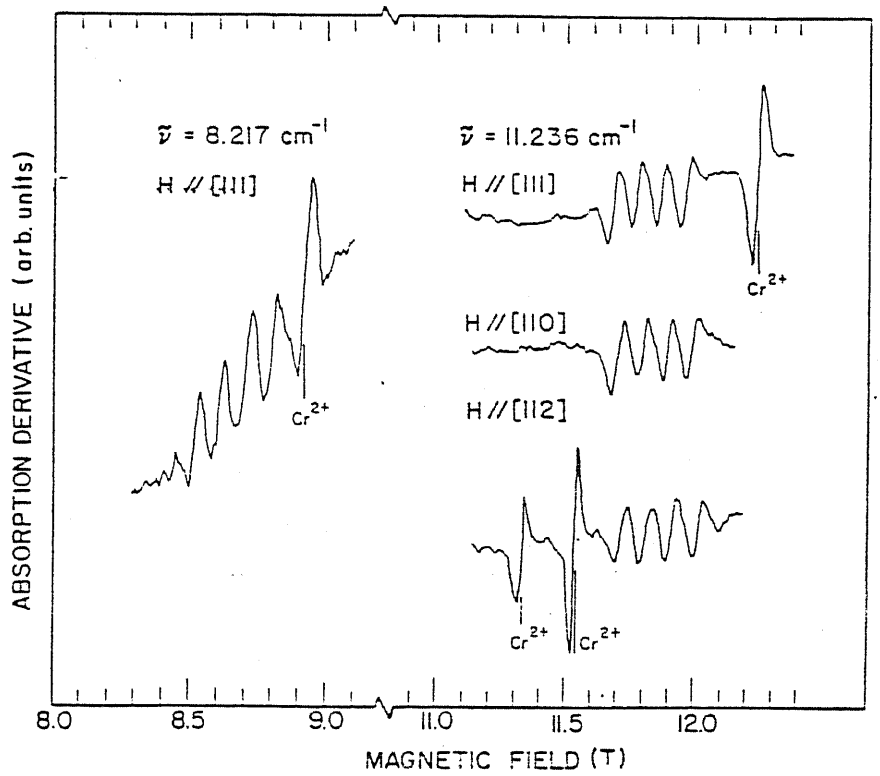

Fig. 4-1 ESR spectra of the isotropic quadruplet, As_{Ga}, in GaAs. (After Wagner et al. 1980)

intensively. Weber et al. (1982) measured the ESR signal of a plastically deformed GaAs under optical excitation. They found that the As_{Ga} defect has two energy levels in the gap; E_c-0.75eV and E_v+0.50eV. The former is in good agreement with the energy level of EL2. They also observed photoquenching of the ESR signal. Photoquenching was also observed for As_{Ga} in as-grown GaAs crystals (Baeumler et al. 1985, Meyer and Spaeth 1985) Recently, Tsukada et al. (1985a) explained the photo-ESR signal using the values of optical ionization cross sections of EL2. A correlation in concentration has been also studied. Elliot et al. (1984) found a positive correlation between EL2 concentration determined by 1um absorption coefficient and As_{Ga} concentration and concluded that EL2 is the first ionization level of As_{Ga}. However, it should be pointed out that As_{Ga} can be measured in a singly ionized state As_{Ga}^{+} while the transition of EL2 to the metastable state occurs at a neutral charge state. In a semi-insulating crystal, a change in As_{Ga} might be caused by a change in Fermi-level due to the metastable transition of EL2.

All these results support the idea that EL2 be the As_{Ga} defect. However, some recent results question such an assignment. Meyer et al. (1984) showed that As_{Ga} and EL2 have different photoionization cross section and concentration. They further found a difference in the minimum excitation power at which photoquenching takes place. An ODENDOR measurement revealed the existence of distorted As_{Ga} together with undistorted isolated As_{Ga} (Hofmann et al. 1984). It should also be noted that there are two types As_{Ga} centers one

of which has a short spin-lattice relaxation time and the other has a longer one by five orders of magnitude. Actually, it has been pointed out (Weber and Omling 1985) that the broad ESR signal which disturbs the ligand-hyperfine lines is not due to a large number of split lines but also due to the existence of distorted centers. The centers which has a short spin-lattice relaxation time is considered to be a complex in which As_{Ga} is involved because formation of a complex may reduce the spin-lattice relaxation time by mixing of the wavefunctions, while an isolated As_{Ga} has a long one due to the A_1 nature of the wavefunction. The existence of a family of As_{Ga} has also shown clearly in the annealing characteristics of As_{Ga} signals in various GaAs crystals as summarized in Fig. 4-2 (Weber 1984).

Observation of As_I defect was made by Fujimoto (1984) from x-ray quasi-forbidden reflection measurements. According to his result, the number of As_I in bulk GaAs crystals amounted to the order of 10^{18} cm^{-3}. Gant et al. (1984) observed the existence of excess arsenic atoms, probably in the form of As_I, by monitoring Auger-electron spectra of cleaved bulk GaAs crystals. Spaeth (1986) found a complex defect, As_{Ga}+As_I, from an ODENDOR measurement and a fitting using a spin Hamiltonian. The result of photo-ODENDOR revealed the energy level of this defect, which is in agreement with that of EL2.

V_{Ga} has been also identified. The first observation of V_{Ga} was made by Goltzene et al. (1983). They deconvoluted a singlet

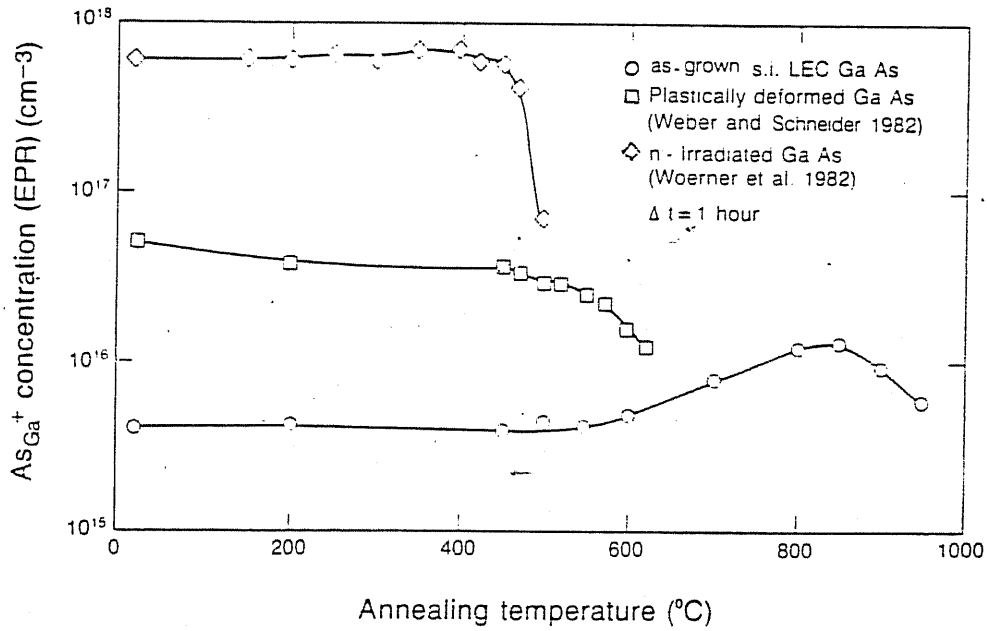

Fig. 4-2 Annealing characteristics of As_{Ga} measured by ESR for as-grown, plastically deformed and n^{O}-irradiated GaAs crystals. (After Weber, 1985).

component from the quadruplet ESR signal in neutron irradiated GaAs and found that this component has a different temperature dependence than As_{Ga}. It has also been reported that the introduction rate of the singlet is not saturated up to the neutron dose of 10^{20} cm^{-2}, while the quadruplet saturates at $2x10^{18}$ cm^{-2} (Beall et al. 1986). Tsukada et al. (1985a) found a peculiar behavior under the condition where the quadruplet is photoquenched. They found that the the singlet in as-grown LEC GaAs signal gradually increases in the time scale longer than that of quenching of the quadruplet. These results suggest that this singlet defect, tentatively attributed to V_{Ga}, are unlikely to be associated with the quadruplet, As_{Ga}. On the other hand, Bardeleben et al. (1986b) showed that the singlet component in electron beam-irradiated GaAs can be well explained assuming an V_{As} which exists in the form of a complex, $As_{Ga}As_4V_{As}$. However, they found no metastability in the singlet defect and what they observed may be different from those observed in the neutron-irradiated materials.

4.3 Change of EL2 by sputtering damage

Changes in concentration and trap parameters of EL2 due to a sputtering damage during Schottky-electrode formation were studied. The metal used was WSi_x (tungsten silicide). Since WSi_x is resistant to high temperature annealing, characterization can be carried out at an identical dot, and thus, an ambiguity caused by a spatial variation can be eliminated.

4.3.1 Experimental

The crystal used was undoped HB GaAs with an electron concentration of $2\text{-}3\times10^{16}$ cm^{-3}. Ohmic contact was formed on the backside by a deposition of InSn followed by alloying. Then the surface was chemically etched with a solution $H_2SO_4:H_2O_2:H_2O=8:1:1$ before Schottky metal deposition. WSi_x or Au Schottky electrode was deposited by RF sputtering. W and Si were co-sputtered from a tungsten target on which slices of crystalline Si were placed to make a composition, x, to be about 0.6. The target was sputtered by Ar plasma at a pressure of 40 mTorr. Two types of WSi_x deposition were carried out. One was done at an RF power of 80W for 30min. The other consisted of two steps: the first deposition at 10W for 10min and the next one at 80W for 30min. In the latter case, it was intended to reduce the damage by sputtering at a low input power during the interface formation. For comparison, a Au-Schottky diode was also fabricated by a vacuum evaporation, in which process no damage is

considered to be introduced.

Characterization of EL2 was performed by DLTS measurement (Lang, 1974). Trap concentration was calculated with a so called "lambda" correction (Zohta and Watanabe, 1982), in which $E_C-E_T=0.75eV$ was adopted.

After the characterization at the as-deposited state, 10W-sample underwent an isochronal annealing for 15min. Annealing was done at 324C and 524C with a H_2 atmosphere.

4.3.2 Results

(1)Dependence on the sputtering power

DLTS spectra for surface regions, bias condition of 0V/-1V, of the as-deposited samples are shown in Fig. 4-3. The sampling gate t_1 and t_2 in the figure are 256ms and 512ms, respectively. The Au Schottky sample is for reference, which was fabricated by vacuum evaporation. Major traps detected have peaks at 150K, 220k and 335K (for the Au case). They can be identified as EL6, EL3 and EL2, respectively. EL6 and EL3 commonly exist in HB GaAs. Their origins are not known but can be speculated to be native defects. When an electrode is sputtered at 80W, another peak (ED5) appeared around 260K for both WSi_x and Au cases. The thermal emission property of this level, $E_a=0.52eV$ and $\sigma=3\times10^{-15}cm^2$, is similar to that of P2 level, which was detected by Pons et al. (1980) in electron beam irradiated GaAs. Concentration of this level rapidly

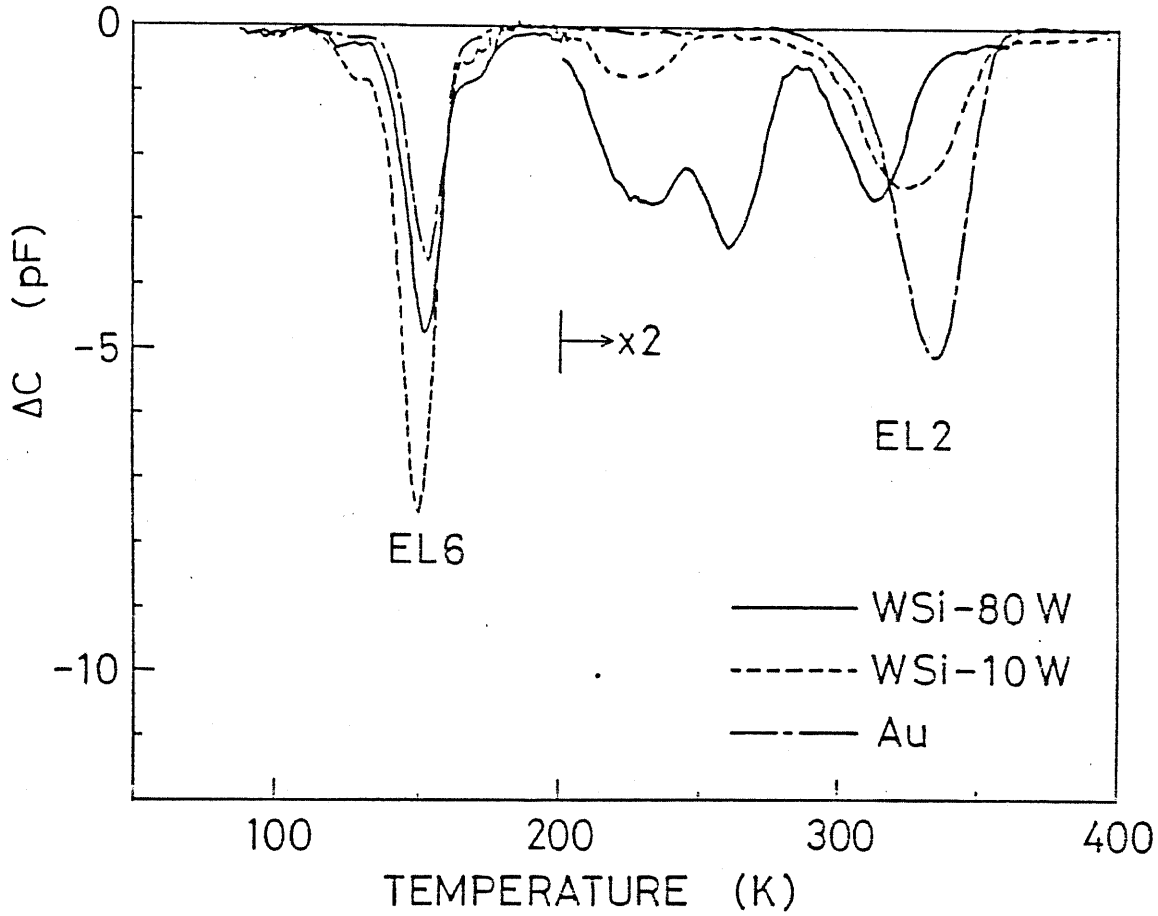

Fig. 4-3 DLTS spectra for WSi_x-Schottky diodes fabricated by RF sputtering with input power of 10W (WSi-10W) and 80W (Wsi-80W). The spectrum for a Au-evaporated sample (Au) is also shown. (t1, t2) is (256, 512)ms.

decreases and no more detected in the region deeper than 0.2um from the surface or after 300C annealing (Ogiwara et al. 1984). These facts suggest that ED5 is related to the native sputtering-induced defect.

A large variety in the EL2 property was observed due to sputtering. The density decreased and the peak shifted to lower temperatures. A larger shift is observed for a larger sputtering power for the deposition. Such a variation was also observed when Au was deposited by sputtering. Therefore, it is not attributed to a chemical reaction of WSi_x with GaAs but to a sputtering-induced damage. Activation energy and capture cross section for electrons (extrapolated value at $T=\infty$) are summarized in Table 4-1 for WSi-80W, Au-80W, WSi-10W and Au (Ref) samples. The applicability of a single level approximation is tested in Fig. 4-4 where the dashed curves were reproduced using the values in Table 4-1.

It is seen that the peak shift is mainly attributed to that in the activation energy. It should be noted that the EL2 spectrum in WSi-10W has a significant broadening. The experimental curve had a broadening in FWHM by 44% compared to a calculated curve assuming a single level. There were also some other dots where the peak temperatures of EL2 spectra were similar to those in the Au (Ref) sample according to the change in bias voltage.

(b)Annealing study

Annealing study was performed on WSi-10W sample. DLTS results

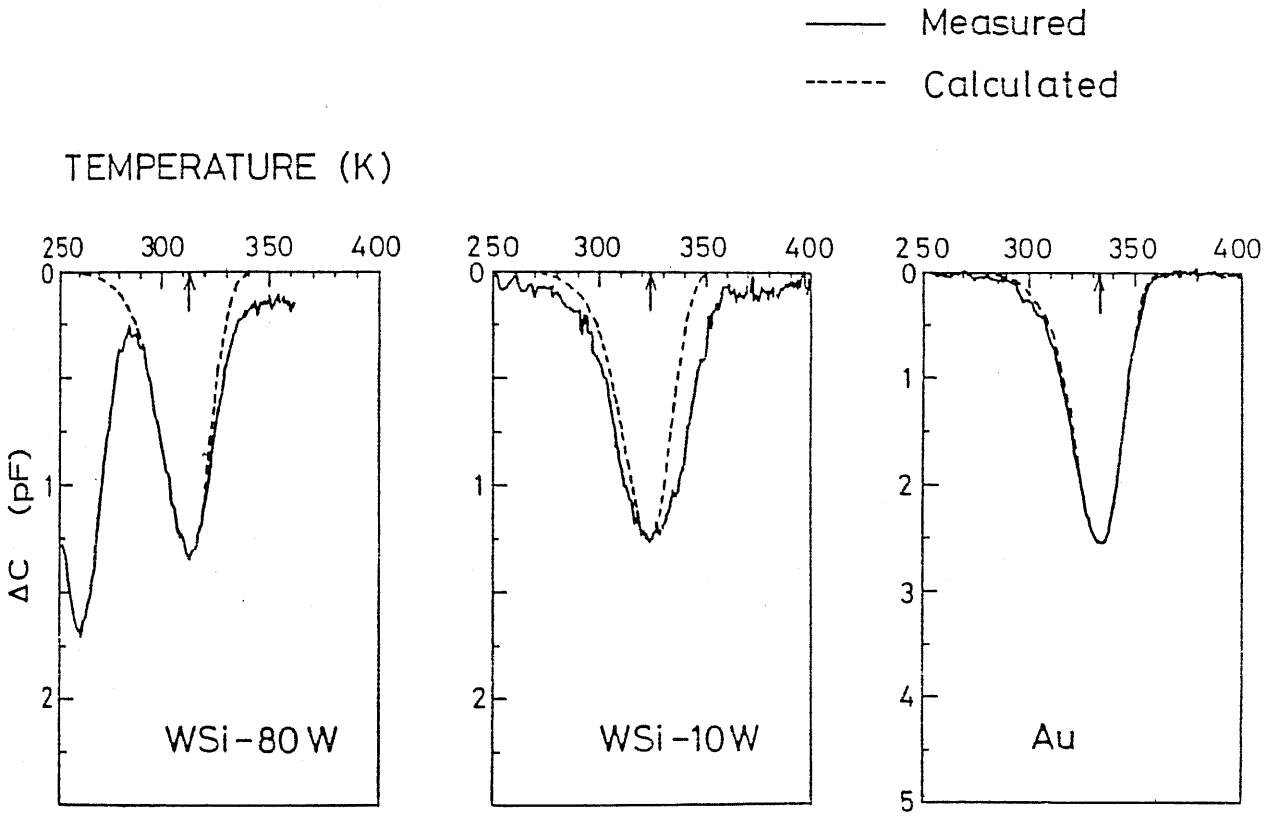

Fig. 4-4 Comparisons of EL2 spectra of as-deposited samples with calculated curves assuming single levels.

Table 4-1 Trap parameters of EL2 in the as-deposited samples

sample	E_a (eV)	σ_n (cm^3)
Au (Ref.)	0.84	4.6×10^{-13}
WSi-10W	0.77	1.0×10^{-13}
WSi-80W	0.74	9.6×10^{-14}
Au-80W	0.74	9.6×10^{-14}

for the EL2 concentration is shown in Fig. 4-5, while those for the peak temperatures of EL2 in DLTS spectra is shown in Fig. 4-6, as a function of the distance of the measurement position from the surface. The depth profiles were measured by changing bias voltage with keeping injection pulse height constant at 1V. After annealing at 324C, EL2 concentration tends to increase to the bulk value by a factor of 1.6. At the same time, the peak position near the surface shifts by 9 degrees. Correspondingly, the activation energy recovered from that in the as-deposited state 0.77eV to 0.85eV which is very close to the energy in the bulk 0.84eV. The broadening was also reduced from 44% to 15%. After 524C annealing, an increase in the EL2 concentration in the deeper region than 0.3um was observed and the profile became rather flat.

In a region around 0.2-0.3um, a behavior of the peak temperature was somewhat different. The sputtering with a power of 10W did not cause a significant deviation of the peak temperature of EL2 from that in the reference sample. The peak temperature shifted rather to lower temperature but the deviation from the reference sample was not so significant after 324C annealing. Annealed at 523C, the peak temperature again shifted to higher temperatures similarly to the result for the surface region. It should be pointed out that EL6 showed no such change due to annealing.

4.3.3 Discussions

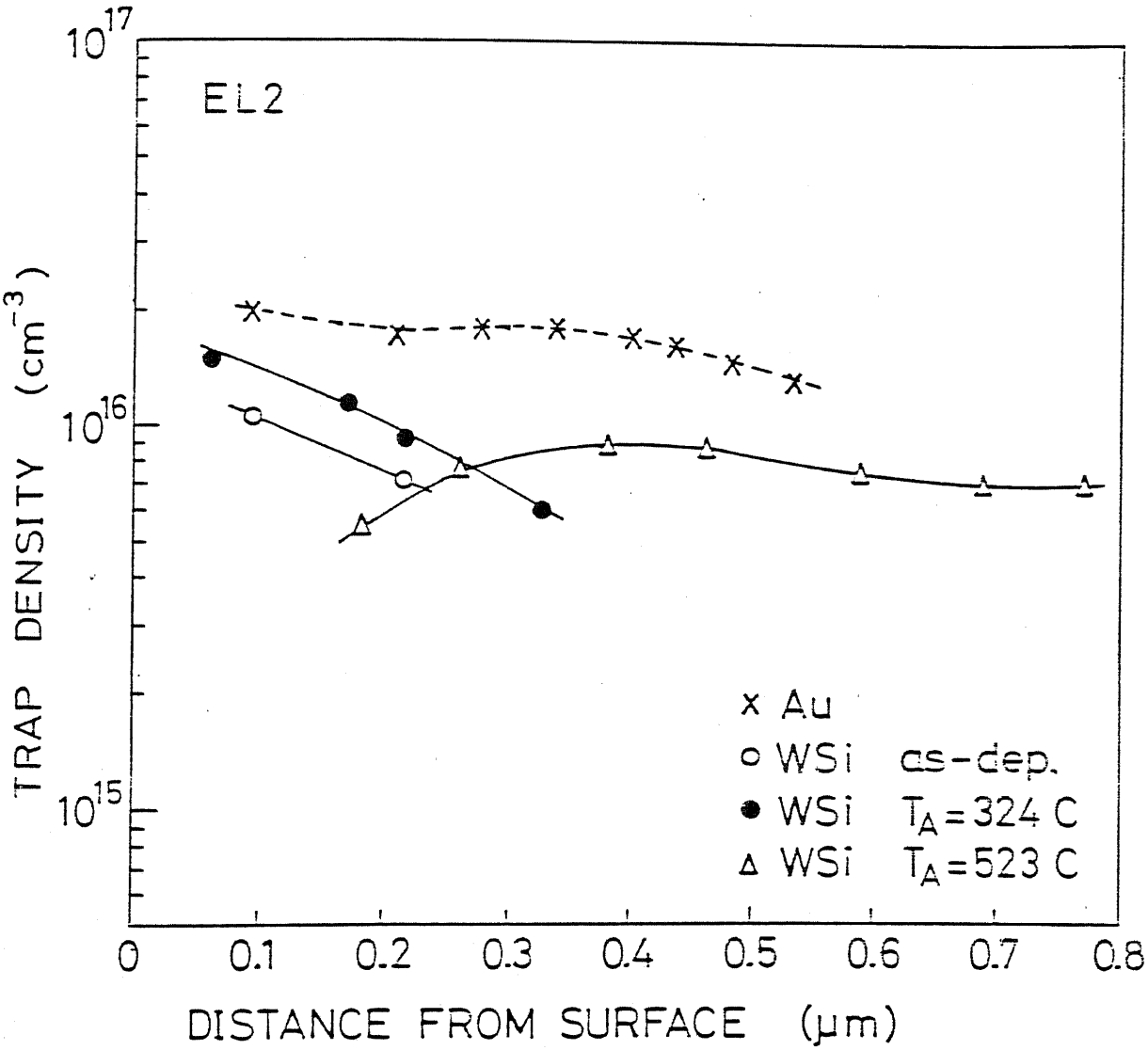

Fig. 4-5 Change of EL2 concentration profile of the WSi-10W sample.

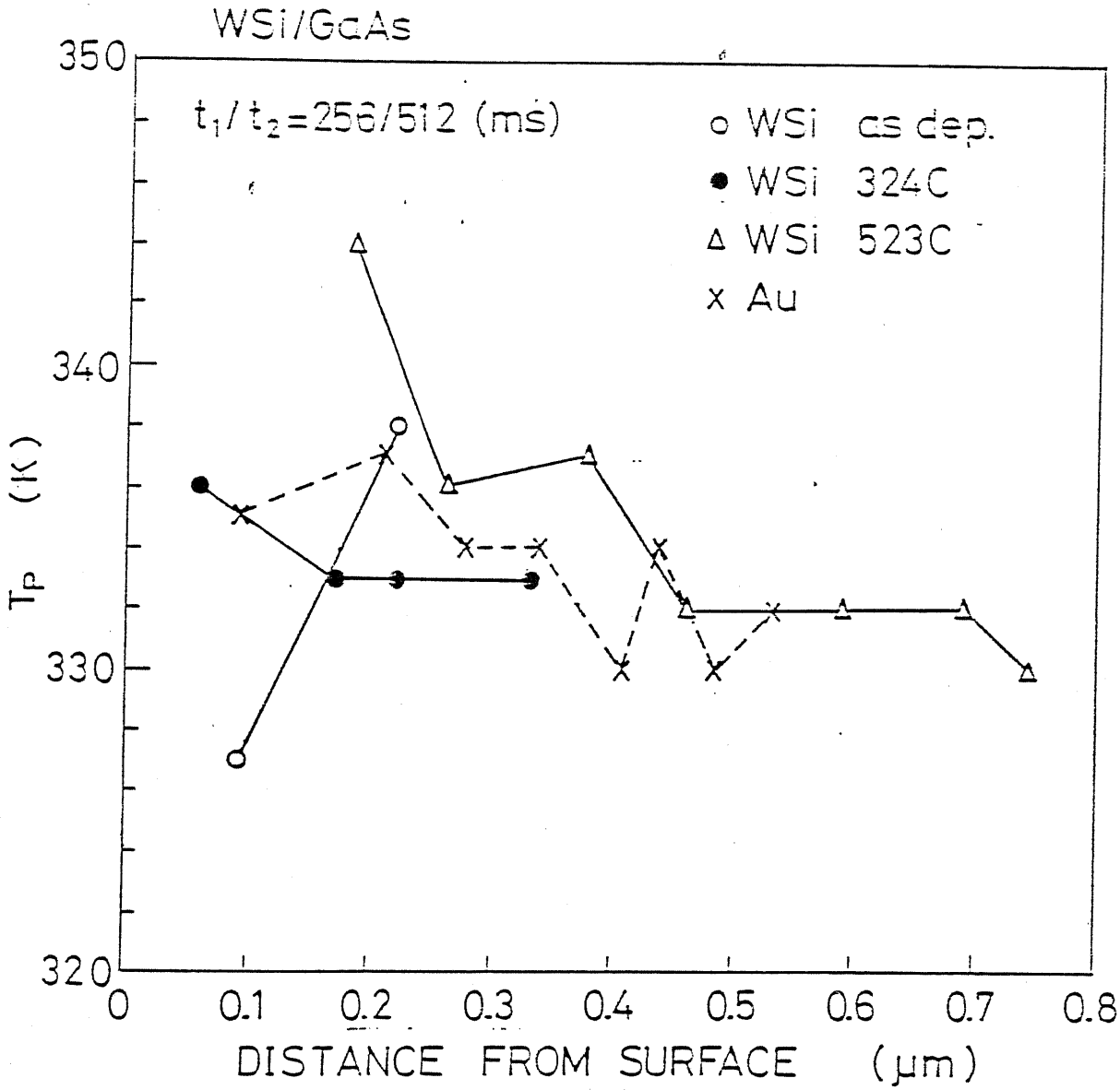

Fig. 4-6 Change of peak temperature of EL2 in DLTS spectra due to annealing.

When results of DLTS on EL2 are to be discussed, one should be careful about the spurious effect on emission rate and concentration which are caused by leakage current in a depletion region (Okumura and Hoshino 1986). According to the simplest DLTS theory, the leakage current in the depletion region, and thus, the electron capture to a trap is neglected. In this case, the emission time constant τ_e, which is directly related to the peak in a DLTS spectrum, is the inverse of the thermal emission rate, e_n. However, leakage current causes an electron capture to the trap in the steady state. Then, τ can no more be expressed as $(e_n)^{-1}$ but $(nC_n+e_n)^{-1}$, where n and C_n are electron concentration and the capture coefficient for electrons, respectively. If the two terms are comparable, a leakage current results in a peak shift to lower temperatures. At the same time, observed concentration of the trap is reduced. If the effect of leakage current can be neglected, one observes a whole change in occupation function because the equilibrium occupation is 0. Under the existence of electron capture, the equilibrium occupation is replaced by $nC_n/(nC_n+e_n)$ and the observed trap concentration, N_{ta}, is $N_t e_n/(nC_n+e_n)$, where N_t is the real trap concentration. Actually, a true value of n is difficult to determine from the measured value of reverse current mainly due to a contribution of peripheral leakage current. However, this effect can be indirectly estimated by plotting $\log(N_{ta})$ vs τ_e as easily seen from a simple algebra. One would obtain a straight line if this effect cannot be neglected. Carrier concentration in the depletion region is determined by quasi-Fermi level.

Based on the thermionic emission model at a Schottky barrier, the contribution of the capture term drastically changes when a trap energy level is close to the Schottky barrier height derived from current-voltage characteristics. The barrier height of Au-evaporated Schottky barrier is around 0.84eV and energy level of EL2, 0.75eV, is well above the quasi-Fermi level in the depletion region. Therefore, the effect of leakage current can be almost neglected. On the other hand, Al Schottky barrier usually has a height around 0.74eV which is very close to the EL2 energy level. This is why different spectra were obtained in Al Schottky diodes (Yahata et al. 1984).

Another effect which affects the DLTS spectra is the existence of persistently ionized deep centers (Okumura 1985). This effect also causes a reduction in trap concentration and a peak shift to lower temperatures. This effect occurs under such a condition when the injection pulse height is much smaller than bias voltage during the carrier emission.

Some results obtained in the present study are qualitatively explained by these two effects but others cannot be. The barrier height derived from I-V measurements, displayed in Fig. 4-7, were 0.56, 0.72. and 0.86eV for WSi-80W, WSi-10W and Au (Ref.) samples, respectively. Therefore, the peak shift to lower temperatures and the reduction of peak height in the sputtered samples may appear to be explained by the capture term. However, the EL2 concentrations in WSi-80W and WSi-10W samples were almost

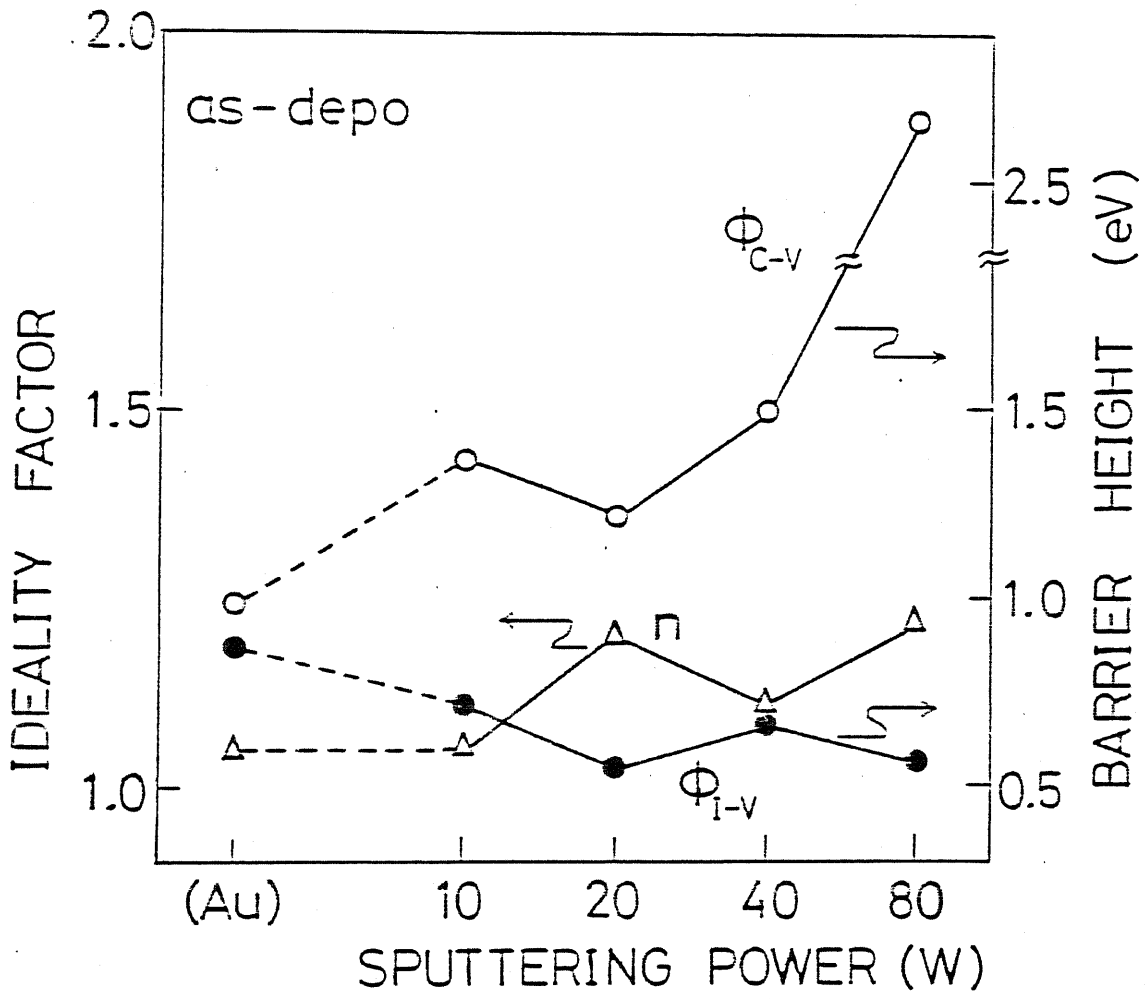

Fig. 4-7 Schottky barrier characteristics of as-deposited samples.

the same, whereas the peak shift from the spectrum of Au (Ref) sample was much larger in WSi-80W. If the behavior were explained by the leakage current effect, a logarithmic relation would be expected. Additionally, the peak temperature of EL2 in WSi-10W measured in the deeper region was higher than that near the surface region and close to the position in Au (Ref) as shown in Fig. 4-6. This behavior cannot be explained by the aforementioned effects, either. Furthermore, the pronounced broadening of the EL2 spectrum was only observed in WSi-10W case and no significant broadening was observed in WSi-80W (or Au-80W) sample as already shown in Fig. 4-4. This result makes an attribution of the peak shift only to the space charge effect difficult. Actually, the spectra in Fig. 4-3 were taken near the surface region and almost all EL2 are occupied during the filling period. It should also be noted that the change in forward current characteristics of WSi-10W after 324C annealing was negligible as shown in Fig. 4-7, while the aforementioned change in EL2 was observed. Based on these facts, it can be concluded that all the behaviors observed in the as-deposited samples cannot simply be attributed to the aforementioned spurious effects although the Schottky barrier are degraded in the sputtered samples and the leakage current effect does exist.

Judging from the power dependence, the change in the EL2 spectra are likely to be caused by a damage introduced by sputtering. During the sputtering process, bombardment by Ar plasma and sputtered metal is expected to disturb the crystalline or defect

structure near the surface more easily than in a vacuum evaporation process. The range of damage introduction can be roughly estimated to be about 0.2um from the distribution of ED5 level. It is interesting to point out that the EL2 peak position of WSi-10W was almost the same as that in the reference sample when the measured region was around 0.2um deep. Damage introduced by 10W sputtering is considered to be not so large but close to the threshold for disturbing the EL2 structure. At the dots which showed little change in EL2 spectra, the amount of damage are likely to be less than this threshold. Furthermore, no systematic variation was actually observed for EL6. Therefore, the damage is estimated to be not so large as to disturb the whole crystal structure but only as to affect the defects which are most easily dissociated. This idea suggests that EL2 should be a sizable complex defect.

The annealing study revealed that the temperature of 324C is high enough for recovering the defect structure of EL2. This result indicates that the specie responsible for EL2 is a fast diffuser even at low temperatures, such as an interstitial site arsenic (As_I). The defect seems to have an equilibrium size to which dissociated As atoms migrate to form a cluster during annealing.

Makimoto et al. (1984) also observed a change of EL2 in emission rate and concentration by a reactive Schottky metal, Pd, deposition and a low temperature annealing. In their system, a reaction of Pd with GaAs caused a change in the depth profile as well as a broadening of DLTS spectra near the surface. These results are

reproduced in Figs. 4-8 and 4-9. The broadening of a spectrum can be evaluated by simply examining $\Delta T/T_p$ where $\Delta T/T_p$ is the half width of a DLTS spectrum normalized by its peak temperature (Goto et al. 1979). In the Pd deposited diodes, the barrier height was always larger than 0.8eV (0.85eV at the as-deposited state and 0.82eV after annealing at 300C, 30min). Therefore, the change in EL2 distribution is not likely to be due to the capture effect. Even at the as-deposited stage, EL2 piled up toward the surface and a broadening of DLTS spectra were observed. This result was explained by assuming an extraction of excess arsenic atoms toward surface which was caused by an reaction of Pd with GaAs. Their result also supports the present speculation that EL2 originates from a sizable defect of mobile As atoms.

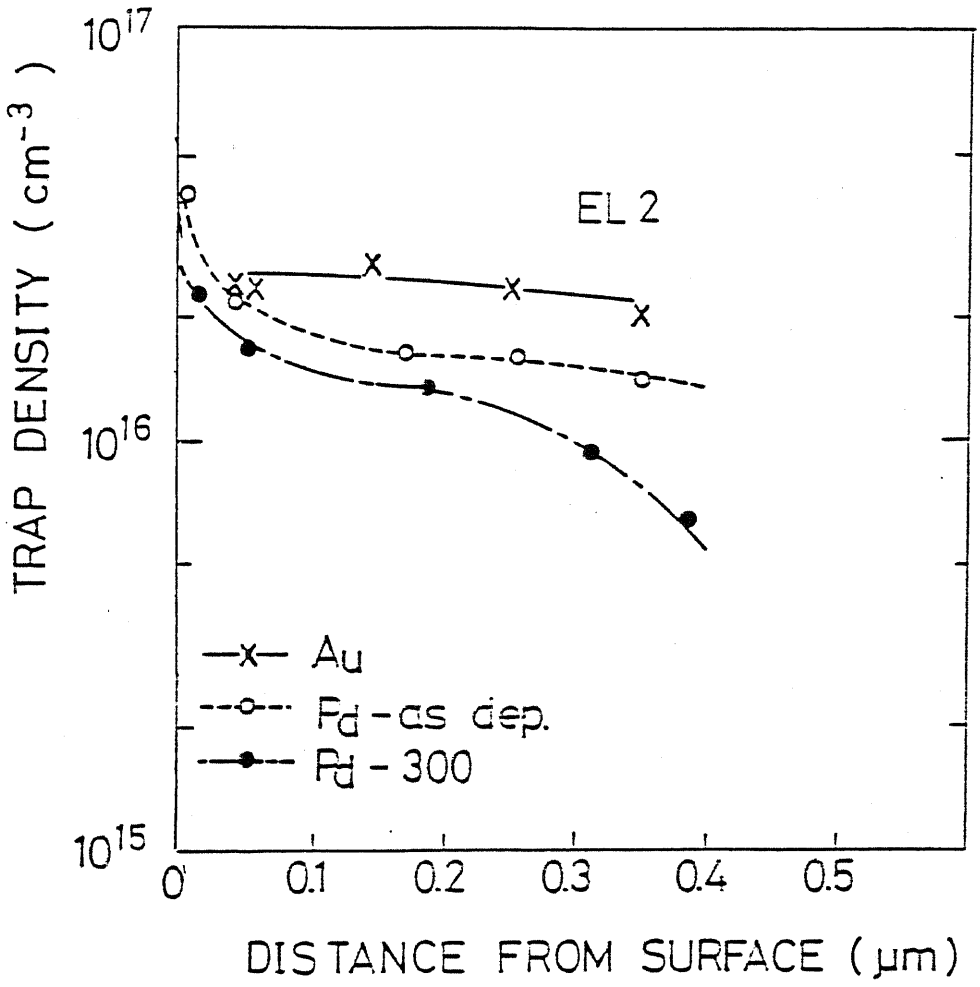

Fig. 4-8 Density profile of EL2 for Au/GaAs, as-deposited and 300C annealed Pd/GaAs. (After Makimoto et al. 1984)

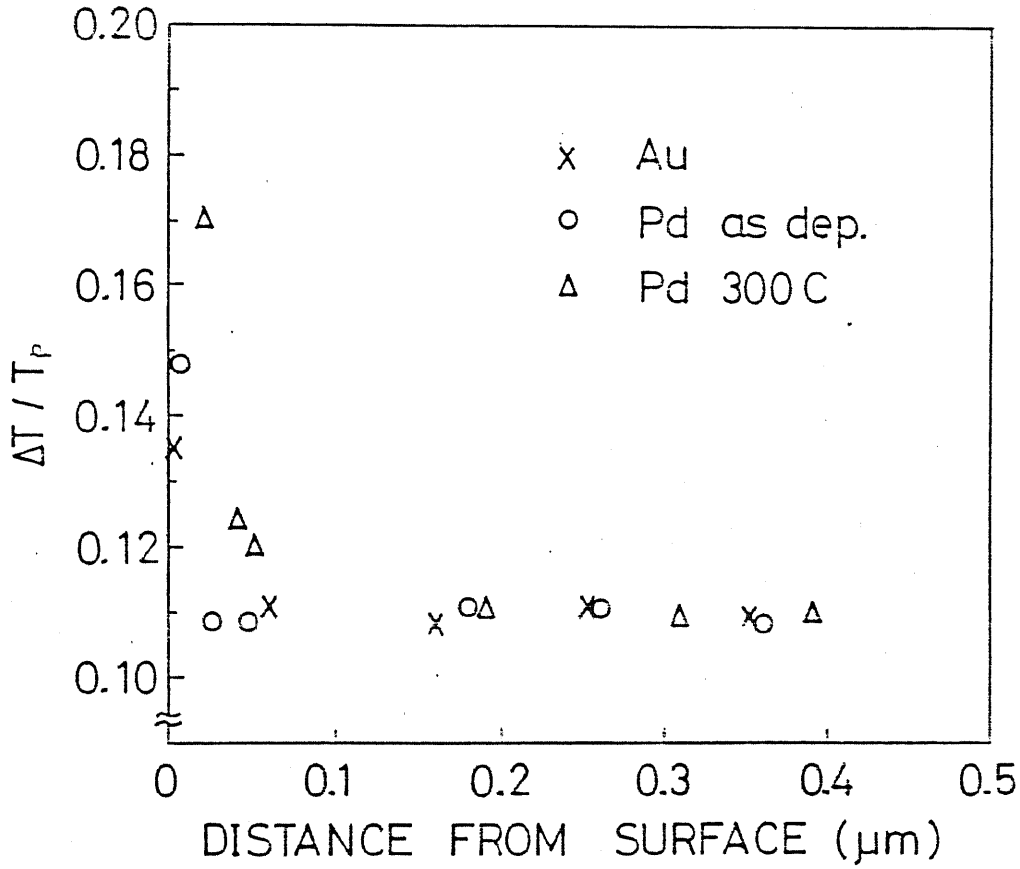

Fig. 4-9 Broadening of DLTS spectra as a function of distance from the surface for Au/GaAs, as-deposited and 300C annealed Pd /GaAs. $\Delta T/T_p$ is a half width normalized by peak temperature.

4.4 Annihilation of EL2 by reactive ion etching (RIE)

Recently, reactive ion etching (RIE) process has come to be widely used for fabrication of small geometry devices. However, damage introduction is expected during RIE because a sample is subjected to plasma bombardment. In this section, the effect of damage which is induced by RIE on EL2 is studied using junction capacitance techniques.

4.4.1 Experimental

The wafers used in the study were undoped n-type HB GaAs. First, SiO_2 (400nm) was deposited by plasma-assisted chemical vapor deposition on the surface of the wafers. Prior to etching, Ohmic electrodes were formed on the backside by evaporating AuGe/Ni/Au and alloying at 400C, 5min. After the patterning of Schottky electrodes, SiO_2 was etched by RIE. The etching ambient was CHF_3 at the pressure of 0.08Torr and the input power was 3.5W/cm^2. Then the wafer was wet-etched with a solution of $HF:NH_4F$=1:6 for 1min. Schottky electrodes were formed by vacuum evaporation of Au with a thickness of 200nm. For reference, Schottky diodes without RIE were fabricated. In this case, SiO_2 was etched by a solution of $HF:NH_4F$=1:6 for 1min. It was found that Au-Schottky electrodes on RIE-etched wafers are easily peeled off, which is likely to be due to the degradation of dry-etched surface. However, Au is suitable for characterization of midgap traps due to a large barrier height of a Schottky diode. As mentioned in the previous section, barrier

height is required to be larger than the energy level of a trap when a junction capacitance method is adopted.

Characterization of the diodes was carried out by I-V, C-V and TDS-ICTS (Okumura 1985) measurements. C-V profiling of deep levels was also performed, which is described in Appendix-1. The measurements were carried out using a Digital Electrometer TR8652 (Advantest), a 1MHz C-Meter/C-V Plotter 4280A (YHP) and a Pulse Generator Model 110C (Systron Donner). A personal computer, PC-9801F (NEC), was used for automated measurements and data processing.

4.4.2 Results

Schottky characteristics for the RIE-etched and the reference samples are compared in Fig. 4-10. From the I-V characteristics, it is seen that the barrier height is lower and the saturation current is larger for RIE samples. In these samples, the extrapolated barrier height from C-V measurement is largely shifted may be due to the reduction of N_D-N_A near the surface regions. Therefore, the dry-etched samples have poorer Schottky characteristics than that of the reference samples. The Schottky characteristics of the reference samples are almost ideal with a large barrier height and small saturation current.

Fig. 4-11 shows a typical TDS-ICTS spectrum at room temperature for the reference sample. The spectrum is shown with a lambda-

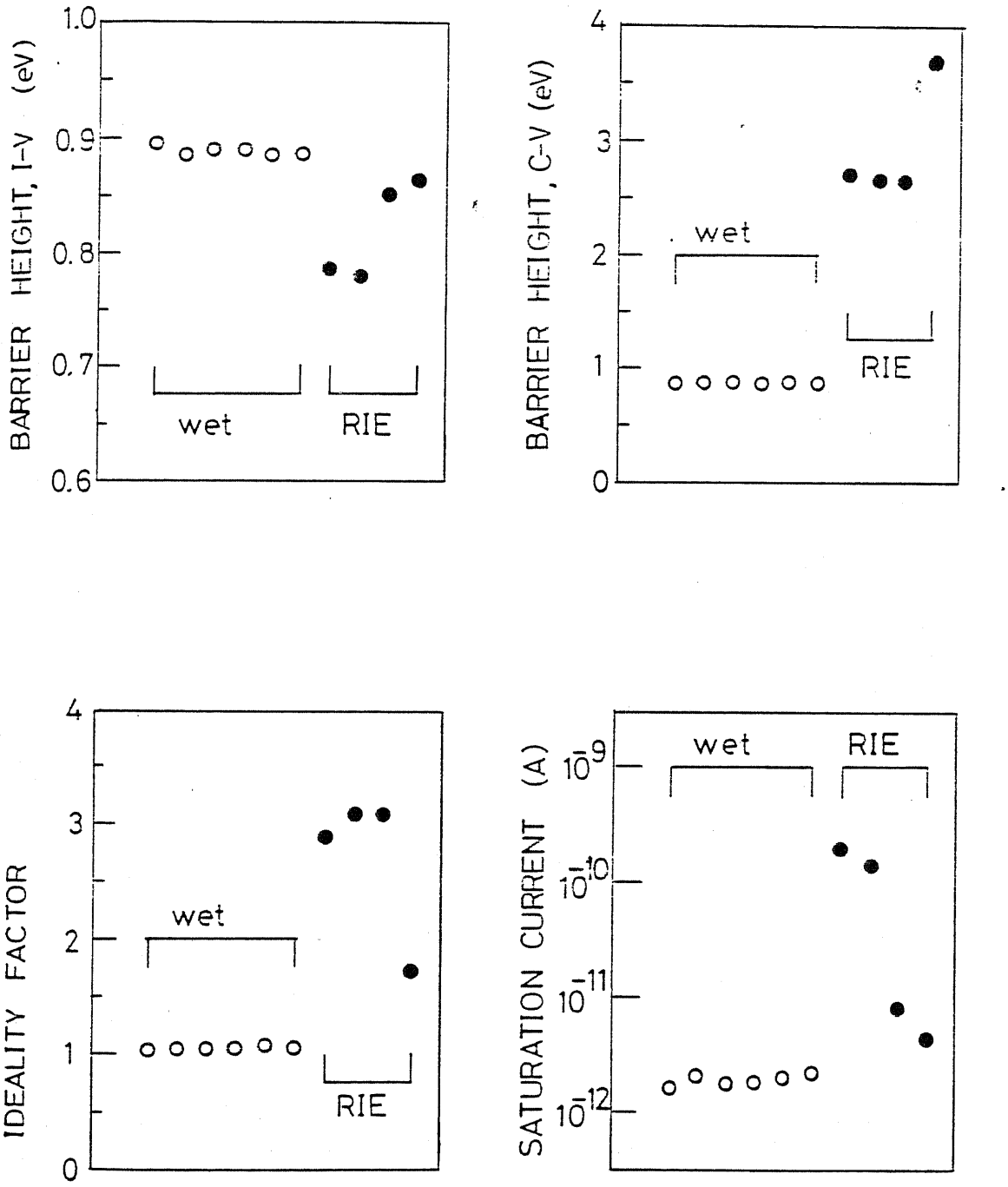

Fig. 4-10 Schottky characteristics (barrier height, ideality factor and saturation current) of the reference and the RIE-etched HB GaAs.

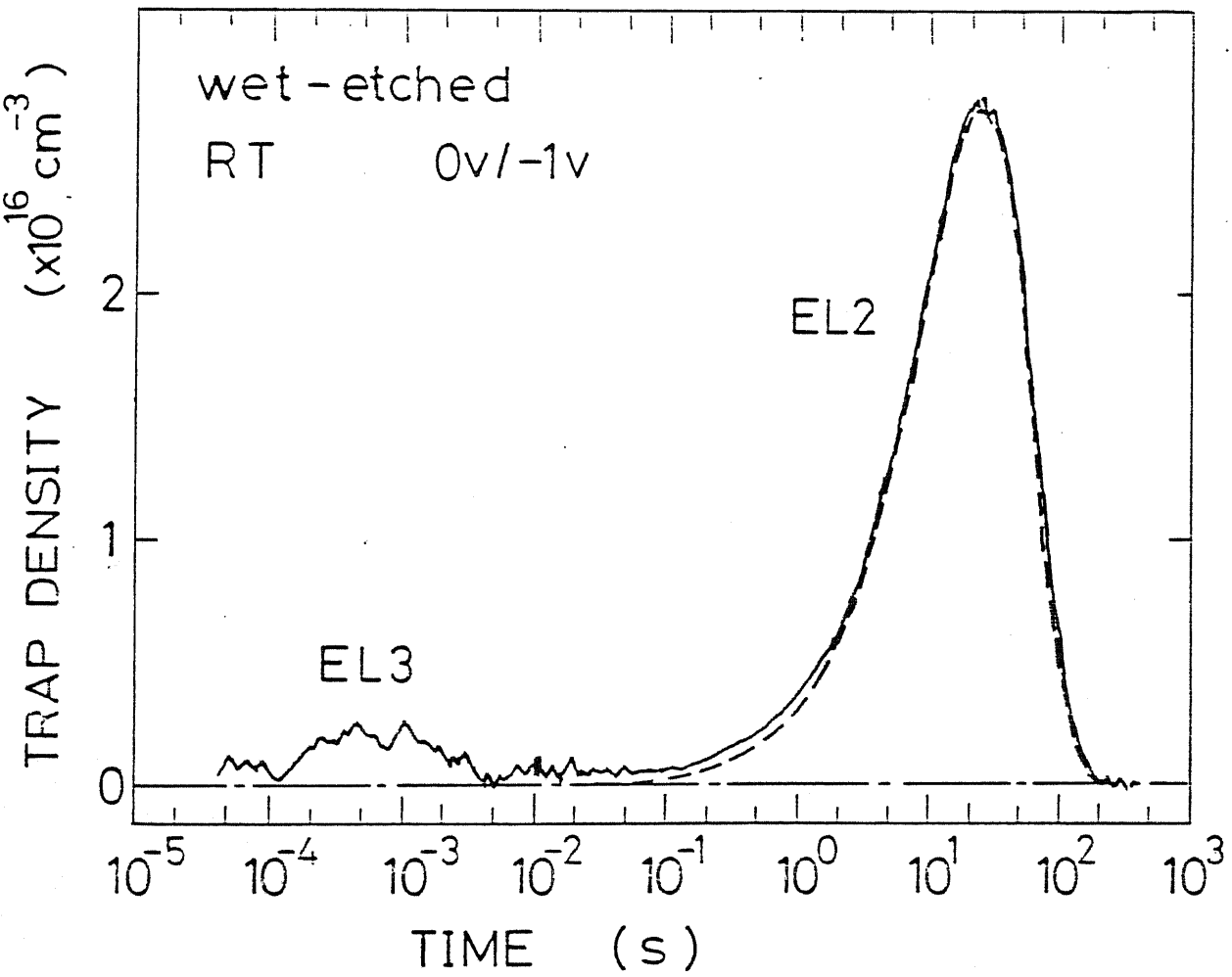

Fig. 4-11 TDS-ICTS spectrum for the reference sample measured at room temperature and the bias condition of 0V/-1V.

correction where $E_C-E_T=0.75eV$ is assumed. In an TDS-ICTS spectrum, a peak position and height immediately gives the emission time constant and the trap concentration. Only EL2 is observed in the reference samples, whose emission time constant is $23\pm2s$ and concentration is $2.7\text{-}4.4\times10^{16}cm^{-3}$, respectively. The variation in the emission time constant is attributed to that in temperature as well as noise in the measured EL2 spectra. However, the spectral shapes of EL2 agreed in general with those reproduced from a calculation assuming single levels. The observed EL2 concentrations are reasonable values in HB GaAs crystals.

On the other hand, no apparent EL2 signal was observed in the TDS-ICTS spectra near the surface regions of dry-etched samples as shown in Fig. 4-12(a) which was measured at the bias voltage of -1V. Instead, a broad signal around 20ms and a very slow transient which exceeds 500s are observed. The former can be identified as ED5 introduced by RIE damage. The origin of the latter transient is not known at present. In the deeper regions, ED5 signal is much reduced and EL2 becomes the dominant signal as shown in Fig. 4-12(b). The unidentified slow transients are still observed. These results indicate that ED5 decreases while EL2 increases toward inside in the RIE processed sample.

To examine the spatial variation more in detail, C-V profiling method was applied. Fig. 4-13(a) shows the profile of EL2 concentration in the reference sample, which was derived from the

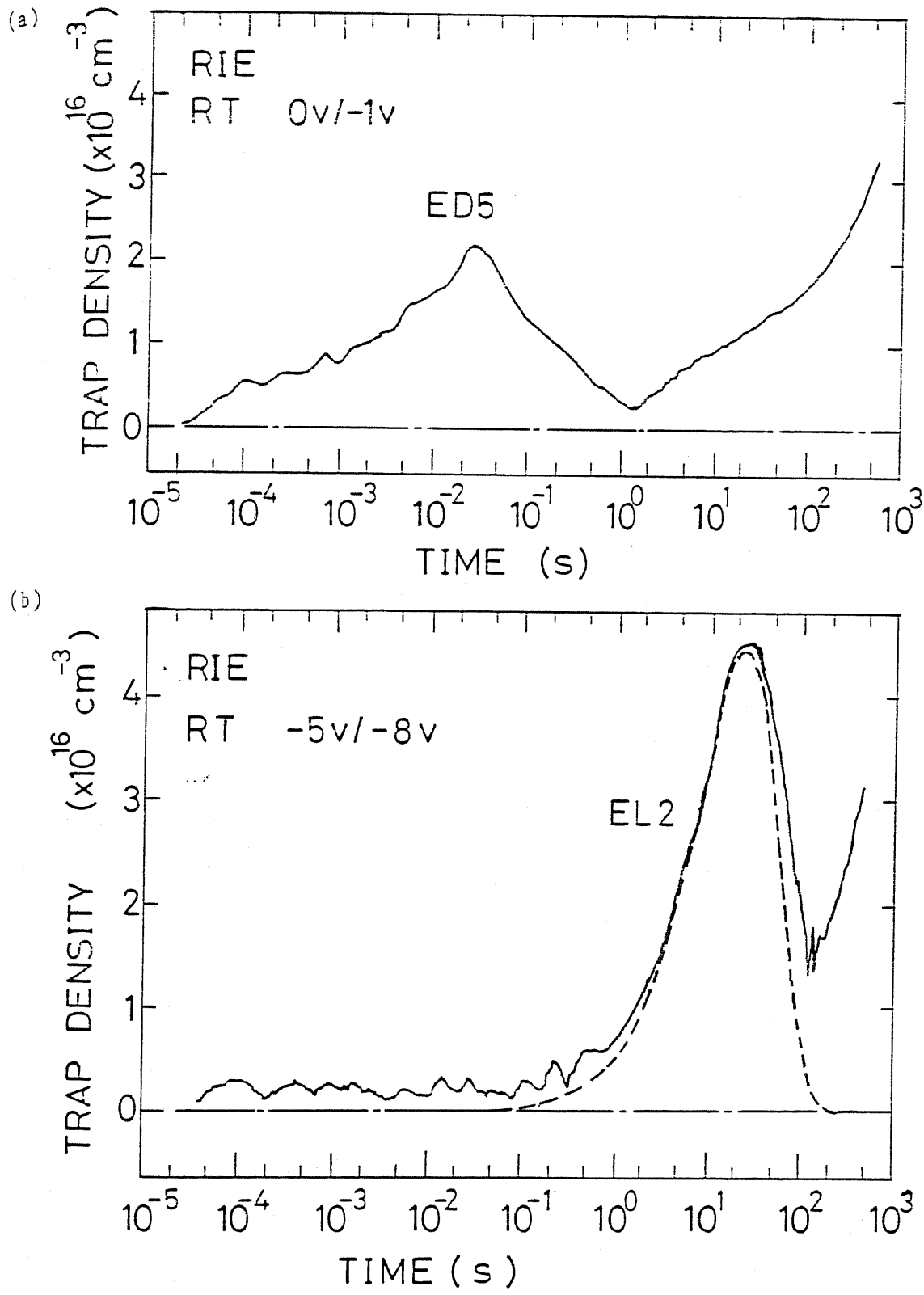

Fig. 4-12 TDS-ICTS spectra for the RIE-etched sample at room temperature. The bias conditions are (a) 0V/-1V and (b) -5V/-8V.

(a)

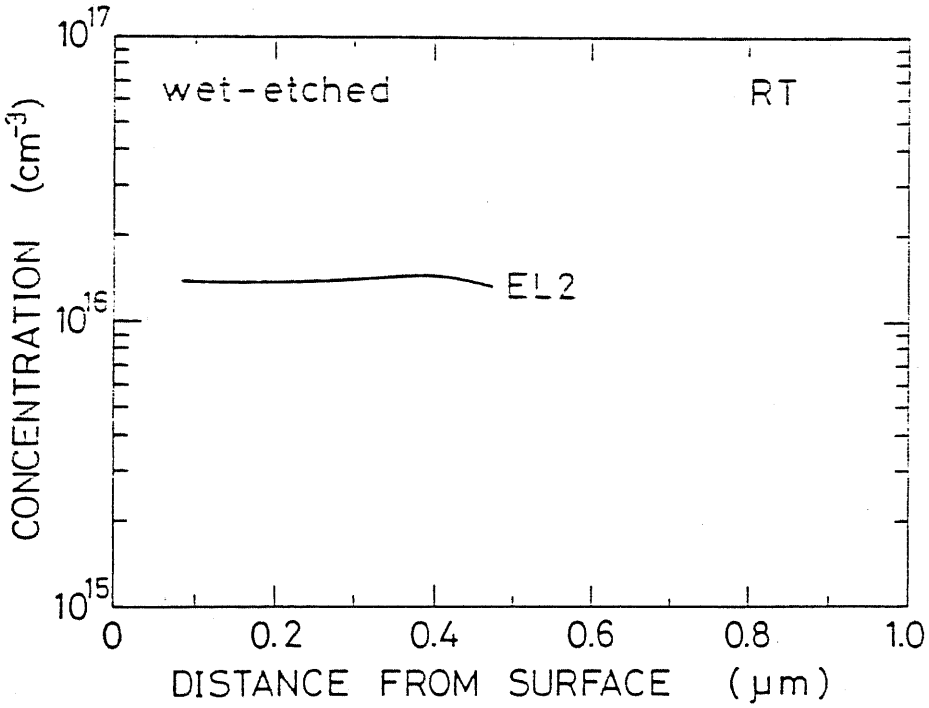

(b)

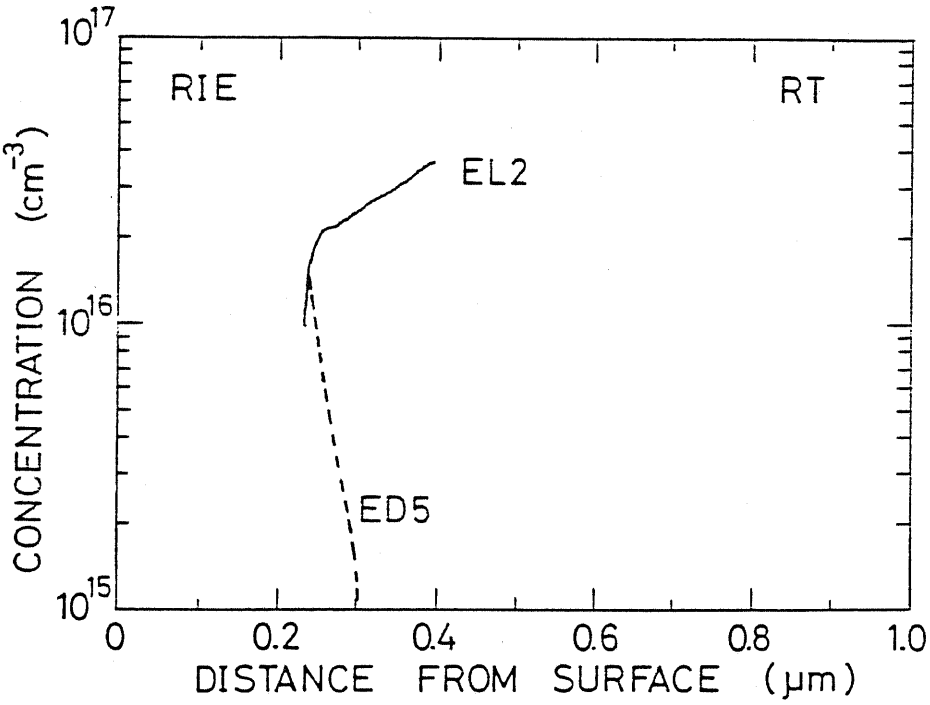

Fig. 4-13 Profiles of the trap concentrations for (a) the reference sample and (b) the RIE-etched sample.

C-V measurements of t_d=10ms and t_d=50s. It is seen that the EL2 concentration in bulk GaAs is almost constant along distance from the surface. However, EL2 concentration in the dry-etched samples were greatly reduced near the surface as shown in Fig. 4-13(b). In this case, C-V measurements with t_d=1s and t_d=50s were carried out to obtain the trap profiles for ED5 and EL2 separately. Since the energy level of ED5 is unknown, λ was calculated using the activation energy 0.52eV of this level, which corresponds to the estimation of the maximum concentration of ED5. In the surface region, ED5 prevails EL2 and rapidly decreases toward inside. Furthermore, a gradual increase of EL2 toward inside was observed. Although a slow ionization co-exists which cannot be attributed to the emission from EL2, C-V measurement with t_d=50s mainly monitors the ionized EL2 centers.

Similar measurements were carried out on RIE-etched n-type VPE GaAs ($n=2\times10^{17}cm^{-3}$). In this case, no EL2 was detected in both unprocessed and dry-etched layers. However, a damage induced level, ED5 was again observed in the surface region of the dry-etched sample as shown in Fig. 4-14.

4.4.3 Discussions

The results of characterization of the dry-etched samples are summarized in the following:

(i) Schottky characteristics were degraded, which showed lower barrier height, larger saturation current and reduction of

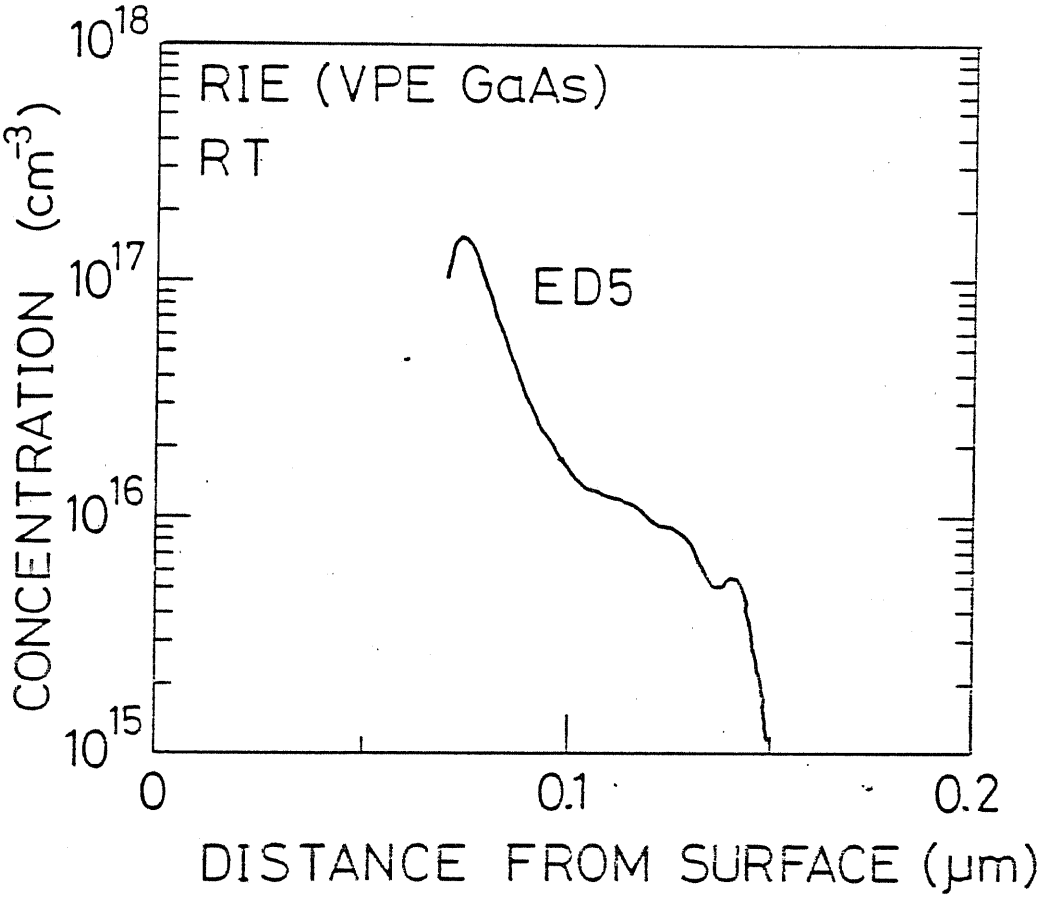

Fig. 4-14 Concentration profile of ED5 in RIE-etched VPE GaAs.

donors or introduction of acceptors near the surface.

(ii) EL2 concentration was largely reduced in the shallower region than 0.25um from the surface. The concentration gradually increased toward inside.

(iii) ED5 was observed in the surface region whose concentration rapidly decreases in the deeper region than 0.2-0.3um.

The degradation of Schottky characteristics and the introduction of ED5 in the surface region are similar to the results of sputtering. This agreement is reasonable because the main factor for the damage introduction in both of the situation is the plasma bombardment. However, in the sputtering experiments, it was difficult to attribute all the change in the EL2 spectra to its real change in characteristics due to a degraded Schottky characteristics. In the present experiments, the increase of EL2 toward inside cannot be explained by the effect of carrier capture by leakage current.

Furthermore, a newly adopted profiling method of deep levels clearly revealed that the annihilation of EL2 has a nice complementary correlation with creation of the damage-induced level, ED5, as can be seen in Fig. 4-13. It should be pointed out that the peak temperature of EL2 spectrum in the WSi-10W sample approached to that of Au(Ref.) sample in the deeper region than 0.2um. Therefore, it is concluded that EL2 centers are affected or annihilated by a bombardment damage which is introduced to the depth of 0.2um.

It is not possible so far as to attribute ED5 as a directly transformed defect from EL2, although ED5 has a complementary profile to that of EL2. Originally, no EL2 was detected in the VPE samples probably due to the large electron concentration (Lagowski et al. 1982a), whereas a large concentration of ED5 was introduced by RIE. The concentration of ED5 rather has a correlation with the original free electron concentration. Therefore, this defect is more likely to be assigned as a displaced shallow donor impurity or a complex of shallow donor impurity with a native defect produced by the bombardment damage. Anyhow, identification of ED5 is beyond the scope of this thesis and not discussed further.

4.5 A model for the atomic structure of EL2 family

4.5.1 As cluster model

Recent assessment is that EL2 is closely related to the excess arsenic conditions. A model for the atomic structure is required to successfully explain the experimental facts which are summarized as follows;

(i) EL2 appears during an intermediate stage of annealing after heavy particle bombardment such as ion implantation.

(ii) EL2 easily dissociates by the sputtering damage, and recovers its structure after a low temperature annealing as low as 300C.

(iii) The trap parameters of EL2 have variations so as to form a family of levels (EL2 family).

(iv) A large metastable relaxation takes place at EL2, which is beyond the harmonic oscillator approximation. Furthermore, The energy configuration of the normal state and the metastable state are not uniquely determined.

(v) The defect responsible for EL2 consists of a rigid point defect similar to As_{Ga} and an easily displaced defect which mainly contributes to the metastability.

Items (i) and (ii) indicate that EL2 is annihilated and created at low temperatures which is considerably lower than that for simple point defects and support the idea that EL2 should be originated from a sizable defect. Furthermore, a defect component of EL2 is

required to be mobile at low temperatures as mentioned above and As_I is the most probable candidate. The trap characteristics as stated in the rest of the items also suggest that EL2 should be a sizable complex defect which enables a variation. Furthermore, its bonding is likely to be "soft" so that the metastability and the family characteristics occur.

As discussed in the previous chapter, the principle characteristics are likely to be determined by $As_{Ga}+V_{As}$ or $As_{Ga}+As_I$. Taking into account the argument above, the latter structure is more probable. It was further pointed out in the previous chapter that it is necessary to assume the third (or more) defect(s) to account for the result on EL2 in LEC GaAs. Again, it is naturally expected that As_I is such a defect(s). Therefore, the atomic structure of the EL2 family can be tentatively expressed as $As_{Ga}+nAs_I$ ($n>=2$). Atomic arrangement is hardly known so far but this defect can be regarded as an aggregate of more than 7 arsenic atoms. In such a phase, it is hardly expected that the coordinations in the host lattice are conserved.

Information on the bulk amorphous arsenic gives an insight into the properties of the As-aggregate. Three-fold coordinated arsenic as shown in Fig. 4-15 is a normal configuration in amorphous arsenic. Defect states in this phase are two-fold and four-fold coordinated arsenic atoms. As shown in Fig. 4-15, ${}_pP_2{}^0$ and ${}_{sp}P_4{}^0$ have an unpaired electron and are spin-active. (We follow the conventional notation: ${}_pP_2{}^0$ means a two-fold coordinated neutral arsenic atom

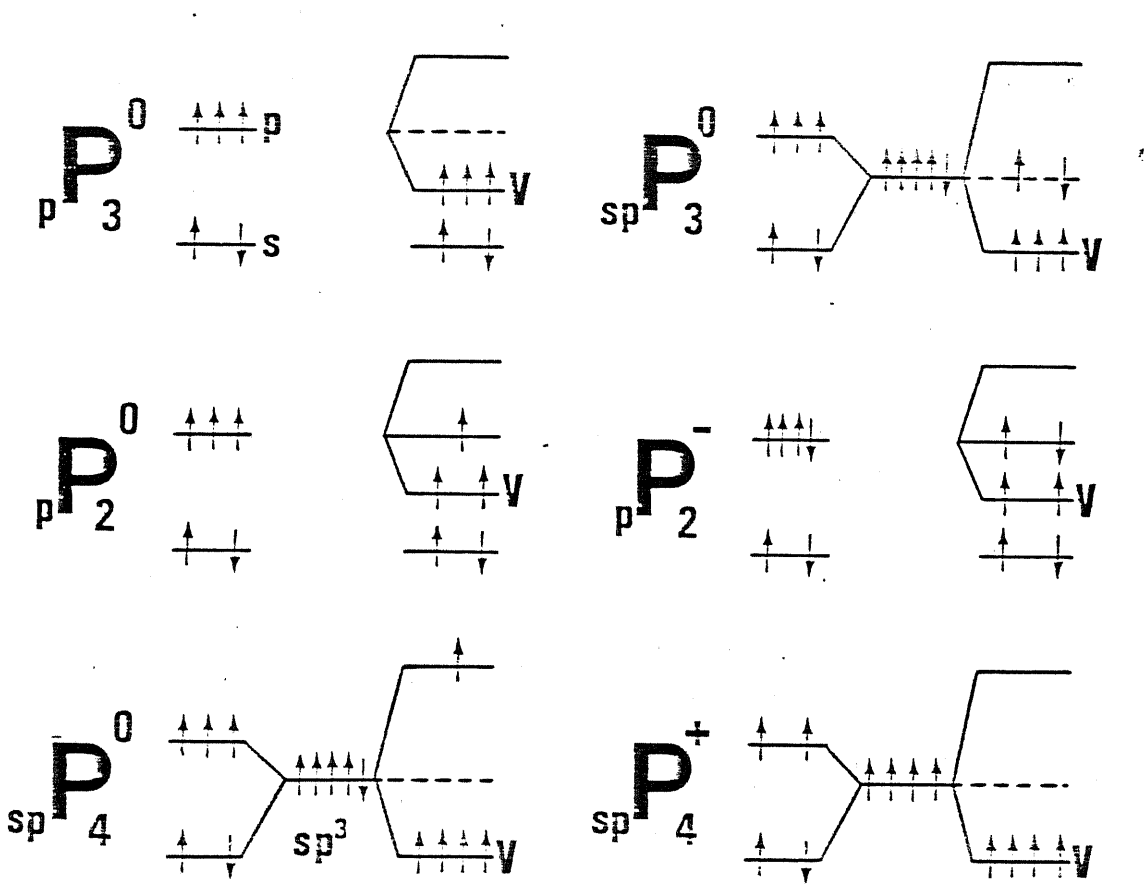

Fig. 4-15 Possible defect states in amorphous arsenic. Electron occupations are also shown before and after bonding. "V" indicates bonding electrons. (After Greaves et al. 1979).

whose predominant type of bonding is p-like.) It is interesting to note that $_pP_4^0$ has a similar atomic configuration to an antisite arsenic As_{Ga}, corresponding to a singly ionized state D^+ in GaAs, which is detected by ESR measurements. According to Greaves et al. (1979), furthermore, $_pP_4^0$ forms a level near the midgap in the band gap (1.25eV) of amorphous arsenic. Optical fatigue phenomena which is similar to photoquenching at the EL2 family are very common in amorphous materials and in fact, photoluminescence quenching by illumination with 1.1eV light, which is identical to photoquenching of the EL2 family, has been observed in amorphous arsenic (Bishop et al. 1976). Photo-induced absorption, instead of photoquenched absorption was observed near the midgap energy in amorphous arsenic (Bishop et al. 1976). These similarities lead to the idea of arsenic clusters for the origin of EL2 family.

When one makes an analogy between an amorphous arsenic and EL2 family in GaAs, it is necessary to consider the effects of periodic crystal potential on energy levels and the dynamic characteristics of amorphous arsenic. Actually, the ESR spectra for both materials show both similarity and dissimilarity, and the effects of crystal potential are obvious. This suggests that sizes of clusters should be neither too large as to isolate the effect of GaAs matrix nor too small as to eliminate the characteristics of amorphous arsenic.

A large metastable relaxation as stated in the item (iv) is very suggestive. It is inferred that various defect reactions take place when charged states are changed by illumination. In fact,

three reactions have been considered in amorphous arsenic by Greaves et al. (1979)

$$2_{p}P_2^{0} \rightleftarrows {}_{p}P_2^{-} + {}_{sp}P_4^{+} \qquad (4\text{-}1)$$

$$2_{sp}P_4^{0} \rightleftarrows {}_{p}P_2^{-} + {}_{sp}P_4^{+} \qquad (4\text{-}2)$$

$$_{p}P_2^{0} + {}_{sp}P_3^{0} \rightleftarrows {}_{p}P_3^{0} + {}_{sp}P_4^{0} \qquad (4\text{-}3)$$

4.5.2 Comparison with other models for EL2

The models for the atomic structures so far proposed are listed in Table 4-2. These models can be classified into three groups; isolated As_{Ga}, vacancy-related complex with As_{Ga} and excess arsenic atom-related As_{Ga}. Besides the family nature of EL2, it should be recalled that the structure is required to explain the arsenic-rich related and the metastable natures of EL2.

A shuttling motion of an arsenic atom between V_{Ga} and $As_{Ga}+V_{As}$ has been shown to have a metastability from theoretical calculations (Baraff and Schluter 1985, Bar-Yam and Joannopoulos 1986). Since this defect has a stable state near the latter configuration, however, the expected symmetry of the stable state is C_{3V} which is in an apparent contradiction to the result of stress measurement (Kaminska et al. 1985). This model has another disadvantage that the defect is not a donor but an acceptor. Bar-Yam and

Table 4-2 Model for the atomic structure of EL2

model	reference		comment
As_{Ga}	Kaminska et al.	1985	ZPL in intracenter absorption has a T_d symmetry.
As_{Ga}-V_{Ga}	Goltzene et al.	1983	ESR singlet = V_{Ga}
As_{Ga}-V_{As}	Lagowski et al.	1982b	Correlation between EL2 and crystal growth condition.
	(Baraff and Schluter,	1985	Total energy calculation. Not EL2 but an "actuator defect")
V_{Ga}-As_{Ga}-V_{Ga}	Van Vechten	1975	Thermodynamical calculation.
V_{As}-As_{Ga}-V_{Ga}	Yuanxi et al.	1985	Reaction of As_{Ga} with $V_{As}V_{Ga}$.
	Bar-Yam and Joannopoulos	1986	Total energy calculation and charge state consideration.
As_{Ga}-As_I	Spaeth	1986	Fitting to ODENDOR data. Photoquenching characteristics.
	Mochizuki and Ikoma	1986	SPTA, a part of As-cluster.
	von Bardeleben et al.	1986b	Annealing characteristics of DLTS and ESR.
	(Baraff and Schluter	1986	Existence of metastability from total energy calculation.)
$(As_{Ga})_2$	Figielski et al.	1985	Theory. Jahn-Teller instability accounts for the metastability.
$(As_{Ga})_{2\sim5}$	Frank	1985	Annealing characteristics of ESR signal.
$(As_{Ga})_2$-$(As_I)_2$	Wada and Inoue	1985	Out-diffusion profile of EL2.
As_{Ga} aggregate	Meyer and Spaeth	1985	Photoquenching characteritics. Spin-lattice relaxation time.
As-cluster	Taniguchi and Ikoma	1984	EL2 family.
	Ikoma et al.	1985	Annihilation and creation of EL2 at low temperature.
	Ikoma and Mochizuki	1985	Similarities to amorphous arsenic.

Joannopoulos, therefore, assumed a divacancy, $2V_{Ga}$, which dissociates into $V_{As}As_{Ga}V_{Ga}$. Although this defect can successfully explain the p-type conversion of SI GaAs after heat treatment (Lagowski et al. 1986), the symmetry problem still remains unsolved. This is the reason why Baraff and Schluter considered this defect to be an "actuator defect" of EL2, which should experience an aggregation with other defect(s).

$As_{Ga}+As_I$ is very similar to the model proposed in the present study. Bardeleben et al. (1986a) performed an annealing study and attributed the regeneration of EL2 at low temperatures to mobile As_I. Thus, they proposed that EL2 is not an isolated antisite but $As_{Ga}+As_I$. They explained the metastability of EL2 by putting the interstitial As atom at the next nearest site of As_{Ga} at the normal state, which preserves the ESR activeness and the T_d symmetry. Assuming As_I to be pulled towards As_{Ga} in the metastable state, As_{Ga} wavefunction is largely disturbed and no more ESR signal is likely to be observed. A total energy calculation was also carried out for this defect and an ESR active center was found in the As_I at the hexagonal site (Baraff and Schluter 1986). It was further predicted that photoexcitation drives the As_I towards As_{Ga} so that the system is transformed to a metastable state. Experimentally, Spaeth (1986) found a number of ODENDOR lines some of which cannot be attributed to an isolated As_{Ga}. He successfully explained these lines by assuming that As_{Ga} exists in a complex form with As_I on the tetrahedral site from the fitting of spin Hamiltonian.

It can be easily seen that there still exist a problem on the identification that EL2 is As_{Ga}+As_I. The ODENDOR result claims that As_I is at the tetrahedral site which is the nearest saddle point to As_{Ga} still preserving the ESR active characteristic. This is in contradiction to the explanation for the metastability of this system. It should also be noted that association with only one As_I can never explain the family characteristics in the stable-metastable configurations described in this study, even if a family of deep levels may be observed according to the As_I movement. It seems therefore advantageous to assume a complex in which more than one As_I is associated. Recently, a thermodynamical consideration was made by Wada and Inoue (1985), in which the outdiffusion data of EL2 were found to be well explained by assuming a four-As_I cluster. They predicted that a final form of $(As_I)_2(As_{Ga})_2$, for instance, would behave like EL2 by trapping two (or more) Ga vacancies.

Aggregate of As_{Ga} also belong to the category of excess arsenic atom-related defects. These models are mainly based on the ESR results and in an attempt to overcome the inconsistencies between the characteristics of EL2 and As_{Ga} signal. Meyer and Spaeth (1985) performed a photoquenching experiment on As_{Ga} signal in MCD with changing the excitation intensity. EL2-type quenching occurred only at a high excitation level, whereas the bleached As_{Ga} had a different recovery characteristics from EL2. They interpreted the result in such a way that EL2-type quenching takes place when As_{Ga} defects form an aggregate and nearby defects are

simultaneously photoexcited and proposed an As_{Ga}-aggregate model for EL2. However, the EL2 absorption was quenched at low intensities at which no As_{Ga} quenching was observed. Aggregation (complex formation) of As_{Ga} requires either an aggregation of V_{Ga} which trap As_I or As_I-aggregate which trap many V_{Ga}. However, a complete occupation of Ga-sites by As_I are hardly expected and it is more likely that V_{Ga} or As_I are also involved in the excess-arsenic defect aggregate. Therefore, this type of defects can be also identified as As-clusters.

4.6 Conclusions

It is found that the atomic structure of EL2 can be easily disturbed during sputtering and RIE keeping a nice correlation with bombardment damage. The defect structure can be easily recovered at low temperature annealing around 320C. These results suggest that EL2 is a sizable defect in which a highly mobile defect such as As_I is involved.

Based on these results together with those obtained in the previous chapters, the arsenic-cluster model for the origin of EL2 is proposed and its validity is discussed. It is shown that this model can successfully account for the family nature of EL2 as well as the involvement of mobile As_I defects. Possibility of photoquenching effect and ESR active centers are also indicated from an analogy with bulk amorphous arsenic. Recently proposed models by other researchers are shown to be rather similar to the concept of the present model of excess arsenic clusters.

CHAPTER 5 CONCLUSIONS

Abstract

The conclusions obtained in the present study are collectively described.

A detailed study has been carried out on the main midgap electron traps, EL2 family which plays an important role in the carrier compensation at semi-insulating GaAs crystals. In spite of intensive works by many researchers and of both practical and physical importance, identification of this center has been controversial. The properties of EL2 are characterized through electrical and optical measurements in an attempt to provide a ground to deduce its defect structure.

Photoquenching effect at the EL2 family was studied in Chapter 2. A systematic characterization was carried out on the transition processes between the normal and the metastable states in various GaAs crystals. In particular, the recovery from the metastable state to the normal state has been studied in detail. A quantitative study on the recovery process by optical excitation has been performed on the EL2 family for the first time using photocapacitance technique. The results obtained in Chapter 2 are summarized as follows:

(i) EL2-O, an oxygen-implantation induced level in LPE GaAs, has a barrier of 0.41eV in the thermal recovery process and exhibits no recovery to the normal state by free electron injection.

(ii) It has been found that the optical recovery occurs only at a part (around 10%) of EL2 centers in LEC GaAs crystals.

(iii) The vertical transition energy for the optical recovery has been determined to be 0.855eV.

(iv) It has been further clarified that even the levels which

recover optically cannot be regarded as a unique level.

(v) No appropriate configuration for the normal and the metastable states was found to consistently explain all the transition energies.

In conclusion of Chapter 2, a large variation observed in the recovery characteristics indicates the existence of a multiplicity in the energy configuration of the normal and the metastable states of the EL2 family. The result-(iv) indicates a possibility of optically induced defect reaction for the photoquenching which occurs in a largely displaced regime and a harmonic approximation no more holds. The increase above 1.3eV rather than the Gaussian shape in the photoquenching spectra is tentatively attributed to the direct excitation process the normal metastable state as a consequence of the variation in the recovery characteristics among the EL2 family.

The optical transition mechanisms at EL2 has been studied more in detail in Chapter 3. An important role of the excited state has been characterized using a newly developed technique, SPTA method. This method has been found to be powerful in observing the final states of charge transfer. The experimental results are summarized in the following:

(i) Fine structures has been observed in a photoquenching rate spectrum for the first time, which consists of ZPL at 1.039eV and its phonon replica.

(ii) The electrons at the excited states have probabilities of

relaxing to both the metastable state and the conduction band.

(iii) The ZPL spectrum at EL2 in LEC GaAs was broader than that at EL2 in MOCVD GaAs.

(iv) The energy positions of the negative peaks in SPTA spectra were in agreement with the peak positions of intracenter absorption as well as those of photocurrent.

Based on these results, the SPTA spectrum has been attributed to the transitions to two excited states; one of which gives rise to the fine structure and is resonant with the conduction band, while the other leads to the Gaussian spectrum and couples with the metastable state. A new configuration coordinate model for EL2 is proposed, which consistently explains the aforementioned experimental results. The model assumes two excited states of EL2 with different degrees of lattice relaxation as a key feature. It has been found that the existence of two excited states is the only solution also from the viewpoint of the stability of the energy levels.

This configuration coordinate model suggested a complex nature for the origin the EL2 center which consists of an As_{Ga}-like defect with rigid bonds and another defect with easily displaced soft bondings. Actually, a comparison with the theoretical predictions by other researchers provided a possibility of identification as $As_{Ga}+V_{As}$ or $As_{Ga}+As_{I}$. However, the result-(iii) indicates an involvement of more defects which is essential

for the family nature to be observed.

An insight into the defect specie which contributes to the formation of EL2 has been given through the annihilation and re-creation properties of EL2 by process-induced damage and low temperature annealing as described in Chapter 4. It has been shown that EL2 is easily dissociated or change its property by damage introduction due to heavy particle bombardment. Its defect structure is restored after low temperature annealing as low as 320C. The results indicate that EL2 is a sizable defect in which an involvement of a highly mobile excess-arsenic defect, probably As_I, is essential.

Based on all of the results, the arsenic-cluster model has been proposed and its validity has been discussed. It has been shown that this model can successfully account for the family nature of EL2 as well as the involvement of mobile As_I defects. Possibility of photoquenching effect and ESR active centers are also indicated from an analogy with bulk amorphous arsenic. Recently proposed models by other researchers are shown to be rather similar to the concept of the present model of excess arsenic clusters.

To make a final statement, it seems that the problem of the identification of EL2, which has been one of the most mysterious ones, has come very close to its goal. The author hopes that the present study plays some role in the "feed back circuit" of a new

phase of controlling defects in semiconductors.

ACKNOWLEDGMENT

The work described in this thesis was carried out while the author was a PhD student in the Department of Electronic Engineering in the Graduate School of the University of Tokyo, 1984-1987.

In the first place, the author wishes to express his sincere gratitude to Professor Toshiaki Ikoma (Institute of Industrial Science, University of Tokyo), the dissertation supervisor as well as the "God Father" of the EL2 family, for encouragement and guidance, which are always full of insights.

Professor Tsugunori Okumura (Tokyo Metropolitan University) and Professor Tadamasa Kimura (University of Electro-Communication) are greatly acknowledged for fruitful and exciting discussions at the weekly meetings of Ikoma Laboratory. The author owes much to Prof. Okumura for kindly supplying the measurement programs of TDS-ICTS and so on.

The author would like to thank Dr. Mitsuhiro Taniguchi (Nippon Mining Co. Ltd.) for giving advice at the early stage of the study and also for many discussions, while he was a research associate in Ikoma Laboratory.

Profs. J.-M. Spaeth (University of Paderborn), E. R. Weber (University of California, Berkeley), and A. M. Hennel

(Massachusetts Institute of Technology) are acknowledged for giving suggestions especially on interpretation of the SPTA spectra. The author is also grateful to Dr. B. K. Meyer, Dr. U. Kaufmann and Prof. J. Schneider for discussions on the origin of EL2.

Many of the samples appeared in this thesis were kindly supplied by courtesy of various people: "beautiful" MOCVD GaAs by Dr. M. O. Watanabe (Toshiba), ingot annealed LEC and "artistic"-thick LPE GaAs by Dr. Ohkubo (Hitachi Cable Ltd.), RIE-processed samples by Dr. K. Inaniwa (Hitachi Ltd.).

The author would like to thank those who helped him in the DLTS and ICTS measurements described in Chapter 4. Mr. M. Tanaka, Ms. S. Tanya, Mr. T. Kakinoki, Mr. T. Kimura, Mr. K. Ogiwara are acknowledged for the sample fabrication and DLTS measurements for sputtering-damage study. Y. Akiyama carried out the TDS-ICTS measurements of RIE-processed samples. Without their assistance, the work would not have been completed.

People who are and are used to be in Ikoma Laboratory are also acknowledged. Dr. M. Takikawa (Fujitsu Laboratories) and Mr. S. Kumashiro (NEC), Dr. H. Noge (Toyota Central Research Laboratories) are appreciated for discussions on DLTS measurements and deep level statistics. Dr. H. Noge is also helped the auther by giving advice on the electrical circuitries for measurements. Dr. T. Saito, Mr. T. Makimoto (NTT) and Mr. T.

Hiramoto helped the auther mainly in sample preparation processes. Dr. J. Yoshino and Dr. K. Hirakawa of Sakaki Laboratory (Institute of Industrial Science, University of Tokyo), and Mr. M. Nishioka are acknowledged for discussions and advice in making measurements. The author is grateful to Dr. K. Iwamoto (Institute of Industrial Science, University of Tokyo) for assistance in FTIR measurements. Finally, the auther would like to express his sincere gratitude to Ms. Y. Kurihara (research associate, Ikoma Laboratory) for encouragement and comfortable management of the laboratory.

APPENDICES

Appendix.1 C-V profiling method of deep levels

A C-V (capacitance-voltage) method of deep levels is described. If a deep level is well resolved in a DLTS or ICTS spectrum, the concentration of the level can be easily estimated from the change in capacitance before and after the emission of carriers. Such a method is actually applied for the estimation of DX center in alloy semiconductors. Since the emission rate of DX center is very large at room temperature and very small at low temperatures, the concentration profile of DX center is calculated by subtracting the C-V data measured at low temperature (77K) from that measured at room temperature. However, This method is hardly applied to midgap levels because they have large emission time constants even at room temperature.

Instead, the method described here calculates a deep level profile by using C-V data measured with different delay times at the same temperature. This method is in an analogous relation to that of DLTS and ICTS. The time sequences of the applied bias are shown in Fig. A-1. Figure A-1(a) corresponds to the measurement of concentration profile of shallow levels. Typically the delay time was 10ms and (V_1, C_1) is measured. In this case ionization of deep levels can be totally neglected and a concentration profile is immediately calculated by taking a derivative (for instance, Sze 1982).

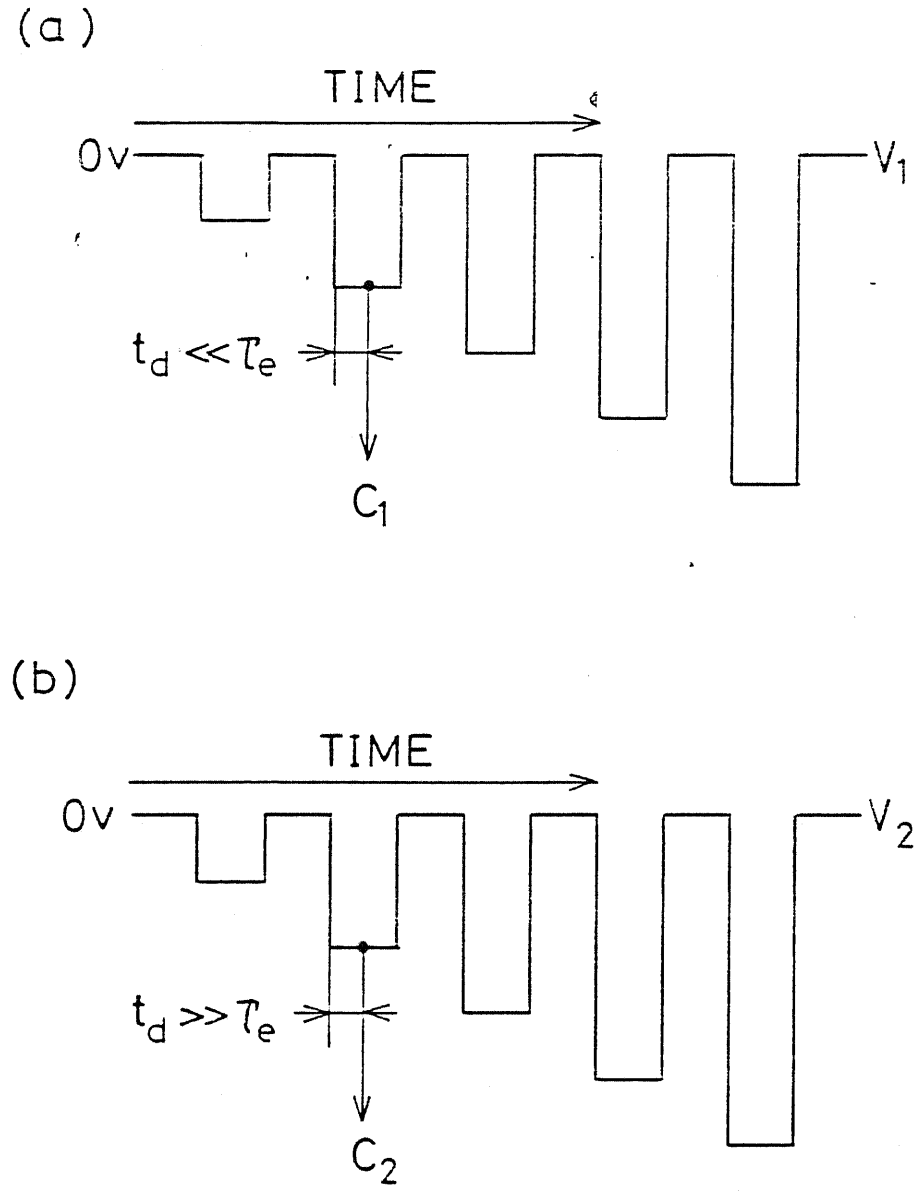

Fig. A-1 Illustrations of the C-V measurements for (a) shallow donor profiling and (b) deep level profiling.

$$N_D = \frac{2\varepsilon_s}{q}\left[-\frac{dV_1}{dW_1^2}\right]^{-1} \qquad \text{(A-1)}$$

$$W_1 = \frac{\varepsilon_s}{C_1} \qquad \text{(A-2)}$$

Here, W_1 and N_D are the depletion layer width and the shallow donor concentration, respectively. q is the unit charge and ε_s is the permitivity.

On the other hand, Fig. A-1(b) corresponds to measuring (C_2, V_2) and the concentration of space charge after the deep levels are also ionized. Let the deep level concentration be N_T, the Poisson's equation is

$$\begin{cases} \dfrac{d^2\varphi}{dx^2} = -\dfrac{q}{\varepsilon_s}(N_D + N_T) & (0 \le x \le W_2 - \lambda) \\ \dfrac{d^2\varphi}{dx^2} = -\dfrac{q}{\varepsilon_s} N_D & (W_2 - \lambda \le x \le W_2) \end{cases} \qquad \text{(A-3)}$$

λ is the distance of the crossing point from the depletion layer edge, at which the trap level crosses Fermi level (Zohta and Watanabe 1982). Emission from the deep level occurs only in the

region $x<W_2-\lambda$. Solving (A-3), the W_2 at a certain V_2 is expressed as,

$$V_2 = -\frac{1}{q\varepsilon_s}\left[W_2^2 N_D + (W_2-\lambda)^2 N_T\right] \qquad (A-4)$$

The same procedure of taking derivative gives

$$N_D + \left(1-\frac{\lambda}{W_2}\right)N_T = \frac{2\varepsilon_s}{q}\left[-\frac{dW_2^2}{dV_2}\right]^{-1} \qquad (A-5)$$

Therefore, the difference of (A-5) and (A-2) gives N_T when a factor $(1-\lambda/W_2)^{-1}$ is multiplied. It should be noted that thus obtained N_T corresponds to the concentration at $W_2-\lambda$.

An example is shown in Fig. A-3 for a case of EL2 distribution in an as-grown HB GaAs, whose emission time constant, τ_e, is 20s. The delay time, t_d, for the slow C-V measurement was 50s and $E_c-E_T=0.75$eV was assumed. When t_d is not sufficiently larger than τ_e, a factor $\exp(t_d/\tau_e)$ should be multiplied.

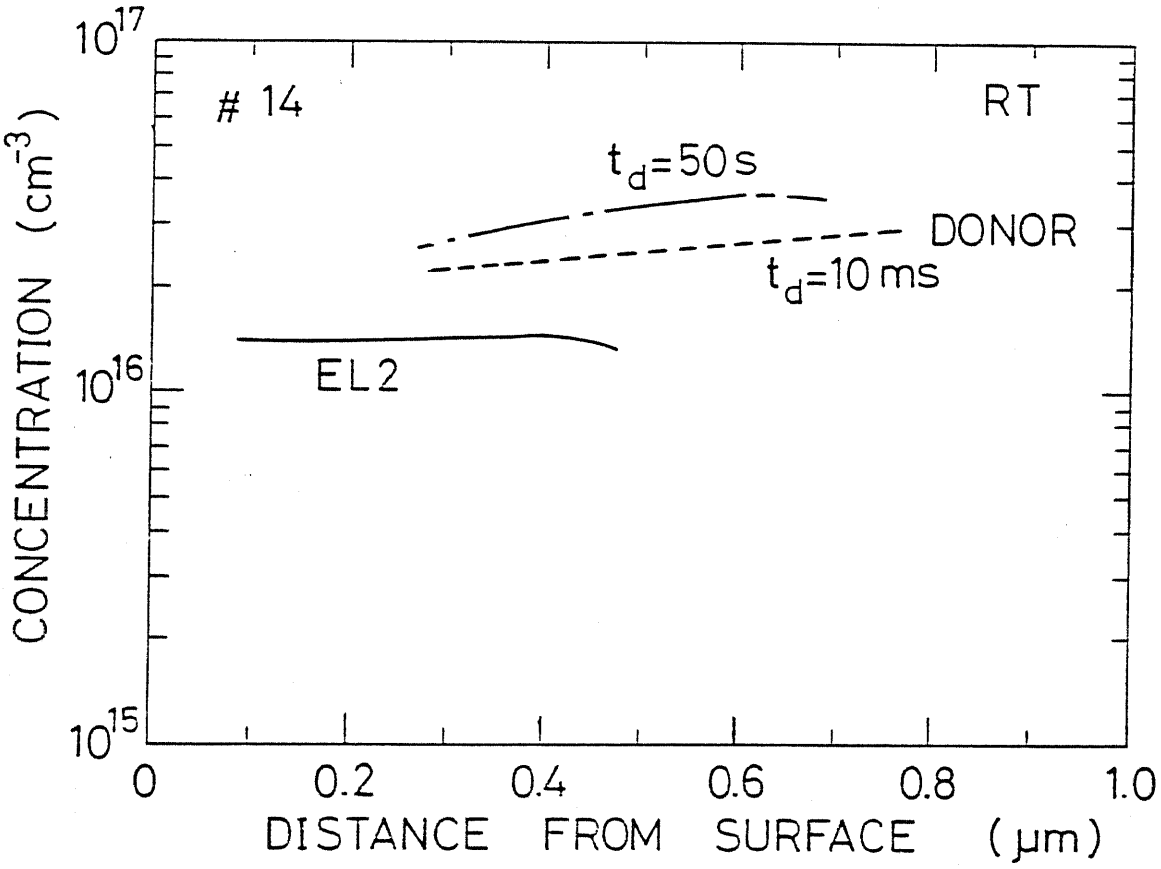

Fig. A-2 An example of the result of the deep level profiling . EL2 distribution in an HB GaAs is shown (solid curve) together with the shallow donor profile (broken curve) and the total space charge profile (dashed curve).

Appendix-2 Lattice absorption of GaAs

A-2.1 Introduction

It is expected that a defect of a large size may give rise to a phase within a crystal, which has a different vibrational density of states than that of the host crystal. If an excess-arsenic defect forms such a phase as amorphous aggregation, corresponding phonon may be observed. It is known that a bulk amorphous arsenic has phonon absorption band around 230cm^{-1} at room temperature as shown in Fig. A-3. In this appendix, the results of far-infrared absorption measurement of GaAs is described.

A-2.2 Experimental

(1)Samples

Samples studied are as-grown LEC (labeled as LECa and LECb), ingot annealed LEC (IASI) and LPE GaAs crystals. Two wafers of as-grown LEC GaAs provided by different vendors, Sumitomo and Cominco, were studied. Several points should be noted. All the LEC crystals examined were undoped semi-insulating to avoid free carrier absorption and absorption due to local vibration or electronic transition at doped impurities. The LPE sample is essential in the present experiment to investigate an effect of different growth conditions, i.e. Ga-rich or As-rich. A thick layer (0.2mm) of LPE was especially grown for the purpose of making absorption measurements. This sample has an electron

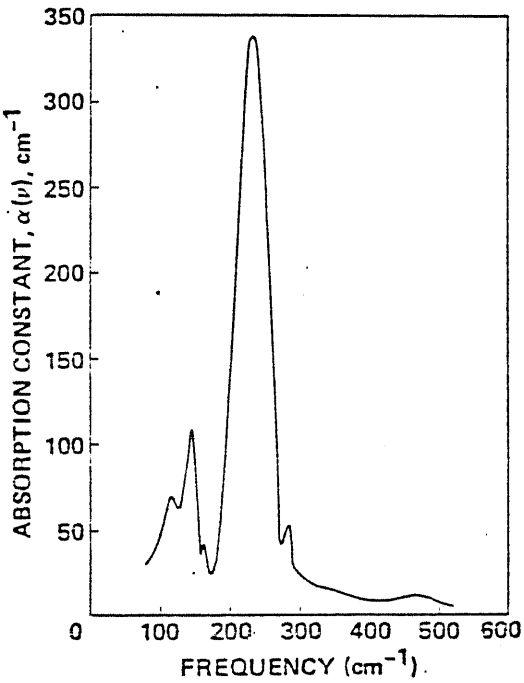

Fig. A-3 Absorption spectrum due to lattice vibration of bulk amorphous arsenic at room temperature. (After Lucovsky and Knights 1974).

concentration of about $1x10^{15}cm^{-3}$.

All the samples were mechanically polished on the backside to a thickness of 0.2mm. This procedure means that only the epi-layer was remained after the polishing for the LPE sample. The sample dimensions are approximately 16mmx16mm, which are larger than the window (14mmx14mm) of the sample holder. The surface of the LEC samples were mirror, while that of the LPE sample was "wiped" (almost mirror), which is characteristic of normal LPE layers.

Another sample for eliminating an effect of reflectance was also prepared by a chemical etching to approximately 20um. This is because the energy range of the present interest is near Reststrahl region where reflectance is expected to dramatically change with photon energy. Transmitted light intensity, T, at a certain photon energy is expressed, assuming a multiple reflection, as follows,

$$T = \frac{R*\exp(-a*d)}{1-R*\exp(-2a*d)} \qquad \text{(A-6)}$$

Here, R, a and d are reflectance, absorption coefficient and thickness of a sample, respectively. If reflectance can be regarded as a constant, relative value of a is obtained by simply monitoring a transmission spectrum. On the other hand, when reflectance largely changes, it is necessary to eliminate this

effect. Reflectance can be determined from a separate measurement. When such a configuration is difficult to achieve, however, a is obtained by using a set of samples with different thicknesses, d_1 and d_2. Let T_1 and T_2 be the corresponding transmitted light intensities, $\log(T_1/T_2)$ gives

$$\log(T_1/T_2) = -a*(d_1-d_2)-\log[(1-R*e^{-2a*d_1})/(1-R*e^{-2a*d_2})] \quad (A-7)$$

using (A-6). If $R*\exp(-2a*d_i)<<1$ (i=1, 2), the second term of the right hand of (A-7) can be neglected and an absorption spectrum is obtained.

The procedure for preparing a thinner sample is schematically shown in Fig. A-4 and described in the following. First, an undoped SI LEC GaAs (the same wafer as LECa) was cut into two pieces, one of which is for the reference. Both of the pieces were polished to a thickness of 0.2mm. The reference piece underwent an additional polishing of 20um, which makes a difference in the thickness of this amount. The etchant used is a mixture of H_2SO_4, H_2O_2 and H_2 with a ratio of 4:1:1 at room temperature. This etchant is known to be a fast etchant (a few micron/min) which preserves mirror surface. However, it suffers from a poor reproducibility and a variation of etch rate within a large wafer. Although a dry etching is superior in the aspect ratio, no mask is available for an etching of hundreds of microns.

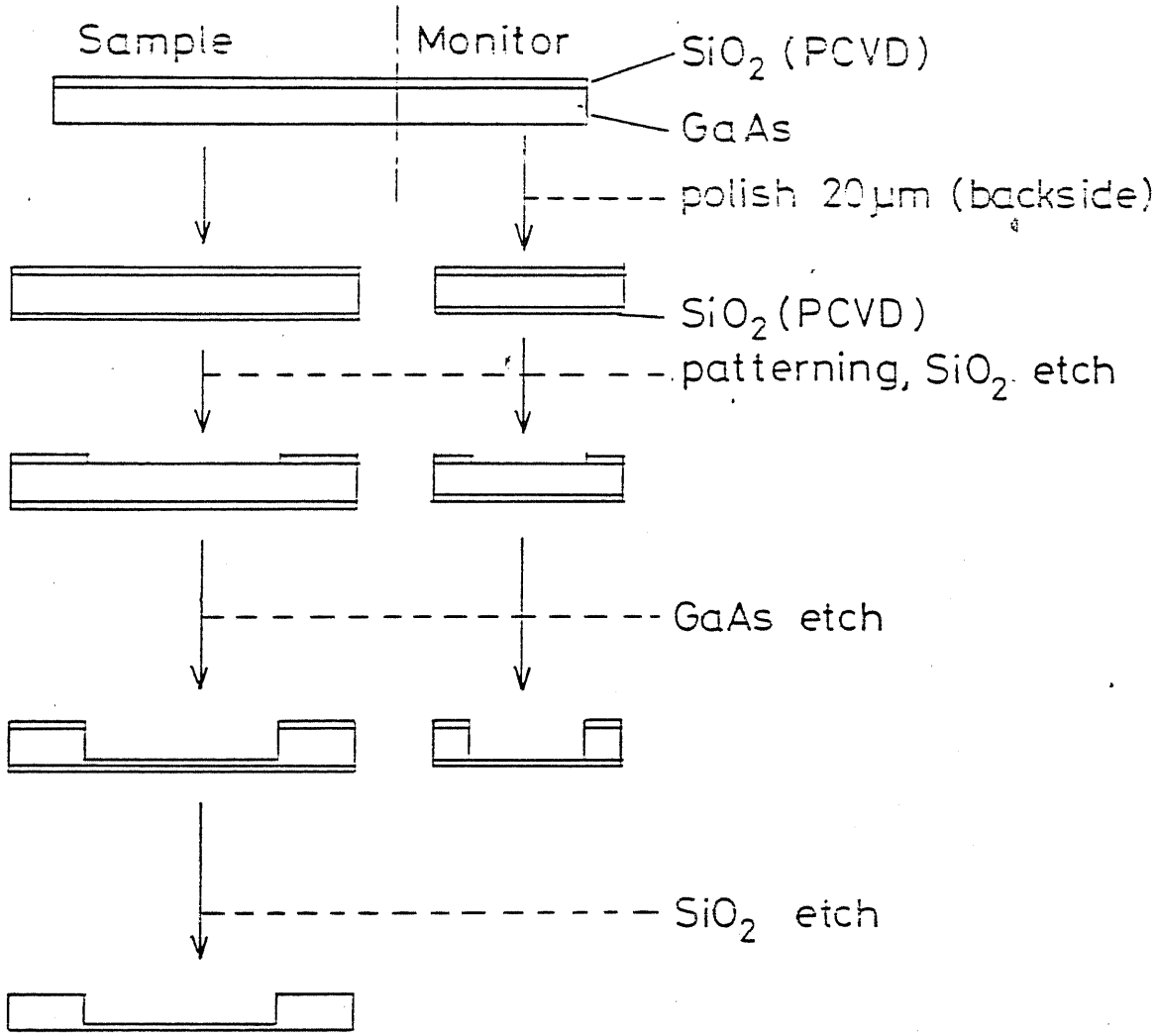

Fig. A-4 A process for the preparation of the thin (20um) sample.

Before etching, a mask is formed by using a photolithography to ensure a mechanical strength. Since a photoresist, OMR-83, is not resistive to the etchant for more than 15min, 1.8um-thick SiO_2 film deposited by plasma-assisted chemical vapor deposition (PCVD) was used as an etching mask. The pattern used was a square with a dimension of 13mmx13mm. The backside was also coated with SiO_2 to avoid the unwanted etching because an etching from backside results in a variation of thickness across a wafer. After opening etching windows, both of the pieces were simultaneously dipped into a etchant until the etching penetrated the reference piece. It actually took approximately 90min to etch and obtain a 20um-thick sample. Finally, SiO_2 was removed by dipping the sample into a solution of $HF:H_2O=2:1$ for 2min.

(2)FTIR Measurement

Optical absorption was measured by using a Fourier-transformation far-infrared spectrometer (FTIR) system, Digilab FTS-16S where a TGS (triglythine sulfate) detector and a Myler beam-splitter are used. This system is capable of measuring absorption in the wavenumber range of $400cm^{-1}$-$40cm^{-1}$. For measurements at cryogenic temperatures, a refrigerator, Air Product Heli-tran LT-3-110, which cools a sample by a flow of liquid helium, was used. When a sample is placed in the cryostat, a pair of CsI (cesium iodide) windows were used, which are transparent to light with a wavelength up to about 50um. Collection of interferogram and calculation of inverse Fourier transform were carried out automatically by a mini-computer.

A-2.3 Results and discussions

Fig. A-5 shows the transmitted light intensity of LECa of different thickness (20um and 200um). In the following, (A/B) means that the transmission of A is normalized by B. It can be seen that at the peak energy around 270cm^{-1}, transmission is not so different although the absorbance should be reduced by one order of magnitude. This is the clear indication that reflectance play an important role in this energy range as discussed in the previous section.

The actual absorbance spectra, where the transmittance of a thin sample should be used for the normalization, at room temperature are not shown. This is because the transmission were not measured with a good S/N due to a small transmittance. Figure A-6 shows the absorption spectra of the four samples measured at 14K. All these spectra have peaks around 280cm^{-1} due to the lattice absorption of GaAs crystals.

To look more in detail, relative absorption spectra of LEC samples are shown in Fig. A-7 where the LPE sample was used for normalization and all the sample thicknesses are 200um. The main feature is that both of the LEC crystals have residual absorption at the tail region. However, it can be clearly seen that this residual absorption is dependent on the wafers. This result indicate a difference in crystalline properties. However, a

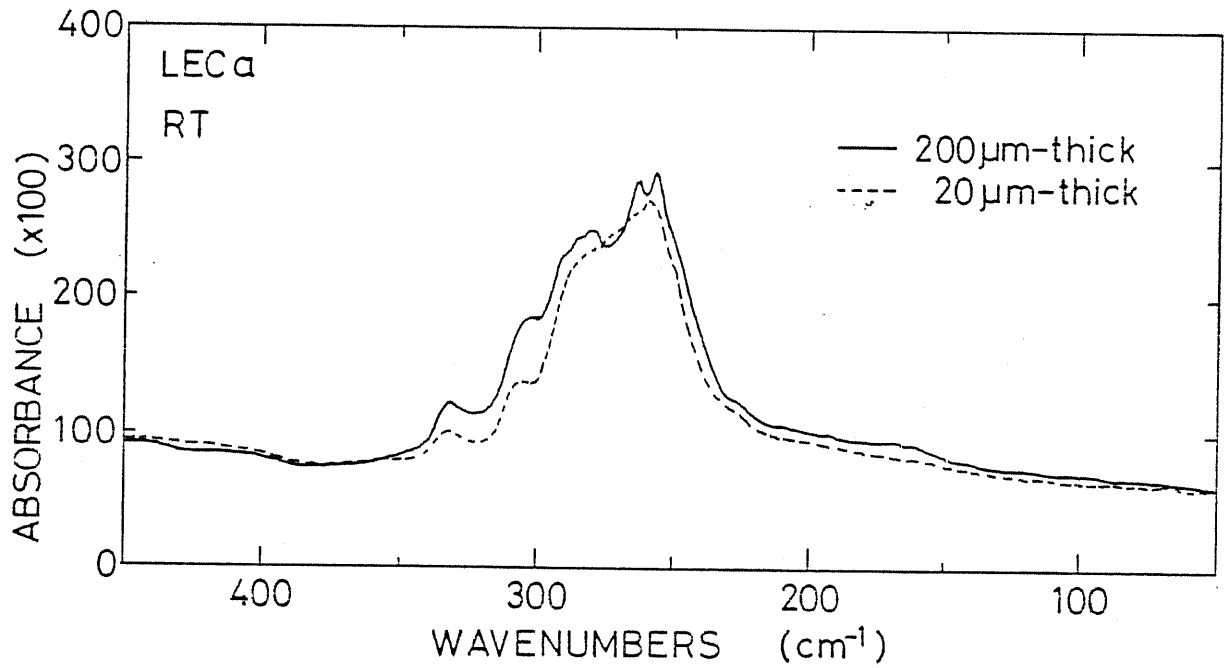

Fig. A-5 Transmitted light intensities of the 20um- and 200um-thick LECa samples.

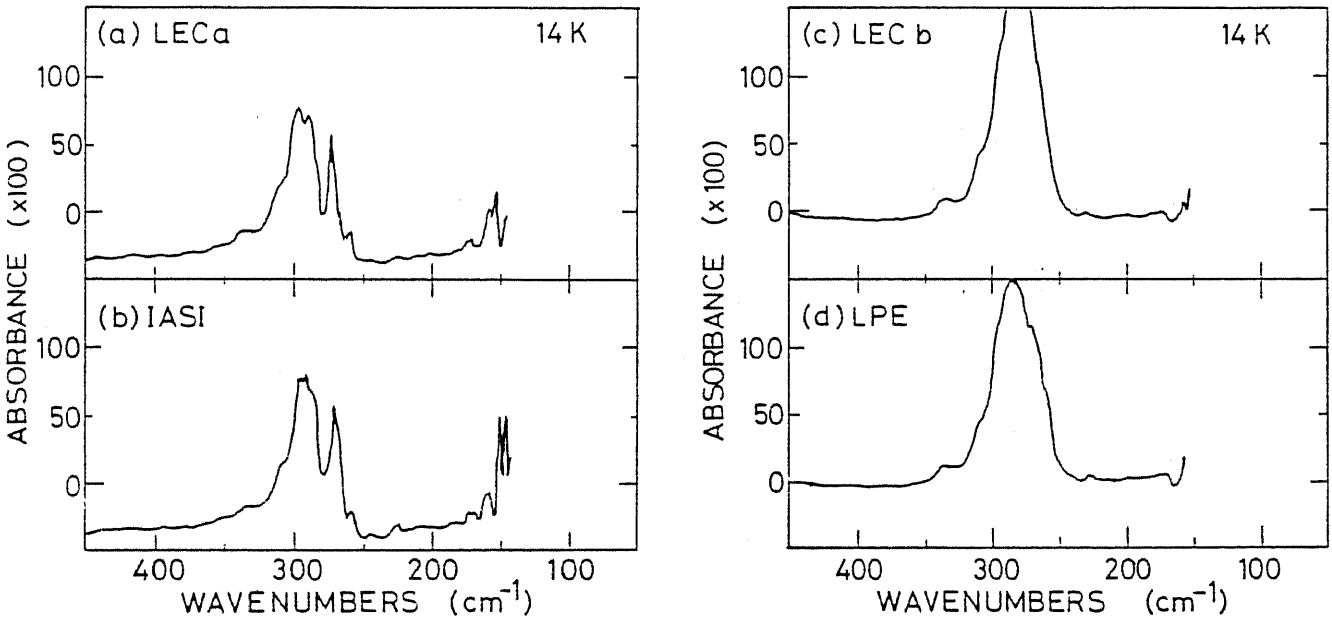

Fig. A-6 Absorbance spectra for LECa, LECb, IASI and LPE measured at 14K.

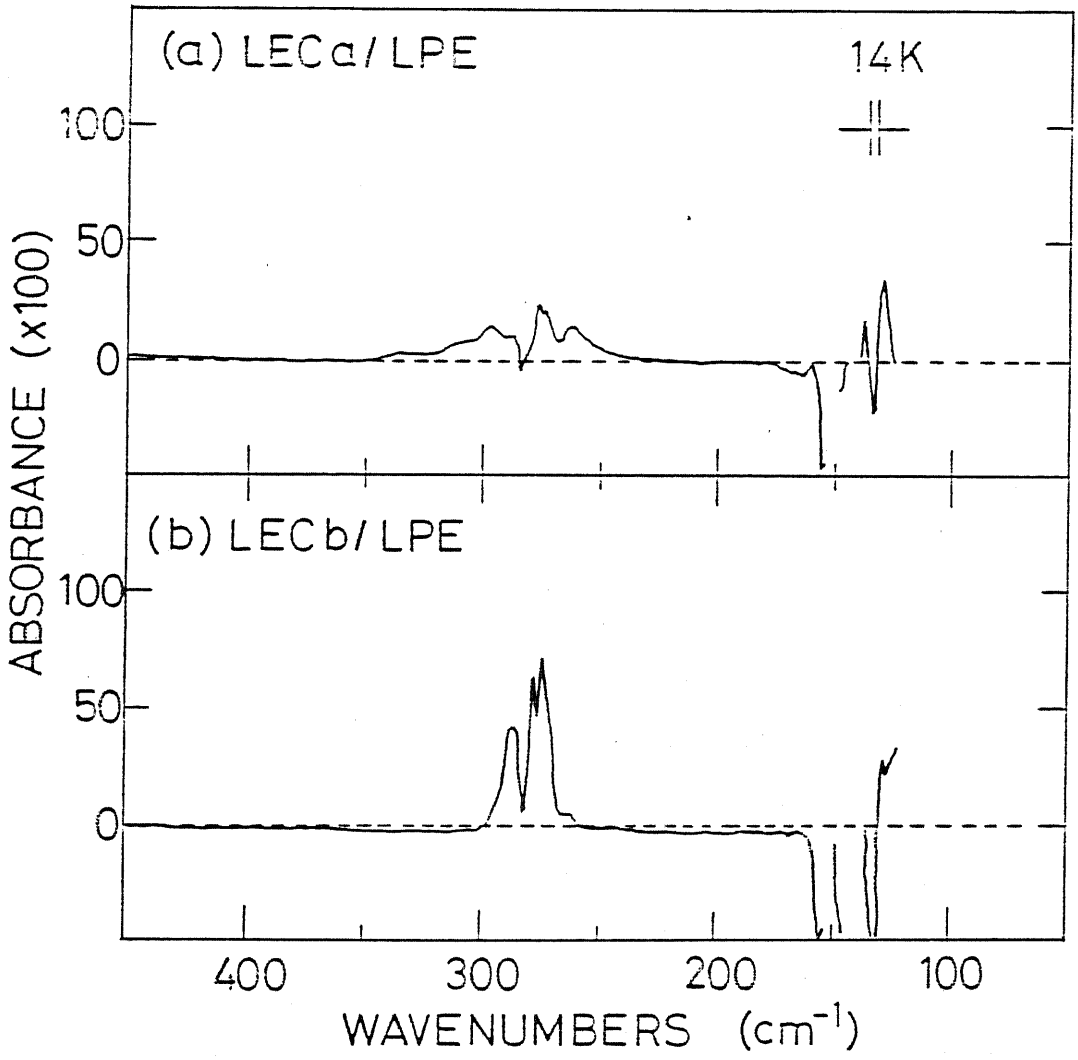

Fig. A-7 Residual absorption in LECa and LECb, where LPE is used as a reference.

vibration spectrum of amorphous arsenic was not observed as shown in the Fig. A-8 which is the enlarged version where LECa was commonly used as the numerator. The reason for this result is likely to be the low oscillator strength of vibration modes of amorphous arsenic even if it is present. When the vibration of As-As bonds is considered, the relevant absorption coefficient can be estimated by a volume effect consideration. Absorption coefficient of bulk amorphous arsenic is $350cm^{-1}$ at its maximum (at room temperature). If it is assumed that one aggregate corresponds to one EL2 center and this phase exists in GaAs crystal with a concentration of $10^{16}cm^{-3}$, the oscillator strength is expected to be reduced by a factor of the order of $N_{As}x10^{-6}$ where N_{As} is the number of As atoms in one aggregate. Experimentally, this value is at largest $1.6x10^{-3}$ which is determined by the detection limit of the present system as well as the spectral background. Therefore, the resultant N_{As} should be less than 1600. This estimation seems to be reasonable since a defect with such a large dimension is hardly expected to act as an electrically active center in a GaAs crystal. At the same time, the total number of excess arsenic atoms should be $10^{20}cm^{-3}$ which seems to be too large. If the aggregate consists of a much smaller number of arsenic atoms, then the absorption by local phonons would be enhanced. Actually, a strong absorption have been observed, for instance, at C_{As}. However, in such a case, it is difficult to identify the absorption band without information on the defect structure.

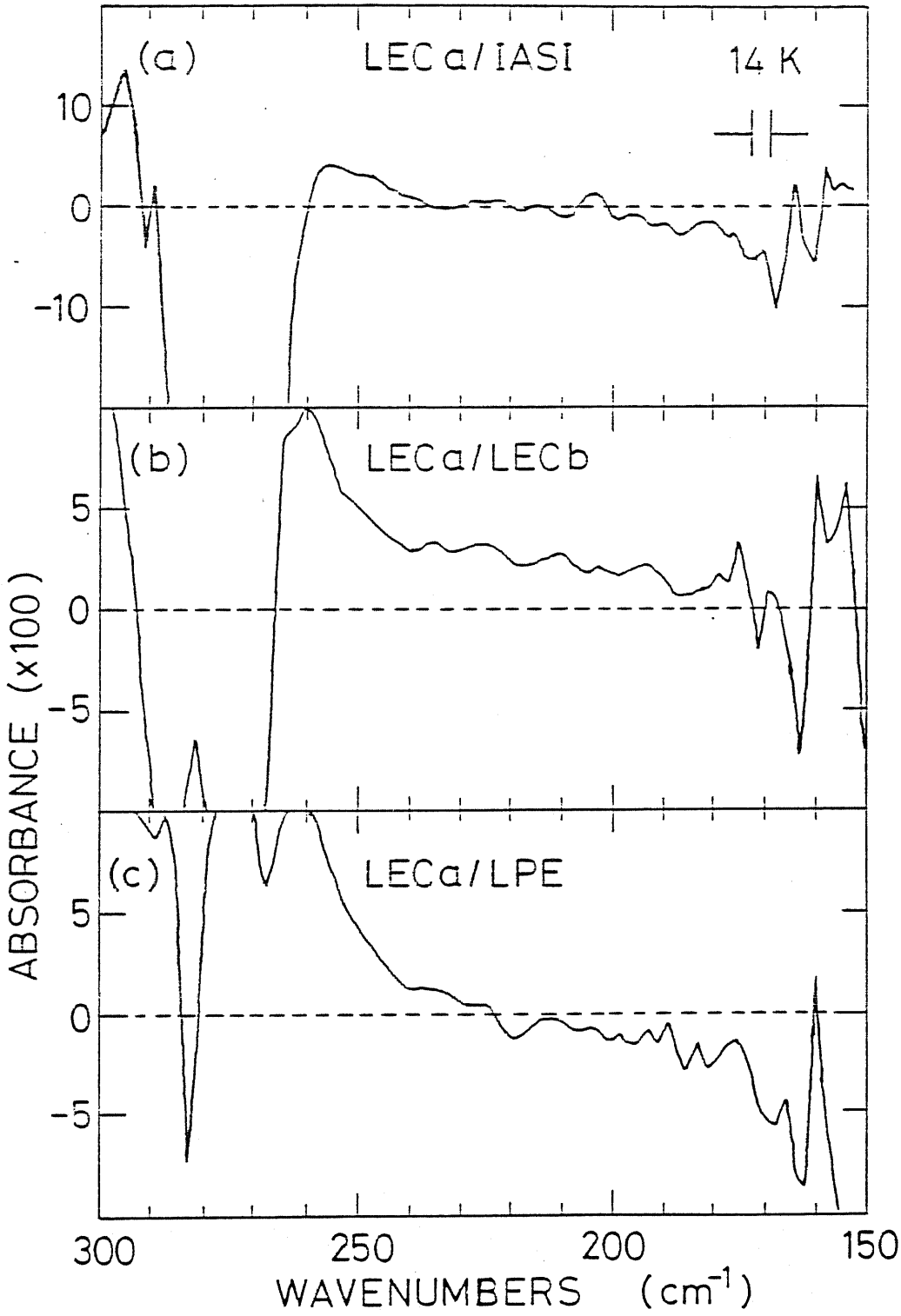

Fig, A-8 Residual absorption in a enlarged scale. LECa is commomly used as a numerator.

A-2.4 Conclusions

An FTIR study of lattice absorption in GaAs was performed on crystals grown by LEC and LPE methods. It is found that LEC GaAs has residual absorption compared to LPE GaAs with a variation depending on crystals. No absorption band was observed which is analogous to the absorption of bulk amorphous arsenic. This result is rather reasonable according to a volume effect consideration.

REFERENCES

Ainslie, N.G., Blum, S.E. and Woods, T.F., (1962). J. Appl. Phys. 33, 2391.

Bachelet, G.B. and Scheffler, M., (1985). Proc. 17th Int. Conf. on Physics of Semiconductors, ed. by J.D. Chaudi and W.A.Harrison, Springer, p.755.

Baeumler, M., Kaufmann, U. and Windscheif, J. (1985). Appl. Phys. Lett. **46**, 781.

Baraff, G.A. and Schluter, M., (1985). Phys. Rev. Lett. **55**, 2340.

Baranowski, J.M., Majewski, J.A., Hamera, M. and Kaminska, M., (1985). Proc. 13th Int. Conf. on Defects in Semiconductors, ed. by L.C. Kimmering and J.M. Parsey, Jr., AIME, Warrendale, p.199.

Bar-Yam, Y. and Joannopoulos, J.D., (1986). 14th Int. Conf. on Defects in Semiconductors, Paris, France.

Beall, R.B., Newman, R.C. and Whitehouse, J.E., (1986). J. Phys. **C19**, 3745.

Bhattacharya, P.K., Ku, J.K., Owen, S.J.T.,Aebi, V., Cooper, C.B., and Moon, R.L., (1980). Appl. Phys. Lett. **36**, 304.

Bishop, S.G., Storm, V. and Taylor, P.C., (1976). Solid State Commun. **18**, 573.

Blanc, J., Bube, R.H. and Weisberg, L.R., (1964). J. Phys. & Chem. Solids **25**, 225.

Blanc, J. and Weisberg, L.R., (1961). Nature **192**, 155.

Chantre, A., Vincent, G. and Bois, D., (1981). Phys. Rev. B **23**, 5335.

Dischler, B., Fuchs, F. and Kaufmann, U., (1986). 14th Int. Conf. on Defects in Semiconductors, Paris, France.

Elliott, K., Chen, R.T., Greenbaum, S.J. and Wagner, R.J., (1984). Appl. Phys. Lett. **44**, 907.

Fazzio, A., Brescansin, L.M., Caldas, M.J. and Leite, J.R., (1979). J. Phys. **C12**, L831.

Figielski, T., KaKaczmarek, E. and Wosinski, T., (1985). Appl. Phys. **A38**, 253.

Fillard, J.P., Bonnafe, J. and Castagne, M., (1984). Solid State Commun. **52**, 855.

Frank, W., (1985). 12th Int. Symp. on GaAs and Related Compounds, Karuizawa, Japan.

Fujimoto, I., (1984). Jpn. J. Appl. Phys. **23**, L287.

Gant, H., Koenders, L., Bartels, F. and Monch, W., (1983). Appl. Phys. Lett. **43**, 1032.

Goltzene, A., Meyer, B. and Scwab, C., (1983). Rev. Phys. Appl. **18**, 703.

Gooch, C.H., Hilsum, C. and Holeman, B.R., (1961). J. Appl. Phys. **32**, S2069.
Greaves, G.N., Elliott, S.G. and Davis, D.A., (1979). Adv. Phys. **28**, 49.
Haisty, R.W., Mehel, E.W. and Stratton, R., (1964). J. Phys. & Chem. Solids **23**, 829.
Hambleton, K.G. and Hall, R.B., (1961). Phys. Soc. London 77, 1147
Henry, C.H. and Lang, D.V., (1977). Phys. Rev. B **15**, 988.
Hofmann, D.M., Meyer, B.K., Lohse, F. and Spaeth, J.-M., (1984). Phys. Rev. Lett. **53**, 1387.
Holmes, D.E., Chen, R.T., Elliott, K.R. and Kirkpatrick, C.G., (1982). Appl. Phys. Lett. **40**, 46.
Huber, A.M., Linh, N.T., Valladon, M., Debrun, J.L., Martin, G.M., Mittoneau, A. and Mircea, A., (1979). J. Appl. Phys. **50**, 4022.
Ikoma, T. and Mochizuki, Y., (1985). Jpn. J. Appl. Phys. **24**, L935.
Ikoma, T., Taniguchi, M. and Mochizuki, Y., (1985). Gallium Arsenide and Related Compounds, Inst. Phys. Conf. Ser. No.74, p.65.
Jaros, M., (1982). Deep Levels in Semiconductors, Adam Higer Ltd., Bristol.
Kaminska, M., Lagowski, J., Parsey, J., Wada, K. and Gatos, H.C., (1981). Gallium Arsenide and Related Compounds, Inst. Phys. Conf. Ser. No.63, p.197.
Kaminska, M., Skowronski, M., Lagowski, J., Parsey, J.M. and Gatos, H.C., (1983). Appl. Phys. Lett. **43**, 302.
Kaminska, M., Skowronski, M. and Kuszko, W., (1985). Phys. Rev. Lett. **20**, 2204.
Keil, T.H., (1965). Phys. Rev. **140**, A601.
Kuszko, W., Walczak, P.J., Trautman, P., Kaminska, M. and Baranowski, J.M., (1986) Int. Conf. on Defects in Semiconductors, Paris, France.
Goswami, N.K., Newman, R.C. and Whitehouse, J.E., (1981). Solid State Commun. **40**, 473.
Lagowski, J., Gatos, H.C., Parsey, J.M., Wada, K., Kaminska, M. and Walukiewicz, W., (1982a). Appl. Phys. Lett. **40**, 342.
Lagowski, J., Kaminska, M., Parsey, J.M. and Gatos, H.C., (1982b). Gallium Arsenide and Related Compounds, Inst. Phys. Conf. Ser. No.65, p.41.
Lagowski, J., Lin, D.G., Aoyama, T. and Gatos, H.C., (1984). Appl. Phys. Lett. **44**, 336.
Lagowski, J., Gatos, H.C., Kang, C.H., Skowronski, M., Ko, K.Y.

and Lin. D.G., (Appl. Phys. Lett. **49**, 892.
Lang, D.V., (1974). J. Appl. Phys. **45**, 3023.
Lang, D.V. and Logan, R.A, (1975). J. Electron. Mater. **4**, 1053.
Levinson, M., (1983). Phys. Rev. B **28**, 3660.
Leyral, P., Vincent, G., Nouailhat, A. ang Guillot, G., (1982). Solid State Commun. **42**, 67.
Makimoto, T., Taniguchi, M., Ogiwara, K., Ikoma, T. and Okumura, T., (1984). Extended Abstracts of the 16th Conf. on Solid State Devices and Materials, p.189.
Martin, G.M., (1981). Appl. Phys. Lett. **39**, 747.
Martin, G.M., Mittoneau, A. and Mircea, A., (1977). Electron. Lett. **13**, 191.
Martin, G.M., Jacob, G., Hallais, J.P., Hallis, J.P., Grainger, F., Roberts, J.A., Clegg, B., Blood, P. and Poiblaud, G., (1982). J. Phys. **C15** 1841.
Meyer, B.K. and Spaeth, J.-M., (1985). J. Phys. **C18**, L99.
Meyer, B.K., Spaeth, J.-M. and Scheffler, M., (1984). Phys. Rev. Lett. **52**, 851.
Miller, M.D., Olsen, G.H. and Ettenberg, M., (1977). Appl. Phys. Lett. **31**, 538.
Mircea-Roussel, A. and Makram-Ebeid, S., (1981). Appl. Phys. Lett. **38**, 1007.
Mittoneau, A. and Mircea, A., (1979). Solid State Commun. **30**, 157
Mochizuki, Y., (1984). Thesis for Master's Degree, Univ. Tokyo.
Mochizuki, Y. and Ikoma, T., (1985). Jpn. J. Appl. Phys. **24**, L895.
Mochizuki, Y. and Ikoma, T., (1986a). Semi-Insulating III-V Materials, Hakone 1986, ed. by H. Kukimoto and S. Miyazawa, Ohm-sha, p.323.
Mochizuki, Y. and Ikoma, T., (1986b), 14th Int. Conf. on Defects in Semiconductors, Paris, France.
Nojima, S., (1985). J. Appl. Phys. **57**, 620.
Ogiwara, K., Taniguchi, M. and Ikoma, T., (1984). unpublished.
Okumura, T., (1985). Jpn. J. Appl. Phys. **24**, L437.
Okumura, T. and Hoshino, M., (1986). Semi-Insulating III-V Materials, Hakone 1986, ed. by H. Kukimoto and S. Miyazawa, Ohm-sha, p,409.
Omling, P., Weber, E.R. and Sammuelson, L., (1985). Phys. Rev. B
Pajet, D. and Klein, P.B., (1985). Proc. 13th Int. Conf. on Defects in Semiconductors, ed. by L.C. Kimmerling and J.M. Parsey, Jr., AIME, Warrendale, p.959.
Pons, A., Mircea, A. and Bourgoin, J., (1980). J. Appl. Phys. **51**, 4150.
Ross, S.F. and Jaros, M., (1973). Phys. Lett. **A45**, 335.

Sakai, K and Ikoma, T., (1974). Appl. Phys. 5, 165.
Samuelson, L., Omling, P. Titze, H. and Grimmeis, H.G., (1981). J. Cryst. Growth 55, 164.
Schluter, M. and Baraff, G.A., (1986). 18th Int. Conf. on Physics of Semiconductors, Stockholm, Sweden.
Shanabrook, B.V., Klein, P.B. and Bishop, S.G., (1983). Physica 117&118, 173.
Skowronski, M., Lagowski, J. and Gatos, H.C., (1985). Phys. Rev. B 32, 4264.
Skowronski, M., Lagowski, J. and Gatos, H.C., (1986). J. Appl. Phys. 59, 2451.
Spaeth, J.-M., (1986). Semi-Insulating III-V Materials, Hakone 1986, ed. by H. Kukimoto and S. Miyazawa, Ohm-sha, p.299.
Sze, S.M., (1981). Physics of Semiconductor Devices, John Wiley and Sons.
Tajima, M., (1984). Jpn. J. Appl. Phys. 23, L691.
Tajima, M., (1985). Appl. Phys. Lett. 46, 484.
Taniguchi, M. and Ikoma, T., (1983a). Gallium Arsenide and Related Compounds, Inst. Phys. Conf. Ser. No.65, p.65.
Taniguchi, M. and Ikoma, T., (1983b). J. Appl. Phys. 54, 6448.
Taniguchi, M. and Ikoma, T., (1984). Appl. Phys. Lett. 45, 69.
Taniguchi, M., Mochizuki, M. and Ikoma, T., (1984). Semi-Insulating III-V Materials, Kah-nee-ta 1984, Shiva Publishing, p.231
Thomas, R.N., Hobgod, H.M., Eldridge, G.W., Barrett, D.C., Braggins, T.T., Ta, L.B. and Wang, S.K., (1984). Semiconductors and Semimetals, vol.20, p.1-87.
Tsukada, N., Kikuta, T. and Ishida, K., (1985a). 12th Symposium on Gallium Arsenide and Related Compounds, Karuzawa, Japan.
Tsukada, N., Kikuta, T. and Ishida, K., (1985b). Jpn. J. Appl. Phys. 24, L302.
Turner, W.J., Pettit, G.D. and Ainslie, N.G., (1963). J. Appl. Phys. 34, 3274.
Van Vechten, J.A., (1975). J. Electrochem. Soc. 122, 419 and 423.
Vasudev, P.K., Wilson, R.G. and Evans, C.A.Jr, (1980). Appl. Phys. Lett. 36, 837.
Vigneron, J.P., Scheffler, M. and Pantelides, S.T., (1983). Physica 117B&118B, 137.
Vincent, G. and Bois. D., (1978). Solid State Commun. 27, 431.
Vincent, G., Bois, D. and Chantre, A., (1982). J. Appl. Phys. 53, 3643.
von Bardeleben, H.J., Stievenard, D., Bourgoin, J.C. and Huber, A., (1985). Appl. Phys. Lett. 47, 976.
von Bardeleben, H.J., Stievenard, D., Deresmes, D., Huber, A. and

Bourgoin, J.C., (1986a). Phys. Rev. B **34**, 7192.
von Bardeleben, H.J., Bourgoin, J.C. and Miret, A., (1986b). Phys. Rev. B **34**, 1360.
Wada, K. and Inoue, N., (1985). Appl. Phys. Lett. **47**, 945.
Wagner, R.J., Krebs, J.J., Stauss, G.H. and White, A.M., (1980). Solid State Commun. **36**, 15.
Walukiewicz, W., Lagowski, J. and Gatos, H.C., (1983). Appl. Phys. Lett. **43**, 192.
Watabnabe, M.O., Tanaka, A., Nakanishi, T. and Zohta, Y., (1981). Jpn. J. Appl. Phys. **20**, L439.
Weber, E.R., Ennen, H., Kaufmann, U., Windscheif, J., Schneider, J. and Wosinski, T., (1982). J. Appl. Phys. **41**, 6140.
Weber, E.R., (1984). Semi-Insulating III-V Materials, Kah-nee-ta 1984, Shiva, London, p.296.
Weber, E.R. and Omling, P., (1985). Festkoerperprobleme, XXV, p.689
Worner, R., Kaufmann, U and Schneider, J., (1982). Appl. Phys. Lett. **40**, 141.
Yahata, A. and Nakajima, M.,(1984). Jpn. J. Appl. Phys. **23**, L313.
Yu, P.W., (1984). Appl. Phys. Lett. **44**, 330.
Yuanxi, Z., Jicheng, Z., Yiang, L., Kwangyu, W., Binghua, H., Bingfang, L., Cuncai, L.,Liansheng, L., Jiuan, S. and Chi, S., (1985). Proc. 13th Int. Conf. on Defects in Semiconductors, ed. by L.C. Kimmerling and J.M. Parsey, Jr., AIME, Warrendale, p.1021.
Zhu, H.-Z., Adachi, Y. and Ikoma, T., (1981). J. Cryst. Growth 55 154.
Zohta, Y. and Watanabe, M.O., (1982). J. Appl. Phys. **53**, 1809.

PUBLICATION LIST

(* indicates a publication which is not directly related to the work described in this thesis)

1. Original papers

(1) "Photoquenching Effect at the Midgap Electron Traps ('EL2 Family') in Different GaAs Crystals"
Semi-Insulating III-V Materials, Kah-nee-ta 1984, edited by D. C. Look and J. S. Blakemore, Shiva Publishing, 1985, p.231
(with M. Taniguchi and T. Ikoma)

(2) "A New Model for the Origin of Midgap Electron Traps (EL2 Family)in Liquid Encapsulated Czochralski GaAs"
Gallium Arsenide and Related Compounds", Institute of Physics Conference Series, No.74 (1985) p.65
(with T. Ikoma and M. Taniguchi)

(3) "Optical Recovery of Photoquenching at the Midgap Electron Traps (EL2 Family) in GaAs"
Japanese Journal of Applied Physics, Vol.24 (1985) pp.L895
(with T. Ikoma)

(4) "Identification of 'EL2 Family' Midgap Levels in GaAs"
Japanese Journal of Applied Physics, Vol.24 (1985)
pp.L935
(with T. Ikoma)

(5) "Charge Transfer at Excited States of EL2 Observed by
Spectral Photocapacitance Transient Analysis"
Semi-Insulating III-V Materials, Hakone 1986, edited by H.
Kukimoto and S. Miyazawa, Ohm-sha Ltd., 1986, p. 323
(with T. Ikoma)

(6) "Optical Transition Mechanisms via Excited State and a New
Configuration Coordinate Model for EL2 in GaAs"
to be published in the Proceedings of 14th International
Conference on Defects in Semiconductors, Trans Tech
Publications Limited
(with T. Ikoma)

*(7) "Point Defects and Their Physical Properties in III-V
Semiconductors", (Invited, in Japanese)
Journal of Japanese Society of Crystallography, Vol.28
(1986) pp.103
(with T. Ikoma)

*(8) "The Role of Gallium Antisite Defect in Activation and
Type-Conversion in Si Implanted GaAs"
Japanese Journal of Applied Physics, Vol.24 (1985) pp.L921

(with T. Hiramoto, T. Saito, and T. Ikoma)

*(9) "Evidence for Creation of Gallium Antisite Defect in Surface Region of Heat Treated GaAs"
Japanese Journal of Applied Physics", Vol.25 (1986) pp.L830
(with T. Hiramoto and T. Ikoma)

2. International Conferences

(1) "Photoquenching Effect at the Midgap Electron Traps ('EL2 Family') in Different GaAs Crystals"
The 3rd Conference on Semi-Insulating III-V Materials, 1984, Kah-nee-ta, USA
(with M. Taniguchi and T. Ikoma)

(2) "A New Model for the Origin of Midgap Traps (EL2 Family) in Liquid Encapsulated Czochralski GaAs"
11th International Symposium on Gallium Arsenide and Related Compounds, 1984, Biarritz, France
(with T. Ikoma and M. Taniguchi)

(3) "Charge Transfer at Excited States of EL2 Observed by Spectral Photocapacitance Transient Analysis"
The 4th Conference on Semi-Insulating III-V Materials, 1986, Hakone, Japan
(with T. Ikoma)

(4) "Optical Transition Mechanisms via Excited State and a New Configuration Coordinate Model for EL2 in GaAs"
The 14th International Conference on Defects in Semiconductors, 1986, Paris, France
(with T. Ikoma)

3. Domestic Conferences (in Japanese)

(1) "Characterization of Undoped LEC GaAs by PL and DLTS"
The 44th Autumn Meeting of the Japan Society of Applied Physics, September 1983, 26a-E-1
(with M. Taniguchi and T. Ikoma)

(2) "Photoquenching Effect at the Main Electron Trap (EL2) in GaAs (I) --- Sample Dependence"
The 31st Spring Meeting of the Japan Society of Applied Physics and Related Societies, April 1984, 1p-O-14
(with M. Taniguchi and T. Ikoma)

(3) "Photoquenching Effect at the Main Electron Trap (EL2) in GaAs (II) --- Transition to the Metastable State and the Recovery Processes"
The 31st Spring Meeting of the Japan Society of Applied Physics and Related Societies, April 1984, 1p-O-15
(with M. Taniguchi and T. Ikoma)

(4) "Photoquenching Effect at the Deep Level in Oxygen-Implanted LPE GaAs (EL2-O)",
The 45th Autumn Meeting of the Japan Society of Applied Physics, October 1984, 12p-J-16
(with T. Ikoma)

(5) "Tunneling of Electrons at the Main Electron Trap (EL2) in GaAs"
The 32nd Spring Meeting of the Japan society of Applied Physics and Related Societies, March 1985, 31p-W-14
(with T. Ikoma)

(6) "Characterization of EL2 near the Interface of WSi_x/GaAs"
The 32nd Spring Meeting of the Japan society of Applied Physics and Related Societies, March 1985, 31a-W-8
(with T. Kakinoki, T. Kimura and T. Ikoma)

(7) "Optical Recovery of Photoquenching at the Electron Traps (EL2 Family) in GaAs"
The 46th Autumn Meeting of the Japan Society of Applied Physics, October 1985, 1p-A-5
(with T. Ikoma)

(8) "A Model for the Main Electron Traps (EL2 Family) in GaAs"
The 46th Autumn Meeting of the Japan Society of Applied Physics, October 1985, 1p-A-9
(with T. Ikoma)

*(9) "Behavior of Copper and Amphoteric Impurities in Ion-Implanted and Annealed GaAs"
The 46th Autumn Meeting of the Japan Society of Applied Physics, October 1985, 2p-C-1
(with T. Hiramoto and T. Ikoma)

*(10) "Role of Ga_{As} Defect in the Activation Process of Si-Implanted GaAs"
The 46th Autumn Meeting of the Japan Society of Applied Physics, October 1985, 2p-C-2
(with T. Hiramoto, T. Saito and T. Ikoma)

(11) "Transitions via Excited States of EL2 --- Characterization by Spectral Photocapacitance Transient Analysis (SPTA) Method"
The 33rd Spring Meeting of the Japan scciety of Applied Physics and Related Societies, April 1986, 1a-V-4
(with T. Ikoma)

(12) "Transitions via Excited States of EL2 --- A Configuration Coordinate Model for Excited State"
The 47th Autumn Meeting of the Japan Society of Applied Physics, September 1986, 29p-D-5
(with T. Ikoma)

*(13) "Defects near the Surface of GaAs Induced by Focused Si Ion-Implantation"

The 47th Autumn Meeting of the Japan Society of Applied Physics, September 1986, 27p-ZG-14
(with T. Hiramoto, T. Saito and T. Ikoma)

4. Others

(1) "Midgap Electron Traps (EL2 Family) in GaAs"
International Symposium on Nanometer Structure Electronics, Ohm-sha Ltd., (1984), p.137
(with T. Ikoma and M. Taniguchi)